THE TIPPING POINT: VISUAL ESTIMATION OF THE PHYSICAL STABILITY OF THREE-DIMENSIONAL OBJECTS

BY STEVEN A. CHOLEWIAK

A dissertation submitted to the

Graduate School—New Brunswick

Rutgers, The State University of New Jersey

in partial fulfillment of the requirements

for the degree of

Doctor of Philosophy

Graduate Program in Psychology

Written under the direction of

Manish Singh

and approved by

_____

_____

_____

_____

New Brunswick, New Jersey

October, 2012

ABSTRACT OF THE DISSERTATION

The tipping point: Visual estimation of the physical stability of three-dimensional objects

by STEVEN A. CHOLEWIAK

Dissertation Director:

Manish Singh

Vision research generally focuses on the currently visible surface properties of objects, such as color, texture, luminance, orientation, and shape. In addition, however, observers can also visually predict the physical behavior of objects, which often requires inferring the action of hidden forces, such as gravity and support relations. One of the main conclusions from the naïve physics literature is that people often have inaccurate physical intuitions; however, more recent research has shown that with dynamic simulated displays, observers can correctly infer physical forces (e.g., timing hand movements to catch a falling ball correctly takes into account Newtons laws of motion). One ecologically important judgment about physical objects is whether they are physically stable or not. This research project examines how people perceive physical stability and addresses (1) How do visual estimates of stability compare to physical predictions? Can observers track the influence of specific shape manipulations on object stability? (2) Can observers match stability across objects with different shapes? How is the overall stability of an object estimated? (3) Are visual estimates of object stability subject to adaptation effects? Is stability a perceptual variable? The experimental findings indicate that: (1) Observers are able to judge the stability of objects quite well and are close to the physical predictions on average. They can track how changing a shape will

affect the physical stability; however, the perceptual influence is slightly smaller than physically predicted. (2) Observers can match the stabilities of objects with different three-dimensional shapes – suggesting that object stability is a unitary dimension – and their judgments of overall stability are strongly biased towards the minimum critical angle. (3) The majority of observers exhibited a stability adaptation aftereffect, providing evidence in support of the claim that stability may be a perceptual variable.

Acknowledgements

This work was supported by NSF Grants CCF-0541185 and DGE-0549115 (IGERT: Interdisciplinary Training in Perceptual Science) and by NIH Grant EY021494.

Many thanks to Chris Kourtev for his technical assistance and the present and past members of the Rutgers University Perceptual Science and Visual Cognition Laboratories (including Kristina Denisova, Shalin Shah, Sung-Ho Kim, Bina Pastakia, Mehwish Ajmal, Roy Jung, Stamatiki "Matina" Clapsis, Omer "Daglar" Tanrikulu, John Wilder, Peter Pantelis, Vicky Froyen, and Seha Kim).

Dedication

This research project would not have been possible without the support and guidance of many of my fellow students and the faculty members in the Rutgers University Psychology Department.

I wish to express my sincerest gratitude to my advisor, Dr. Manish Singh, whose invaluable support and guidance over the years has helped me "find my way" in academia and to help strengthen my desire for knowledge. His insightful comments and constructive criticisms of my projects have been instrumental in strengthening my research. Thank you.

Deepest gratitude is also due to the members of the supervisory committee, Dr. Jacob Feldman, Dr. Eileen Kowler, and Dr. Roland Fleming, without whose knowledge and assistance – over the course of these past few years –, this research would not have been successful.

I also wish to express my gratitude to my family and friends, especially my best friend (and wife!) Sara and parents Roger and Linda, who have put up with endless discussions about "whether or not this beer glass will fall", "How might I perceptually represent this [or that]?", and "What's the functional form for this surface? I want to calculate its properties analytically...". You are all saints.

Table of Contents

Chapter 1

Introduction

Vision research generally focuses on currently visible surface properties, such as color, texture, luminance, orientation, and shape. Representing these properties provides a useful visual description of a scene and the objects therein: what the various objects are, where they are located relative to each other, and relative to the observer. There are some notable exceptions to the focus on visible surface properties, where researchers investigate the perceptual representation of surfaces (or portions of surfaces) that are not currently visible – that is, have no counterpart in the retinal images – as well as predicting where objects will be in the near future. Both modal completion, where observers perceive an illusory contour occluding another shape (e.g., Kanizsa triangle & illusory contours), and amodal completion, where a complete shape is perceived even though contours are partly occluded, involve the inference of contours and surfaces that are not visible (Anderson, Singh, & Fleming, 2002; Singh, 2004). Similarly, observers can visually extrapolate the trajectory of a moving object (Becker & Fuchs, 1985; Pavel, Cunningham, & Stone, 1992; Verghese & McKee, 2002), and predict where an object that disappears behind an occluder is likely to re-emerge from (Scholl & Pylyshyn, 1999; Graf, Warren, & Maloney, 1995; Shah, Fulvio, & Singh, 2012).

However, these representational processes do not involve the inference of physical forces acting upon the objects. This inference of forces is critical in predicting the physical behavior of objects because the application of forces can lead to translation, rotation, and acceleration, or non-rigid deformation of real-world objects. Therefore, although it is important for the visual system to represent the shape and other surface properties of objects as they currently exist, it is also important to be able to also infer forces and predict the behavior of physical objects in the immediate future – e.g., for

the purpose of guiding motor action.

The inference of forces is crucial for the manipulation of physical objects; without it, one could not interact with the world. Mounting evidence supports an internal, mental model of physics that is applied during object interaction. For example, observers are sensitive to the effects of gravity (I. K. Kim & Spelke, 1992; Friedman, 2002; McIntyre, Zago, Berthoz, & Lacquaniti, 2001). The inference of forces also allows for the prediction of how colliding objects will interact (Cooper, Birnbaum, & Brand, 1995; Newman, Choi, Wynn, & Scholl, 2008) and how frictional forces will affect the movement of objects (by decelerating their motion). Visual surface properties can provide some of the necessary information for inferring forces, such as texture providing information about friction, but visible surface properties alone cannot be used to predict object behavior. The brain must also have an internal model of how physical forces act and how they influence the behavior of objects.

A growing body of research has shown that individuals use models of forces, similar to the classical "Newton's Laws", when predicting object behavior and interactions with other objects. The visual system uses inferred – unseen – forces to plan motor actions (e.g., predicting the trajectory of an arrow or calculating the contact angle for a billiard cue stick in order to strike a ball to sink another) and to assist in decision making. The area of psychology that investigates how humans infer information about forces and use it in the service of future action is known as "naïve physics". This research project's goal is to study how we judge physical attributes of objects and to determine if our judgments of stability conform to the beliefs of the traditional "naïve physics" literature, which had largely concluded that people apply inaccurate physical models, or whether our inference of forces allows us to make judgments in a more physically-correct manner in more perceptual contexts.

1.1 Naïve physics

Humans are constantly interacting with the world around them, observing the behavior and interaction of objects in the environment and using these observations to inform

future decisions and motor actions. The study of naïve physics – how people represent and use models of physical forces and causes of motion – has focused on answering the question of whether or not humans embody physically-correct representations of physics and if they can accurately predict the physical behavior of objects. In order to make physically-accurate predictions, humans must have a system that embodies a model of physics.

In the "real world", the physical behavior of objects of the environment can be physically defined using statics and dynamics (branches of classical mechanics) and, in many cases – where objects move at a constant velocity or are only affected by the force of gravity – the physical behavior of objects can simply be described using Newton's laws of motion. For people to accurately predict object motion and future behavior, their internal models must use the object's velocity and acceleration to infer the physical forces acting upon the object (e.g., as described by Newton's laws). An important question is whether these internal models are consistent with Newton's laws and whether or not people use physically-derived models of motion and object behavior. The naïve physics literature has sought to determine how well people use the behavior of moving objects to predict how they will behave in the near-future. Do they use a physically-accurate dynamic model – using correctly inferred forces – or a simpler model that, while not always physically-correct, can provide reasonably accurate answers most of the time (e.g., a model that utilizes heuristics)?

A representational model of physics would allow people to observe object behavior and estimate the forces acting upon the object, so that the visual system can predict the object's future location. Naïve physics research has focused on describing perceptual and cognitive models of inferred forces and how people use them – correctly and incorrectly – to predict object motion. And, as with most representations, these motion predictions are constantly, unconsciously updated, allowing us to use prior perceptual information with a representation of the the physical world in the service of future action (e.g., to catch a falling ball).

Do people use physically-accurate models when representing object motion? There is evidence that people can do this for the simpler, less complex situations. Human

observers can easily identify the position of objects and track/extrapolate the motion of objects that move at constant velocity (i.e., motion that conforms to Newton's 1^{st} law) (Pavel et al., 1992). There is also evidence that people use a representation of implied motion when observing object behavior and recalling its location/orientation some time in the future.

Representational momentum (RM) is a subarea of naïve physics that has found that representations of object motion interfere with observers' memories of the object's location and/or orientation (Freyd, 1983; Freyd & Finke, 1984; Freyd & Jones, 1994). Freyd (1983) suggested that observers generate a dynamic mental representation of an object's motion when shown a series of images implying object motion and that this dynamic representation can continue to change, based upon the object's prior motion, interfering with "static" memories of the last seen state.

Freyd and Finke (1984) showed observers a rectangle spinning counter-clockwise in a series of images, then presented a frame that was either the same or different from the last image shown and asked, "Is this image the same or different from the last one shown?" (see Fig. 1.1). Observers had more difficulty identifying frames that continued the motion as different from the last presented frame compared to images that showed motion in the opposite direction, which were readily identified as different. Observers appeared to misjudge the orientation of the last frame when presented with a sequence that implies motion. Freyd and Finke (1984) posited that observers generate a representation of the motion and that this representation was interfering with their memories of the last frame in the motion sequence. They found that this RM interference requires coherent motion – that is, a series of images that continue motion in a single direction – otherwise, no dynamic mental representation of the object's motion is generated and people can readily identify images that are different. Because observers are automatically computing the predicted trajectory and using constant velocity information, they cannot help but be influenced by that representation.

People are able to use constant velocity information, but how do they integrate this information over time, for example with accelerating objects? As predicted from a computational complexity argument, observers have more difficulty when predicting

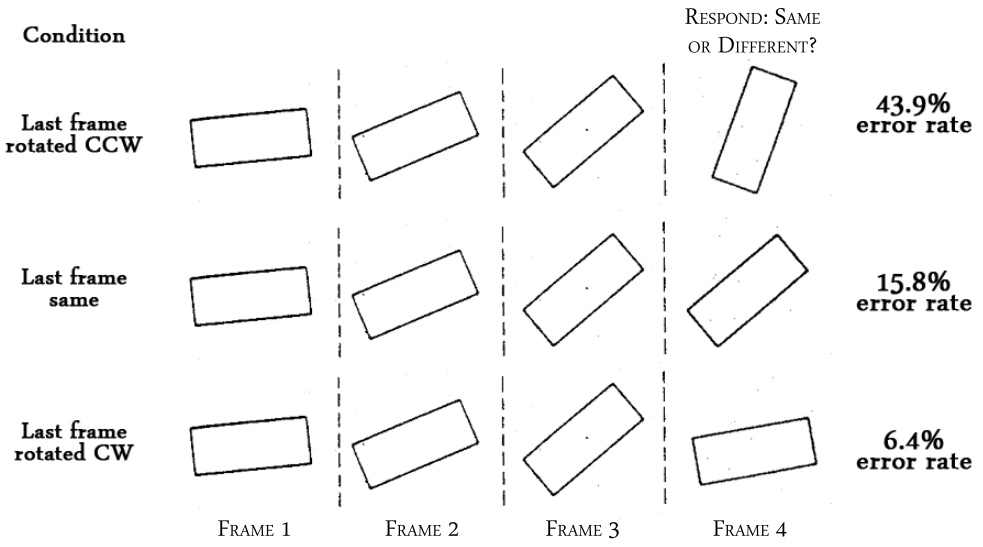

Figure 1.1: Sequence of test images demonstrating representational momentum (Freyd & Finke, 1984).

motion affected by the acceleration due to a net force (i.e., motion that conforms to Newton's 2^{nd} law). Extrapolating motion becomes more difficult for people when the object(s) undergo acceleration due to an implied force, even when the acceleration is a constant centripetal acceleration (e.g., a ball on a string being swung in a circle).

If observers always used position, velocity, and linear acceleration in a physically-consistent, mathematically-derived manner when predicting object motion, then they should be able to predict how forces acting upon an object will affect an object's trajectory. In the gross majority of circumstances, we are able to track movement and account for changing direction – whether due to internal or external forces. And this fact is reflected in evidence that people utilize a physically accurate model that incorporates acceleration due to gravitational forces.

All objects with mass on Earth have a gravitational force acting upon their bodies and it appears as though humans develop a representation at an early age (I. K. Kim & Spelke, 1992; Friedman, 2002) and account for gravity when trying to grab a falling object (McIntyre et al., 2001; Zago & Lacquaniti, 2005). Real-time motor tasks, such as predicting time-to-impact (TTI) in order to catch an object, require relatively quick responses and observers often do not have much of time – on the order of a few hundred milliseconds – to compute a detailed prediction of the trajectory. However, it appears

as though these observers use a physically-accurate model of gravity when predicting the TTI of objects moving under the force of a constant gravitational field.

As McIntyre et al. (2001) and Zago and Lacquaniti (2005) demonstrated, although people sometimes use acceleration correctly, they do not always correctly infer how forces will affect a moving object's velocity and acceleration. White (1983) provided additional evidence that observers have difficulty understanding how forces affect the trajectory of moving object. Specifically, White (1983) showed that undergraduate students had difficulty describing force impulses necessary for a spaceship to fly in a circular path (i.e., centripetal acceleration), a square path (i.e., using impulses to slow the ship and turn at each corner), and in any trajectory that required multiple temporally-separated force impulses (see Fig. 1.2). When people are required to predict motion affected by an external force, they have difficulties using a physically-correct model and often fail to correctly incorporate the temporal component.

One possibility is that higher-level cognitive intuitions lead a person to use a physically-incorrect model. This will often occur when observers are asked to answer paper-and-pencil questions (with static diagrams), or solve a specific physical problem where they must predict the trajectory of an object dropped or propelled.

The curved trajectories of objects moved using "external" forces are often mistakenly believed to continue their trajectories once those forces are removed (McCloskey, 1983a). These are often every-day situations where an accurate mental model (such as the gravitational force model described earlier) would be ecologically important. For example, a ball on a string is illustrated as being swung in a circle and observers are asked what trajectory the ball will take if the string breaks. The majority of observers describe the resulting trajectory as continuing in a circle, as if centripetal force continued to act upon the ball after it has been released (see Fig. 1.3).

Research into how people apply implied forces to motion has shown that observers will use the wrong physical model – as opposed to one simply missing higher-order terms that incorporate acceleration – to guide their intuitions/judgments about an object's future motion (McCloskey, Caramazza, & Green, 1980; McCloskey, 1983b, 1983a). The wrong model that most people use, in this case, is this impetus theory – where

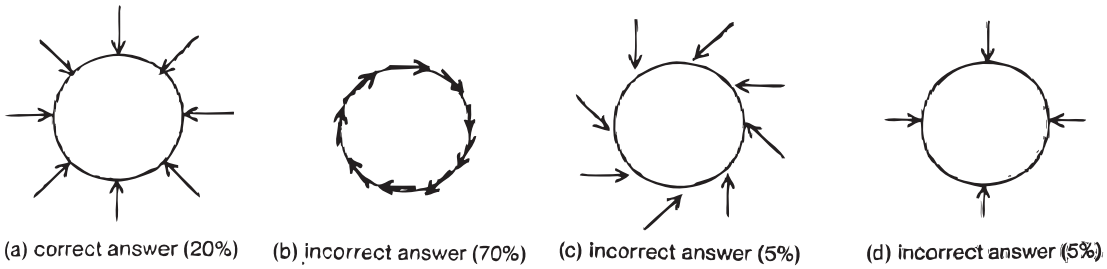

(a) Responses for forces for circular path

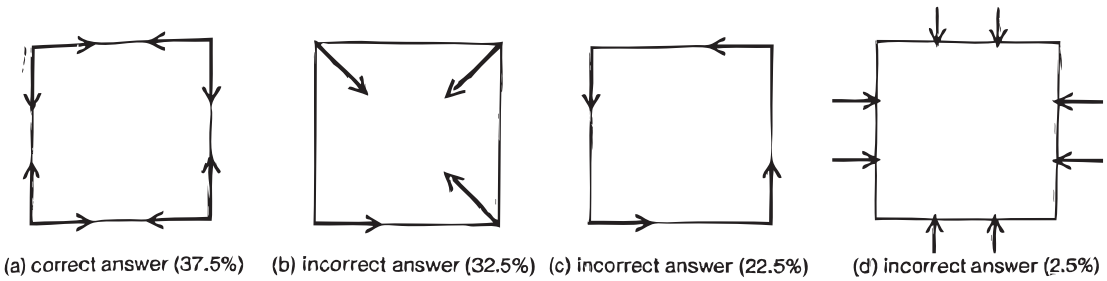

(b) Responses for forces for square path

Figure 1.2: Examples of White (1983)'s paper and pencil task questions where observers fail to demonstrate a working knowledge of how external forces can affect the trajectory of an object. Percentages of responses for each option are in parentheses. In (a), observers were asked "Can you draw a picture and explain how you would get your spaceship to fly in a circular path?". Note that the majority of responses were incorrect. In (b), observers were asked "Can you draw a description of how you would get your spaceship to fly in a square path?" and most observers could not correctly determine the appropriate forces.

objects are believed to embody an internal force that propels them, which gradually dissipates over time – that makes very different predictions for an object's trajectory than Newtonian motion. The majority of the naïve physics research investigating how people perceive implied forces has focused on tasks where the observers have had to extrapolate future motion based upon their intuitions of the physical forces acting upon the object(s) (McCloskey et al., 1980; McCloskey, 1983b, 1983a; McCloskey & Kohl, 1983; McCloskey, Washburn, & Felch, 1983).

A common feature of these studies was that they were all tasks where observers made a decision about the motion of a system (i.e., a bomb dropping from a plane or the trajectory of an object tossed by a catapult), where subjects were shown pictures or given descriptions from which they had to make future predictions. When observers were asked how the object would continue its motion, their performance on these tasks

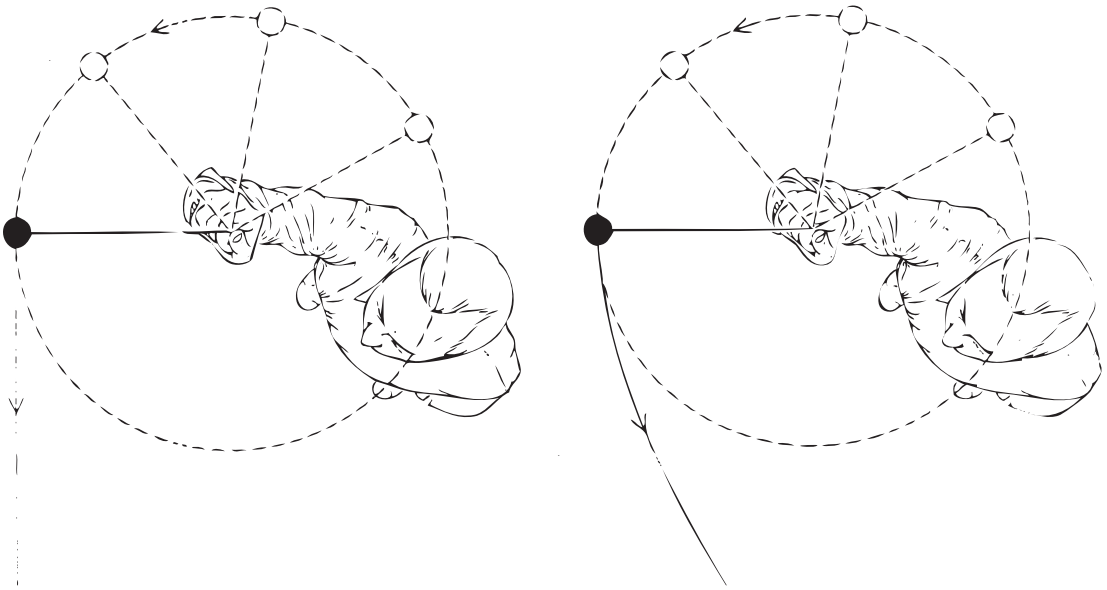

Figure 1.3: Although a ball swung on a string will continue in a straight path once the string breaks (left), most observers believe that the ball will continue on a curvilinear path (right) (McCloskey, 1983a).

was severely degraded and most had false intuitions about how objects would behave under the changing dynamics. However, providing *dynamic simulated motion* of the objects before and after release, either through animation or real displays, leads subjects to readily identify if the simulated motion shown looks "right" or "wrong" and a complete restoration of observer accuracy for the task (Kaiser, Proffitt, & Anderson, 1985; Kaiser, Proffitt, Whelan, & Hecht, 1992).

As a result, when experiments similar to those by McCloskey et al. (1980) and McCloskey (1983b, 1983a) are conducted, but the questions are presented to the observers in a different manner, a very different pattern of results is obtained. For example, if people are shown animations illustrating the possible outcomes of a ball being launched out of a C-shaped tube, observers will overwhelmingly select the physically-correct trajectory, rather than the the one guided by the incorrect cognitive intuition (e.g., the impetus model, see Fig. 1.4 for examples) (Kaiser et al., 1985). When observers observe the different possible motion trajectories, they are able to compare the observed motion to their internal, physically-informed perceptual model and make a more accurate prediction (Proffitt & Gilden, 1989).

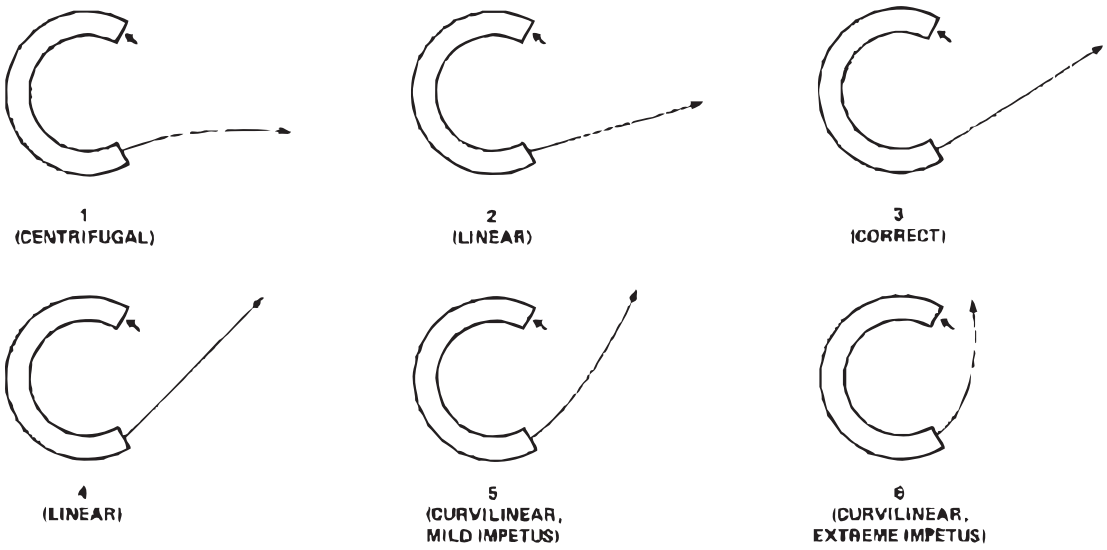

Figure 1.4: Example possible trajectories for a ball exiting a C-shaped tube (Kaiser et al., 1985). Note that providing animated displays illustrating the different possible outcomes leads to observers choosing the correct trajectory (3) while paper-and-pencil tasks often lead to incorrect responses.

To answer the question, "How well can people infer motion and forces acting upon objects in motion?", we can say that although humans often effectively use motion to extrapolate an object's location at a future point in time, it is not necessarily an easy task. More often than not, people appear to revert to simplified physical models that rely on the velocity of the object to describe its motion and fail to take into account acceleration. This seems to reflect a competition between high-level intuitions and perceptual judgments when viewing dynamic simulated motion sequences because people's performance depends on the way in which the question is posed: whether they are asked to report a high-level intuition, or make a perceptual judgment about whether a simulated scene looks "right."

1.2 Perceptual inference of motion and forces from static images

All of the previously discussed naïve physics experiments involve inferring forces from dynamic scenes (i.e., scenarios that include a motion component). Each experiment involved the inference of forces acting upon a moving object and using prior motion information to make a judgment about where the object will go. However, continuous

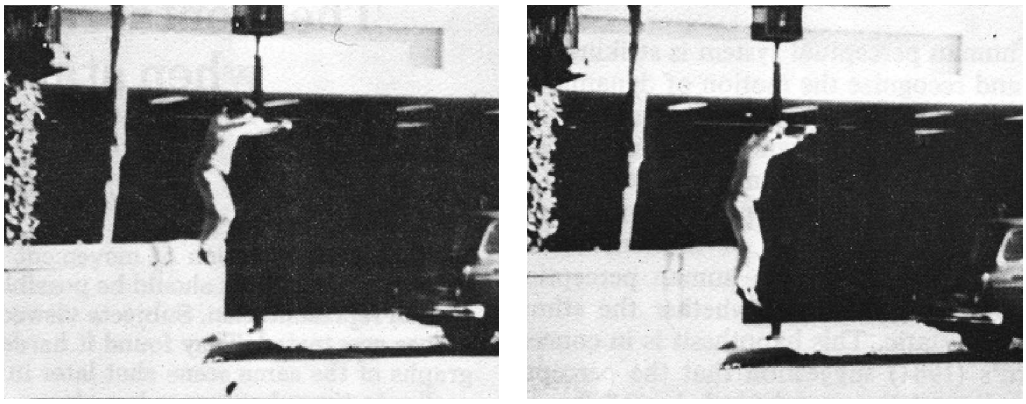

(a) Frame n (b) Frame n+1

Figure 1.5: Before (a) and after (b) frames of an action sequence from Freyd (1983), where a person was shown jumping off a small ledge.

smooth movement/animation is not necessary for people to perceive motion. People perceive motion with as few as two frames of animation (Wertheimer, 1912; Korte, 1915).

Apparent motion in photographic sequences can give such a strong perception of motion that people readily generate a dynamic mental representation of the motion, which interferes with their memory of the scene and, subsequently, change detection. An example from Freyd (1983) used two frames from a video of a person jumping off a ledge (see Fig. 1.5). When observers were shown a future frame from the video where a person's body has translated down due to the force of gravity, observers had difficulty detecting the change and took longer to respond that the image was different and that the body had moved, consistent with an RM account.

There are many cases where forces and motion are inferred from a single static image, where we see implied motion without additional temporal frames. For example, when shown an image of a person in mid-air with his legs bent back and his body over the precipice of a ledge, people will usually assume that the person had jumped off the edge (e.g., Fig. 1.5b alone). That is, observers do not simply describe the static image of the person's body as floating in mid-air, instead they perceive him as in motion and falling. Adding cues, such as blur (Gibson, 1954; Geilser, 1999) or speedlines (Burr & Ross, 2002), strengthen the percept of motion and may lead observers to apply physical

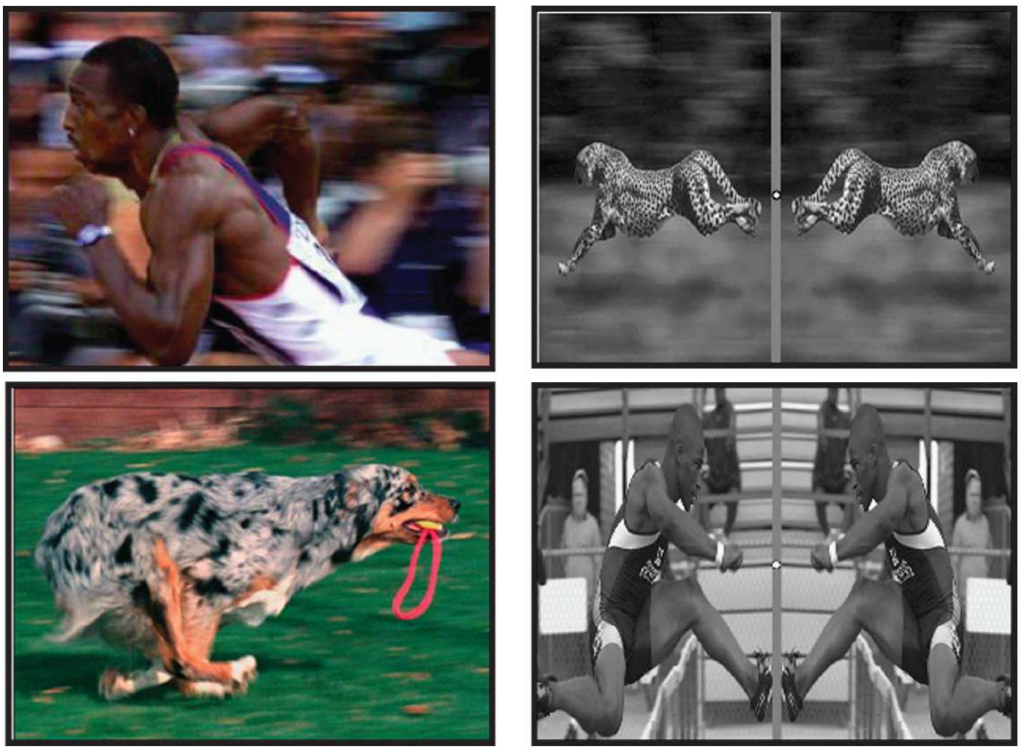

(a) Leftward/Rightward (b) Outward/Inward

Figure 1.6: Example stimuli from Winawer et al., illustrating photographs with implied leftward and rightward motion (a) and outward and inward motion (b).

models when judging the person's past, present, and future states.

These dynamic motion representations have been shown to adapt observers to future motion in the direction of the implied motion. Winawer, Huk, and Boroditsky (2008) showed observers a series of implied motion photographs with either leftward, rightward, inward, or outward motion (e.g., see Fig. 1.6) and then presented them with a moving dot field and asked observers to respond what direction the dots moved. They found that observers became adapted to the direction of motion present in the implied motion photographs and responded that null motion stimuli – with no net motion in any given direction – moved in the opposite direction (a motion aftereffect). Therefore, when we see a static image of an object in motion, we may create a dynamic representation that leads us to expect motion in the direction of the implied motion.

Research has also shown that implied motion in photographs tune observers' perceptual systems to expect motion in the direction of the motion and leads to enhanced

(a) Implied Motion (b) Non-implied Motion

Figure 1.7: Stimuli from Moscatelli et al. (2011) illustrating implied motion (a) and no implied motion (b) for the same scene context, Olympic speed skating.

temporal sensitivity (Moscatelli, Polito, & Lacquaniti, 2011). This increased temporal sensitivity has been shown to lead to increased precision when judging the timing of two events, as though implied motion primes a person for movement. Moscatelli et al. (2011) showed observers photographs from the same context that either had implied motion (e.g., Fig. 1.7a) or no implied motion (e.g., Fig. 1.7b) and then measured observers' difference thresholds for the presentation times of noise displays. The researchers found that implied motion photographs made observers more sensitive to the presentation times of random noise images.

Cartoonists and illustrators often take advantage of the fact that static images can produce percepts of implied motion – and the forces that cause motion – in order to strengthen a scene's realism and the percept of dynamic motion in action sequences to draw readers into a story. These static images can imply acceleration and forces, for example, gravity or forces acting upon objects due to an explosion/percussive force (i.e., "comic book" effects, see Fig. 1.8). The fact that static images can produce such strong percepts of forces acting upon objects in a scene has been exploited by artists and illustrators for hundreds of years (Lasseter, 1987) (e.g., see Fig. 1.9). For example, an image of a runner, crouched and ready to sprint, draws the viewers' eyes to the runner's body, emphasizes the contraction of the muscles and stored energy, and

Figure 1.8: Panels from Action Comics, No. 1 (p.5), illustrating how static images can convey supportive forces (center panel), motion (right panel), and percussive forces.

primes the viewers to anticipate an explosive force from the runner's legs.

Still images only provide a snapshot of a dynamic scene at any given moment in time and cannot provide information about an object's previous states that would cue the observer to future motion (Freyd & Finke, 1984; Freyd & Jones, 1994). Given the lack of temporal cues that multiple frames of video/animation can provide and the relatively small amount of information that can lead to such a strong percept of motion in a static image, the question is posed: How do we perceptually infer forces from static images?

Experiments by Freyd, Pantzer, and Cheng (1988) demonstrated that static images can convey an implied force structure and that this force information may be encoded in the representation of the scene. Observers were first presented with static scenes where a hanging plant had supportive forces – either a pedestal/stand that supported the object from the bottom or a hook that supported it from the top – then an image of the plant unsupported and then the plant above, below, or in the same position. Freyd et al. (1988) found that observers had greater difficulty when making same/different judgments if the test image of the plant was below its previous location (as opposed to above), consistent with motion due to a gravitational force. This result suggests that people inferred the force of gravity acting upon the plant and this inferred force and

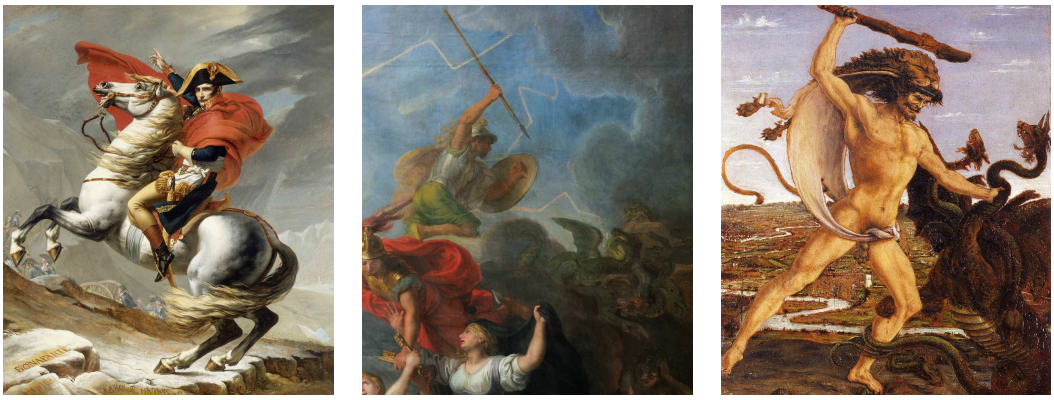

(a) (b) (c)

Figure 1.9: Examples of classical artwork illustrating static images capturing dynamic scenes:
(a) Bonaparte Crossing the Frand Saint-Bernard Pass, May 20, 1800, Jacques Louis David
(b) Inset from Capture of the city and citadel of Gand in six days, 1678, Charles Le Brun
(c) Hercules and the Hydra and Hercules and Anteo, Antonio del Pollaiolo

it's implied motion interfered with observers' memory of the plant's last location.

Roncato and Rumiati (1986) found that although people can perceive the forces acting upon suspended objects in static images, their judgments often do not match physical reality when asked to make a judgment of an object's orientation in the future, after the forces have acted upon it. They showed observers scenes where a bar was suspended by a wire and supported by props from the underside (see Fig. 1.10). The bars were suspended at different points along their axes, including at the center of gravity. Observers were asked: "will [the bar] change its actual orientation after the props have been removed and, if so, at what point it will come to rest when it has stopped swinging" (Roncato & Rumiati, 1986, pp. 363). Observers had difficulty judging how the gravitational force would affect the bars in each scenario and often incorrectly stated that bars supported at the center of gravity would reorient to be vertical or horizontal, when they would be in neutral equilibrium and would not move. Moreover, they misjudged how far bars would rotate when supported off the center of gravity (physically, they would always come to rest in a vertical position).

As previously noted, when people generate a model of the underlying forces acting

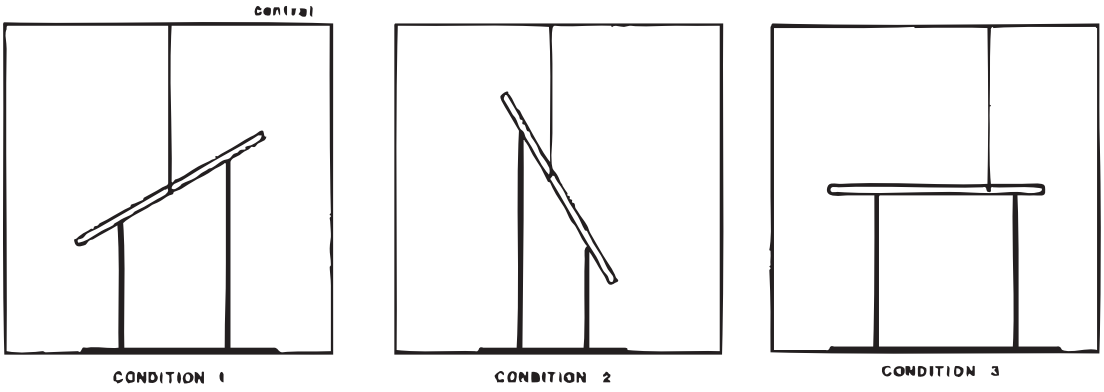

Figure 1.10: Example stimuli from Roncato and Rumiati (1986). In Condition 1, the bars were shown suspended from a central pivot – the center of gravity – at varying degrees of rotation. In Conditions 2 and 3, the bars were suspended from a point to the left or right of the center of gravity.

upon an object, they can then make predictions in the service of motor action, for example to catch a ball (McIntyre et al., 2001). However, the story of how well people can represent these physical forces is not straightforward.

Static images convey information about the physical interaction between objects (e.g., a Jenga tower, cantilevered buildings/designs, see Fig. 1.11). If people want to interact with objects in a scene, it is important for them to understand not only what and where objects are, but how the objects interact and support each other in equilibrium (Cooper et al., 1995). That is, we need to judge their stability. When judging how a scene can be stable and assessing its physical integrity – for example, the images in Fig. 1.11 – the perceptual system should take these static images and ultimately evaluate:

> "What forces are acting on and within the object? How are these forces transmitted through the object? How do these forces balance? What is holding the object together? Which parts are supporting which? ... [And most importantly,] *Why doesn't this object fall down?*" (Cooper et al., 1995, pp. 217).

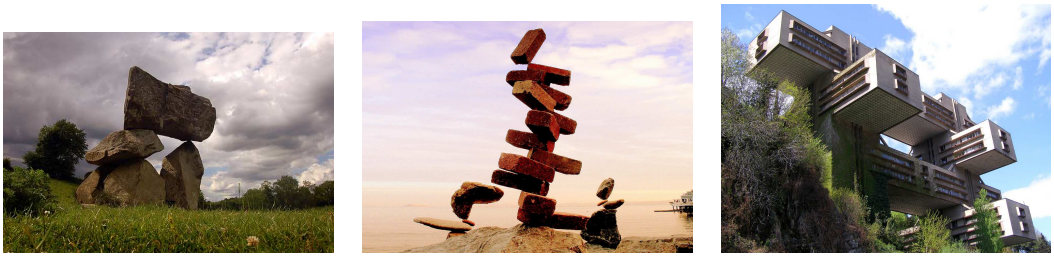

(a) Stones balanced at Aghnacliff dolmen in Ireland (Dempsey, 2008)

(b) Bricks carefully balanced (Dan, 2007)

(c) Former Transport Ministry of Georgia (Zollinger, 2008)

Figure 1.11: Photographs illustrating how static images can convey the physical interactions and support relations between objects in a scene. Sometimes the support structures and interactions are clear, (a) and (b). Other times, foundations conceal the forces that support the objects, (c)

1.3 Perception of Physical Stability

As Cooper et al. (1995) pointed out, knowing the relationships between physical objects and whether they are physically stable or not is truly an ecologically important judgment. Having a perceptual estimate of stability allows for the prediction of an object's physical behavior and assists in guiding motor behavior. The preceding research on naïve physics and inference of forces from static images has demonstrated that while, in general, individuals are able to successfully judge forces in their day-to-day lives, there are certain situations where they have difficulty inferring physical forces and their effects on dynamic and static representations of object movement.

We find ourselves able to interact with the world, balancing objects and applying appropriate forces to open/close/move/throw/catch/clutch objects, on a daily basis. The gross majority of inanimate objects humans interact with on a daily basis are in a static equilibrium, that is, they will not move unless acted upon by an external force, but different objects have varying degrees of stability and the perceptual systems must take this fact into account when predicting object behavior and making decisions about object interaction. For example, a circular manhole cover laying on the ground is extremely stable, while a long steel reinforcement bar (rebar) balanced on its end is very unstable. More subtly, we can readily tell that the object depicted in Fig. 1.12a is more stable – i.e., more resistant to the influences of perturbing forces – than the

(a) (b)

Figure 1.12: Although the bottles in (a) and (b) are both in stable equilibrium, (a) appears more stable – i.e., more resistant to the influences of perturbing forces – than (b).

identical object inverted in Fig. 1.12b. And even though we may be able to interact with and infer the forces that these objects might exert, there are many instances where humans misjudge the stability of objects and their environments.

Any waiter/waitress is likely familiar with the sound of breaking glass. A mispositioned cup or an unbalanced tray can lead to a cacophony of broken glass as the unstable table settings topple. Although people feel as though they can visually judge the stability of many objects, accuracy varies and is dependent upon their ability to infer the forces acting upon the objects. Although many interactions with objects allow us to dynamically correct our stability estimates (e.g., if you notice the laptop you placed on the edge of a table is tipping off), there are some situations where a purely visual estimate is necessary and where misperceived stability can sometimes lead to disastrous consequences. One [extreme] example is Aron Ralston, a canyoneer who became pinned between a boulder and the side of a canyon when he misjudged the stability of the boulder. His father, Larry Ralston, described the misperception:

> "The boulder seemed to be stable, positioned on top of a narrow slot canyon, and as [Aron] started to lower himself over the side, the boulder rotated and came down towards him. But he felt he had tested it out thoroughly ahead of time. But it was just balanced differently than he realized it was." (Morales, 2009)

Aron survived. Although the consequences are usually not as dramatic, the perception of an object's stability is clearly an ecologically important judgment for guiding motor behavior and balance.

In general, the physical stability of an object is a function of the magnitude of the perturbing force needed before an object will leave its equilibrium state. Given knowledge of the mass distribution, one can use the object's center of mass (COM) and supporting base to determine object stability. It is important to note that an object's mass distribution cannot be judged without prior knowledge or physical interaction. But if, in the absence of any information to the contrary, the visual system assumes uniform density, it could readily compute the COM, given a representation of the object's surface structure[1].

Research has shown that the visual system routinely computes the COM when perceptually localizing objects and directing eye movements (saccadic localization). The visual estimation of COM has been studied in a variety of contexts, including 2D objects (Vishwanath & Kowler, 2003; Denisova, Singh, & Kowler, 2006), 3D objects (Vishwanath & Kowler, 2004), and dot clusters (Morgan, Hole, & Glennerster, 1990; Melcher & Kowler, 1999). In most of these studies, observers' judgments corresponded to the object's physical COM, but other studies, such as Baud-Bovy and Soechting (2001) and Baud-Bovy and Gentaz (2004), found that observers used a different, physically incorrect, location when asked to locate the balance point – the alternative location was the orthocenter, the center of the object's circumscribing circle. And so, although individuals can clearly generate multi-modal estimates of physical stability, in a large majority of cases, they must rely primarily on vision to do so.

---

[1]Indeed, the studies reported in this research project suggest that people do make this default assumption.

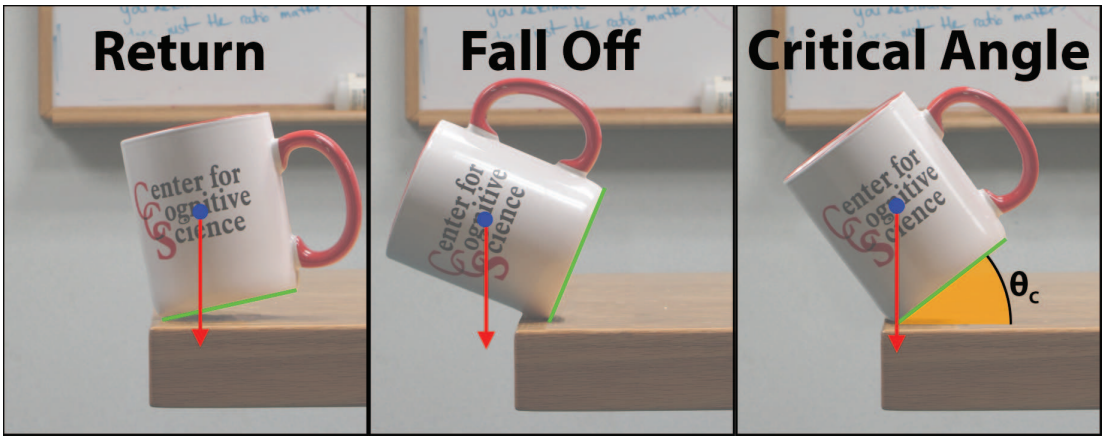

Figure 1.13: Coffee cup with COM vertically above the base (left), outside the base (center), and directly over the contact point (right).

Recall that the COM is the centroid (or average) of the shape's mass and that the supporting base is the surface that is in contact with the ground plane. If the COM is vertically above the base, it will return to its upright position (see Fig. 1.13). If the COM is outside the base, the object will fall.

For example, if an object has a very large base and the COM is vertically above it, then the object is in a static equilibrium and will not change its position or orientation unless a large external force acts upon it (recall Fig. 1.12a). Conversely, objects with smaller bases will be less stable because even a small perturbing force is more likely to lead to the gravity-projected COM going outside of the supportive base (recall Fig. 1.12b). The lower the COM and the larger the supportive base, the more force will be required and therefore, the more stable the object will be. So, for two objects with identical COMs but differing base widths, the object with the smaller base width will be less physically stable.

There is a third possibility where the COM is directly over the contact point, which is physically defined as an unstable equilibrium. Once in an unstable equilibrium, the object will be balanced, but the slightest perturbation will cause the object to leave its equilibrium and returning to a stable equilibrium. When an object has been tilted to its unstable equilibrium, the angle of tilt is defined as the critical angle and, at that angle, the object has an equal likelihood of falling versus returning to its upright position. This critical angle of stability ($\theta_{critical}$) is defined as the angle where the center of mass

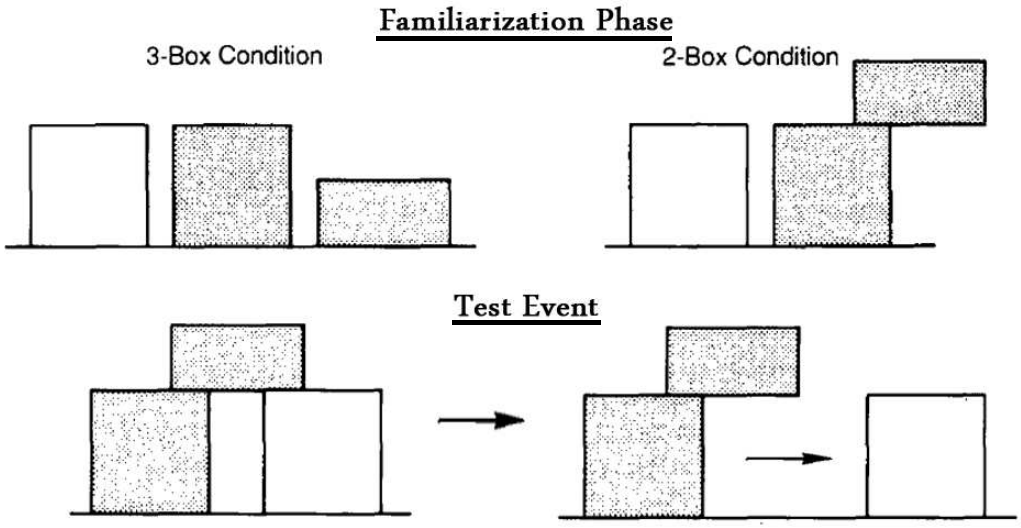

Figure 1.14: Example stimuli from Baillargeon and Hanko-Summers (1990).

is directly vertically above the point of contact and can be calculated physically using the object's COM and base radius (see Equation 1.1).

$$\theta_{critical} = ArcTan\left(\frac{COMy}{r_{base}}\right) \tag{1.1}$$

Researchers have found that human observers are able to judge support relations (whether an object is physically supported by another) based solely upon visual input at an early age. Baillargeon and Hanko-Summers (1990) tested infants' (mean age 8 months, 11 days) abilities to identify anomalous/unstable support relations (see example stimuli in Fig. 1.14). They found that infants stared longer at physically impossible conditions, suggesting that the infants were aware of how separate objects interact and can physically support each other, and were surprised when the scene defied their expectations. Baillargeon and Hanko-Summers (1990) used other experimental conditions to confirm that the infants were surprised by physically impossible events, but that this ability to identify inadequate support conditions was limited for more complex objects (i.e., non-rectangular objects).

Baillargeon, Needham, and DeVos (1992) also tested infants' intuitions about partial-contact support conditions. In their experiments, a small box was placed on top of a

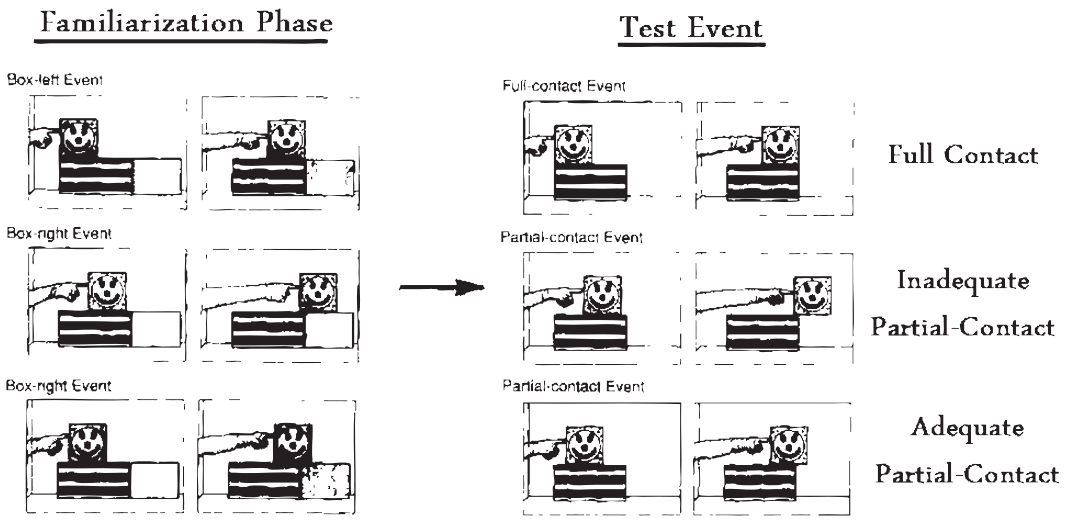

Figure 1.15: Example stimuli from Baillargeon et al. (1992).

larger supportive box and then pushed until 100% of its base was supported (full contact), 70% was supported (adequate partial contact), or 15% was supported (inadequate partial contact) (see Fig. 1.15). The researchers found that 6.5 month old infants looked longer at the inadequate partial contact events, indicating that they were able to identify physically impossible support relations. Further experiments have shown that 5.5 - 6 month old infants did not look longer at the anomalous inadequate partial support event, meaning that intuitions about support relations develop over time (Baillargeon et al., 1992). However, in a later study, Needham and Baillargeon (1993) found that 4.5 month old infants were able to identify a physically impossible support event with a different set of stimuli, where a box moved off of its supportive base and released mid-air does not fall.

Note that although objects may be physically stable, they may not appear to be stable. Perceived stability can use information from multiple modalities, such as visual and haptic shape information, to generate a unitary estimate of an object's stability. Each modality contributes information that allows the perceptual system to generate a cue-combined estimate of the COM location and the object's stability. Vision (see previous section), active touch (Carello, Fitzpatrick, Domaniewicz, Chan, & Turvey, 1992; Lederman, Ganeshan, & Ellis, 1996), and the vestibular system (Barnett-Cowan,

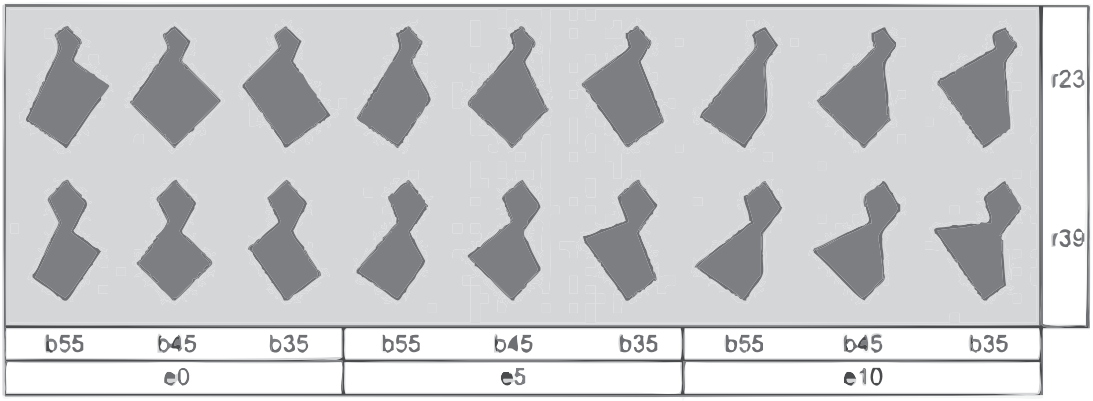

(a) Experiment 1 Stimuli

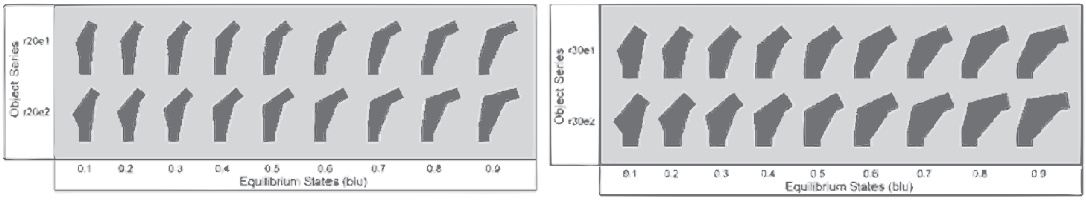

(b) Experiment 2 Stimuli

Figure 1.16: Example stimuli from Samuel and Kerzel (2011).

Fleming, Singh, & Bülthoff, 2011) can all provide information to inform and refine our perceptual estimate of an object's physical stability.

There is some evidence that the visual system uses the shape of an object to judge whether and, if so, in which direction it will fall. Samuel and Kerzel (2011) used a two-alternative forced choice paradigm, where observers were required to respond whether a 2D polygonal object supported on a vertex would fall to the left or to the right (see Fig. 1.16). Samuel and Kerzel (2011) found that observers used different shape heuristics when making judgments about whether the shape would fall to the left or the right. Observers' judgments were overly influenced by the eccentricity of the top part. For example, if the top part was highly eccentric to the right, observers were biased to say that the object would fall on the right, even though physically it would to the left (see Fig. 1.16a for example shapes at their unstable equilibrium).

In addition, in a second experiment, where subjects had to judge whether objects would fall or stay upright, observers in the Samuel and Kerzel (2011) study misjudged the stability of asymmetric 2D objects (see Fig. 1.16b) to be less perceptually stable

than they physically were. The observers' responses exhibited a conservative, or anticipatory, bias – a bias in the direction of perceiving an object to be unstable, even though physically it would maintain its upright posture. This bias was reduced after the observers were given specific instructions about the physical definition of stability. However, some conservative bias remained for these 2D shapes, so Samuel and Kerzel (2011) concluded that observers made their stability judgments about whether or not they would fall "on the safe side."

1.4 Research Questions

The visual system has evolved to evaluate physical attributes very efficiently from limited information. Although its estimates often provide useful information about scenes, it cannot necessarily have a complete representation encompassing every parameter of the objects therein and therefore it must make simplifying assumptions when evaluating scene dynamics. For example, although one may have an accurate representation of an object's shape based upon its visual attributes at one point in time, it is impossible to accurately judge its weight or mass distribution without physically interacting with it or watching it interact with other objects. Even then – when one has developed a dynamic representation of the object and the scene parameters – these representations are lossy and can lose precision over time, leading to decreased precision when inferring the object's future state.

Because an object's shape and distribution of mass density ultimately determine its physical COM, physical critical angle, and stability, our estimates should be as close to the physical parameters as possible in order to accurately evaluate scene dynamics. But do people use physical information correctly when making a judgment about the the object's stability and how forces (e.g., gravity) will affect its state in the future?

As reviewed above, previous work suggests that people use some, but not all, of this information when inferring an object's future state. And, as described in the preceding sections, individuals fail to accurately infer forces acting upon an object in some situations, leading to misjudged scene dynamics and inaccurate physical predictions.

When people determine whether an unstable object is going to fall or not, they often appear to use strategies that produce judgments that can conflict with the physical prediction (fall or return to upright). The perception of stability and support relations should use the object's perceived COM – which has been shown to be close to the physical COM – when estimating the object's critical angle. Determining the computational strategies that the visual system actually uses in estimating object stability remains an interesting question that this research project intends to address. Although our visual system can evaluate many aspects of the physical world with a large degree of precision, it does not always use a model of physics.

This research investigates the perception of stability and addresses whether people use a perceptual model of physics and inferred forces that concurs with the physical world when making judgments about object stability. There are a number of unanswered questions about how people use shape representation when judging the stability of an object, so in this research project, I will address some of the ways that we judge physical attributes of objects and address in the following chapters (Chapters 2, 3, and 4, respectively):

1. How do visual estimates of stability compare to physical predictions? Can observers track the influence of specific shape manipulations on object stability?

2. Can observers match stability across objects with different shapes? How is the overall stability of an object estimated?

3. Are visual estimates of object stability subject to adaptation effects? Is stability a perceptual variable?

Chapter 2

Perception of physical stability of 3D objects: The role of aspect ratio and parts

2.1 Introduction

Research on visual perception focuses primarily on the representation of overtly visible surface properties, e.g., color, texture, orientation, curvature etc. In addition to estimating such properties—i.e., representing what the objects in view are, and where they are located (e.g., Marr, 1982)—an important goal of the visual system is to *predict* how visible objects are likely to behave in the near future. Predicting the physical behavior of objects is, among other things, crucial for the perceptual guidance of motor actions. Consider, for example, the visual guidance of motor actions aimed at intercepting an object in motion, or at catching a precariously placed object that is about to fall. Predicting the physical behavior of objects in these, and other, situations requires observers to infer hidden forces acting on objects, e.g., gravity, support, friction, etc.—and often to do so from vision alone.

Research on intuitive physics has shown that people often hold erroneous physical intuitions. For example, many people expect that a ball being swung at the end of a string will, if the string breaks, fly off along a curved trajectory; or that an object dropped from a flying airplane will fall vertically straight down (e.g., McCloskey et al., 1980). On the other hand, our visuo-motor interactions with objects in everyday life suggest that we usually have a good comprehension of physical attributes such as gravity, friction, and support relations. Indeed, subsequent research has shown that people are much more sensitive to violations of physical laws when they view real-time dynamic displays, rather than when explicitly asked about their intuitions (Kaiser et

al., 1985).[1] In visuo-motor interactions involving catching a falling ball, for instance, McIntyre et al. (2001) have shown that, in timing their hand movements, observers take into account acceleration due to gravity in a manner that is consistent with Newton's laws of motion.

Even more impressive than perceptual predictions involving moving objects, perhaps, are cases where observers can infer the action of underlying forces from a static scene or image. Infants as young as 6.5 months implicitly understand the action of gravity, for example, and expect that objects that are not supported will fall down (Baillargeon et al., 1992). By 8 months they can also judge, to some extent, whether a simple (cuboidal) object is inadequately supported (Baillargeon & Hanko-Summers, 1990; Baillargeon et al., 1992). Such judgments about how an object is likely to behave can have important implications for judgments involving physical objects. In experiments with adult human observers, Freyd et al. (1988) found that when subjects were shown a static image of an unsupported object (that was previously shown to be supported), their memory of its vertical position was systematically distorted in the lower direction (i.e., consistent with how the depicted object would behave if its support were in fact physically removed). Based on this and other evidence, the authors argued that the representation of static scenes includes not only a kinematic component, but a dynamic one as well—in other words, a representation of underlying forces.

An ecologically important judgment that relies on the implicit inference of underlying forces is the perceptual estimation of the physical stability of an object. Fig. 2.1 shows the same object tilted through different angles from its vertical upright position. We can judge in a quick glance that in Fig. 2.1a the object is likely to return to its vertically upright position, whereas in Fig. 2.1b it will probably fall over. These expectations make physical sense. All forces acting on an object in a uniform gravitational field can be summarized by a single net force that acts on its COM. Hence when the gravity-projected COM lies within the supporting "base" surface (as in Fig. 2.1a), the

[1]This is especially true for physical problems where each object can essentially be treated as a point mass located at its center of mass COM, and is correctly treated by observers as such (Proffitt & Gilden, 1989).

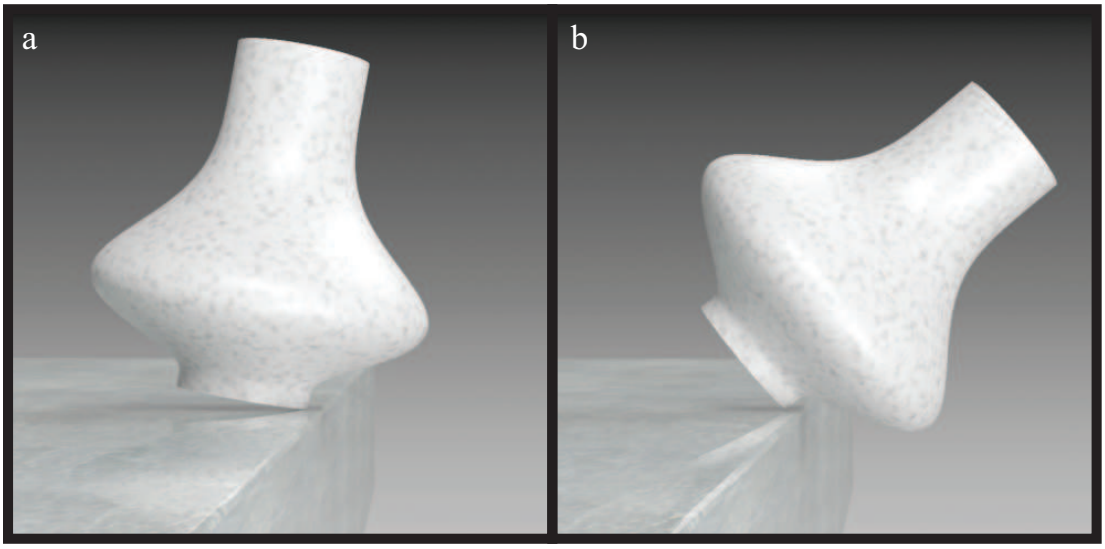

Figure 2.1: Examples of tilted objects where the COM is vertically above (a) or outside (b) the "base" surface.

net torque acting on the object causes it to return to its upright position. However, with a large enough tilt—once the gravity-project COM lies outside the support area (as in Fig. 2.1b)—the object topples over. In everyday situations, rapid judgments such as these allow us to plan appropriate motor movements designed to, say, prevent an object from falling, or perhaps moving quickly out of the way. How good are observers at making such judgments?

In recent work, Samuel and Kerzel (2011) examined the perceptual estimation of balance of planar polygonal objects (see Fig. 2.2). In one experiment, objects consisted of two polygonal parts, and the object rested on one of its vertices (see Fig. 2.2a). Subjects adjusted the orientation of the object until it was perceived to be equally likely to fall to the right or to the left—which, physically speaking, requires that its center of mass (COM) be vertically aligned with its the supporting vertex. Their results showed although subjects could perform this task, they were overly influenced by the eccentricity of the top part of the object (i.e., its lateral shift relative to the lower, larger part), which led to some errors in their judgments. In a second experiment, Samuel and Kerzel used polygonal objects sitting on a supporting edge, with varying degrees of equilibrium states (Fig. 2.2b)—which they defined in terms of where the COM of the object was located relative to the supporting edge (and measured in normalized

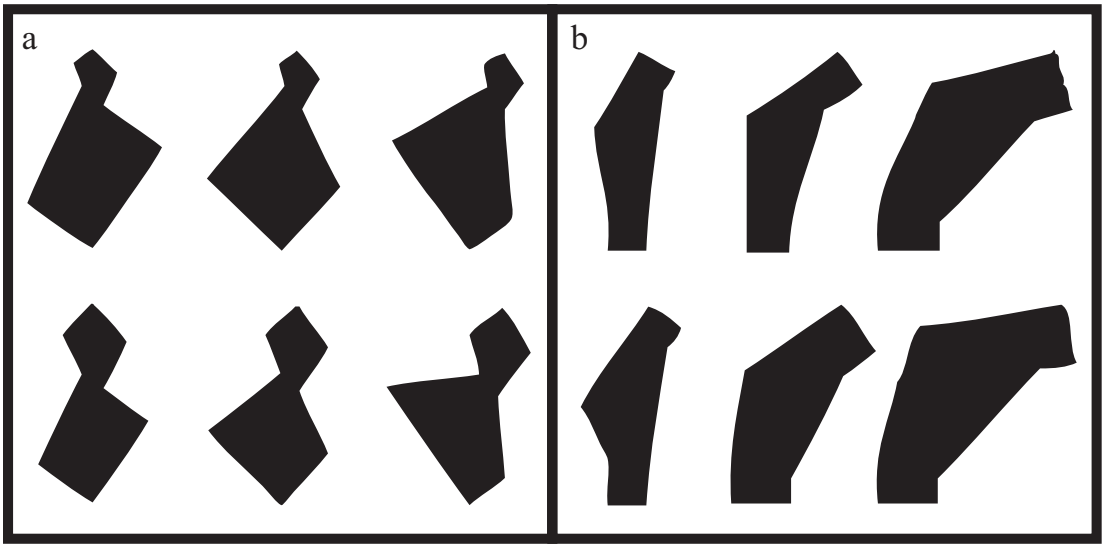

Figure 2.2: Example stimuli adapted from Samuel and Kerzel (2011).

base-length units—as a ratio of the length of the supporting edge). Physically, an object stays upright as long as the gravity-projected COM falls within the supporting edge. Subjects indicated whether a given object (shown resting on the supporting edge) would stay upright, fall to the left, or fall to the right. Their responses exhibited a conservative (or anticipatory) bias—i.e., a bias in the direction of perceiving an object to be unstable, even though physically it would maintain its upright posture. This bias was reduced after the subjects were given specific instructions about the physical definition of stability—and specifically, the importance of the relationship between the COM and the supporting edge. Some bias remained, nevertheless, even after taking into account subjects' own perceptual estimates of the objects' COM. The authors proposed that subjects' responses may be guided by a tendency to stay "on the safe side."

In the current paper, we investigate the perceptual estimation of physical stability of three-dimensional objects. Consider the two objects depicted in Fig. 2.3: Human observers can readily judge from vision alone that the object shown in Fig. 2.3a is in all likelihood more physically stable than the one in Fig. 2.3b. In other words, we naturally expect that the object in Fig. 2.3a would be more resistant to the action of perturbing forces.

A natural way to quantify the above difference in physical stability is in terms of

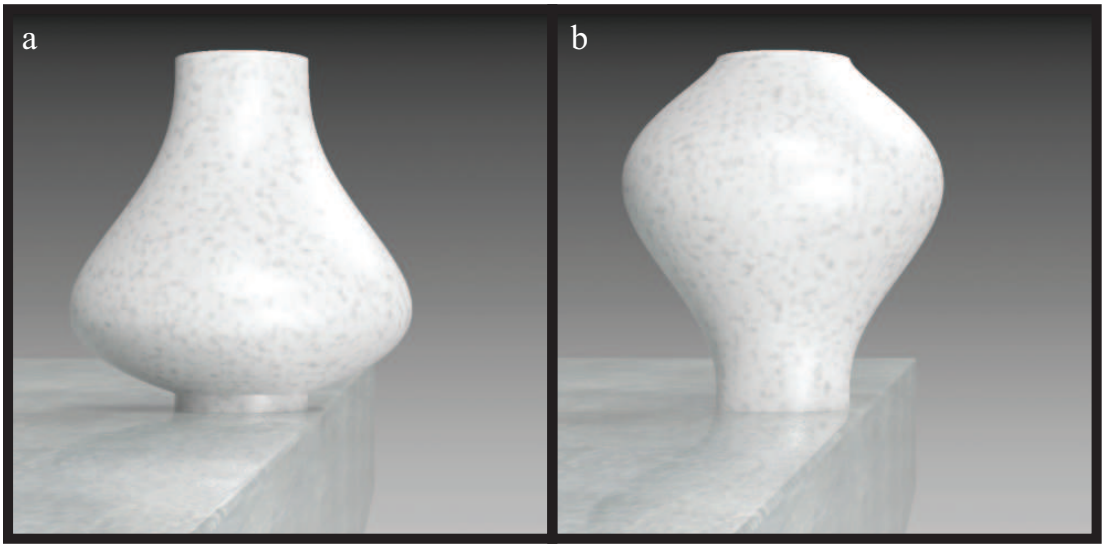

Figure 2.3: Two objects sitting near the edge of a table, one that is very perceptually stable (a) and one that is very perceptually unstable (b).

the "critical angle," i.e., the angle through which an object in a given state of stable equilibrium can be tilted before it will topple over. With a small tilt angle, the net torque acting on the object's COM causes it to return to its upright position (see Fig. 2.4a). However, with a large enough tilt—once the gravity-project COM lies outside the support area (as in Fig. 2.4c) – the object topples over. The boundary between these two regimes is the critical angle of tilt (see Fig. 2.4b). The critical angle thus corresponds to a state of unstable equilibrium in which the object is equally likely to fall over versus return to its upright position. As can be seen in Fig. 2.4b, the critical angle is a function of both the width of the object's base as well as the height of its COM. Physically speaking, then, the object in Fig. 2.3a is more stable because it has a larger critical angle than the one in Fig. 2.3b.

The current study investigates the visual estimation of physical stability of 3D objects, and its dependence on simple shape attributes. We begin with simple conical frustums in Experiment 1, i.e., upright truncated cones, and then consider conical frustums with an attached part. Our experiments measure observers' perceived critical angles, and compare these against the corresponding physical critical angles. This approach to measuring perceived stability has been successfully employed in recent work to show how subjects' estimates of object stability are influenced by visual as well as

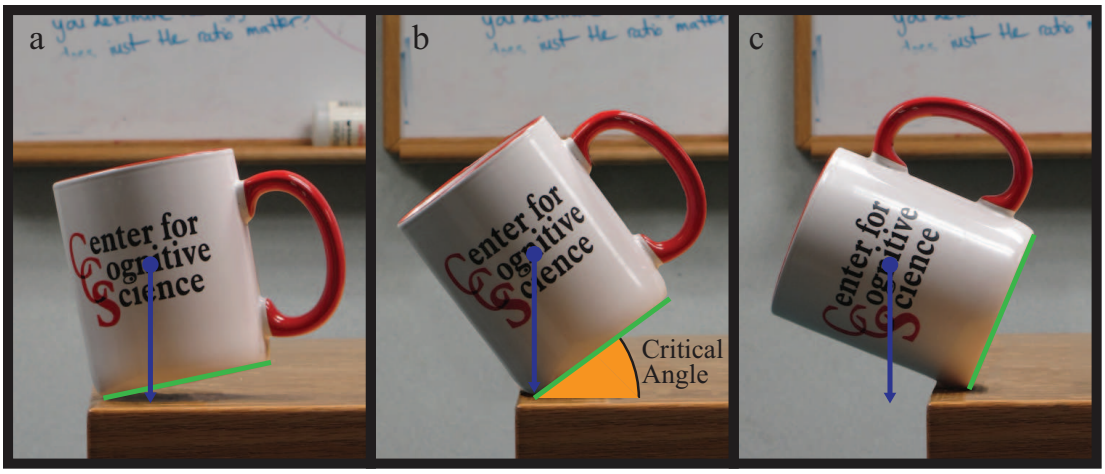

Figure 2.4: Coffee cup with COMs – represented by the blue circle and blue line representing gravity vector – vertically above the base (green) (a), directly over the contact point when the object is at its critical angle (b), and outside the base (c).

vestibular and kinesthetic cues to gravity, when the subjects lie on their sides while judging the physical stability of objects (Barnett-Cowan et al., 2011).

It is clear from the above analysis that the physical notion of stability involves an object's COM in a fundamental way. Previous research has shown that observers use the COM to visually localize a shape—both in perceptual tasks, such as estimating the separation between two dot clusters (Morgan et al., 1990), as well as for saccadic localization (Vishwanath & Kowler, 2003, 2004). Some systematic errors in perceptual estimation of the COM have also been reported in specific contexts, however (Baud-Bovy & Soechting, 2001; Baud-Bovy & Gentaz, 2004; Bingham & Muchisky, 1993).[2] Thus, if the estimation of perceived critical angle is found to deviate from the corresponding physical prediction, one must consider the possibility that perhaps a perceptual mislocalization of the COM is at least in part responsible. In Experiment 1B, we therefore include a task involving the perceptual location of COM for the same set of shapes.

The objects used here are three-dimensional. Research on the visual perception of 3D shape has often focused on the estimation of local geometric properties, such as surface orientation or curvature (Koenderink, 1998; Koenderink, van Doorn, & Kappers,

[2]The term Center of Gravity (COG) is commonly used in this literature. For all practical purposes, the concepts of COG and COM are identical. Physically speaking, the two become distinguishable only in situations where the gravitational field is non-uniform.

1992). Visually estimating the physical stability of a 3D object is, by contrast, a global judgment that requires observers to integrate information across the entire shape. This task thus offers an opportunity to examine how the visual system organizes and integrates local information across a 3D shape. We explore this issue in Experiment 2 using two-part shapes that contain a large conical frustum with a smaller part attached the side. Such two-part objects provide an interesting context where information must be integrated across two different parts to arrive at a single global estimate (e.g., Cohen & Singh, 2006; Denisova et al., 2006).

2.2 Experiment 1A: Perception of Object Stability

Experiment 1 examined the perception of physical stability of conical-frustum objects (Experiment 1A) as well as their perceived COMs (Experiment 1B). Experiment 1A used a critical-angle task to measure perceived physical stability of these objects, while manipulating their aspect ratio and overall volume. The first variable provides a simple manipulation of their shape, whereas the second allows us to test for size invariance—whether, consistent with physical predictions, visual estimates of object stability are a function of intrinsic shape.[3] Experiment 1B examined the visual estimation of the center of mass on the same set of objects by the same group of observers. Although the physical definition of object stability involves the COM in a fundamental way, a natural question is whether observers' perceptual estimates are consistent with the physically correct strategy. The combination of the two experimental tasks allows us to address this question: We can, for example, examine whether any misperception in the physical stability of an object (Exp. 1A) can be explained in terms of a corresponding misperception its COM (Exp. 1B).

[3]Physical stability depends on the mass distribution within an object, which is a function of (i) the object's shape, and (ii) variations in the object's density. It is reasonable to suppose that, in the absence of any information to the contrary, observers make the default assumption of uniform density. In that case, the critical angle is fully determined by the object's 3D shape.

2.2.1 Methods

Observers

Fifteen observers at Rutgers University participated in the experiment. All were naïve as to the purpose of the experiment, and received course credit for their participation.

Apparatus

Stimuli were displayed on a Sony Trinitron 20 inch CRT with a 1024 × 768 pixel resolution at a refresh rate of 120 Hz. Observers were comfortably seated with a chin-rest supporting their head 80 cm from the screen. The experiment was programmed in MATLAB using the Psychtoolbox libraries (Brainard, 1997; Pelli, 1997; Kleiner, Brainard, & Pelli, 2007), including the Matlab OpenGL (MOGL) toolbox for 3D presentation. The rendered scenes were presented stereoscopically using CrystalEyes LCD shutter glasses and E-2 IR emitter by StereoGraphics.

Stimuli and Design

Stimuli were rendered three-dimensional scenes containing a table surface, with a single object placed near its left edge (see Fig. 2.5 for an example scene). Each object was an upright conical frustum, rendered with a wood-grain texture to mimic the visual appearance of a solid block of wood. It could take one of four aspect ratios (Height/Base Diameter): 1, 1.5, 2, and 2.5. Aspect ratio was manipulated in such a way that the overall volume of the frustums was preserved (see Fig. 2.6). The four aspect ratios were repeated with two different volumes that differed by a factor of 2. The heights of the frustums ranged from 4.12 DVA for the shortest frustum with volume = 1 to 11.42 DVA for the tallest with volume = 2. The taper angle of the conical frustums was fixed at 82°.

The experiment was tested using a 4 × 2 factorial design, with aspect ratio and volume as the independent variables (see Fig. 2.6). Each observer made 14 adjustments of critical angle for each combination of aspect ratio and volume, for a total of 112 adjustments. The initial tilt of the object, at the start of each trial, was 0° (vertically

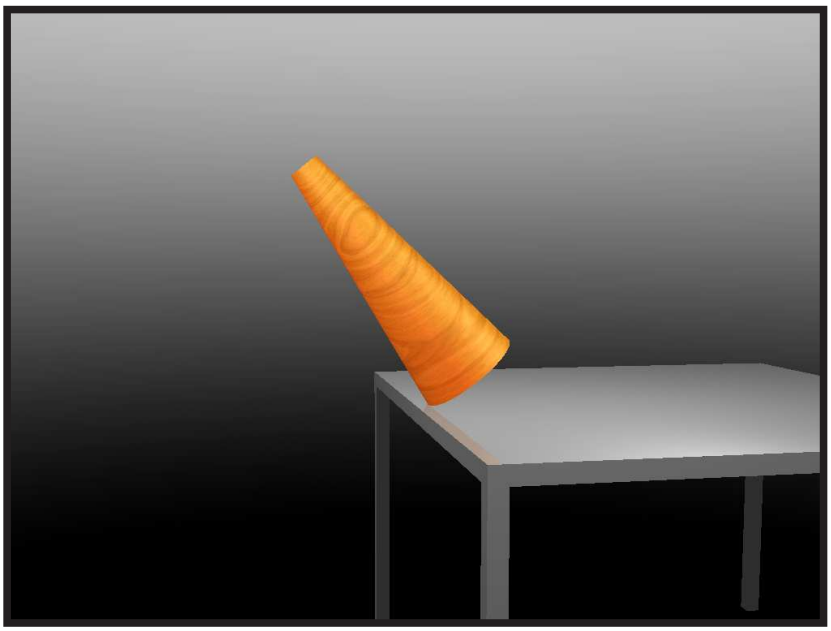

Figure 2.5: Example scene with conical frustum (aspect ratio = 1.5, volume = 2) tilted so that it at its critical angle (38.90°).

upright) on half the trials, and 90° (horizontal, rotated in the direction of the precipitous edge) on the other half.

The method of adjustment was used to estimate observers' perceived critical angle for each object. At the start of each trial, the object near the edge of the table was oriented either vertically or horizontally. Observers used the left and right arrow keys to adjust its angle of tilt. The rotation of the object occurred about the point on its supporting base that was closest to the edge of the table (see Fig. 2.5 for an example of a tilted object).

Observers were instructed to adjust the tilt of the object until it was perceived to be equally likely to fall off the table versus return to its vertical upright position. Pressing and holding the Shift key while pressing the left or right arrows allowed observers to adjust the tilt angle at a faster rate (2°/press instead of 0.2°/press). Releasing the Shift key was useful in making finer adjustments once they were close to the desired angle of tilt.

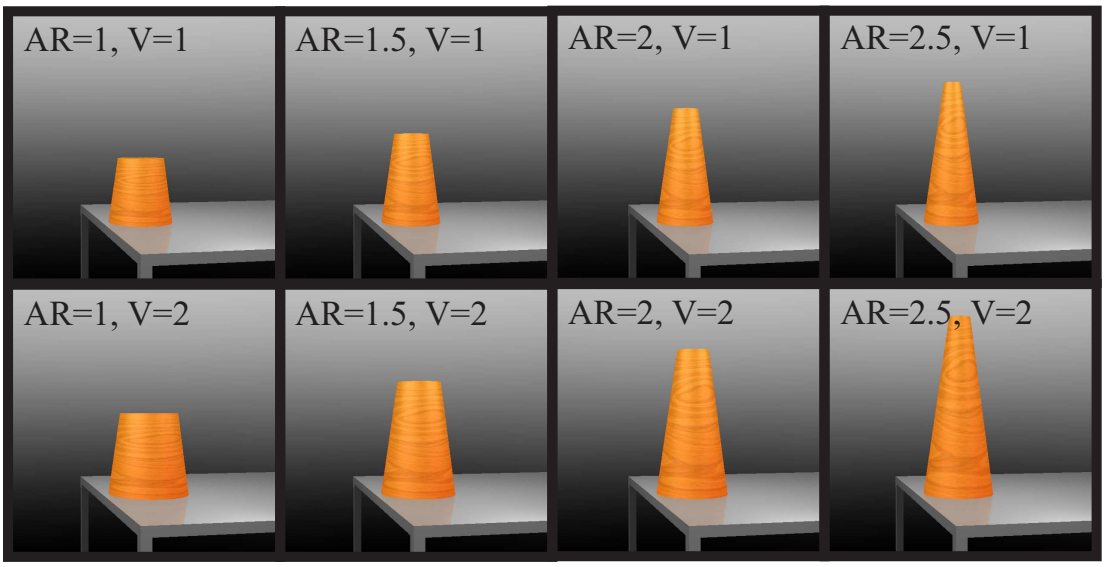

Figure 2.6: Cropped examples for Exp. 1A showing the four aspect ratios of the conical frustums (1, 1.5, 2, and 2.5) and the two volumes (1 and 2). Note that the 3D volumes were equated.

2.2.2 Results

Because we were using observers from an undergraduate subject pool in an adjustment task, we established a criterion to exclude observers with highly noisy data—namely, that the overall SD of their settings (averaged using RMS across all conditions) should not exceed 10°. Data from two observers were excluded based on this criterion.[4] Fig. 2.7 shows the group data across the remaining 13 observers: average critical angle settings are plotted as a function of frustum aspect ratio, for the two volumes and two initial tilt angles. The black dotted curve shows the physical predictions for the critical angle. Overall observers are quite good at estimating the critical angle for the conical frustums. However, on average the critical angle—and hence object stability—tends to be somewhat underestimated for small aspect ratios (short-and-wide shapes) and overestimated for large aspect ratios (long-and-narrow shapes).

A repeated-measures ANOVA revealed a highly significant effect of aspect ratio, $F(3, 36) = 50.89, p < 10^{-12}$. All 13 observers exhibited a significant influence of aspect ratio in their individual data. A small but statistically reliable effect of initial tilt angle

[4]We confirmed, however, that including the data from these two observers does not alter any of our conclusions.

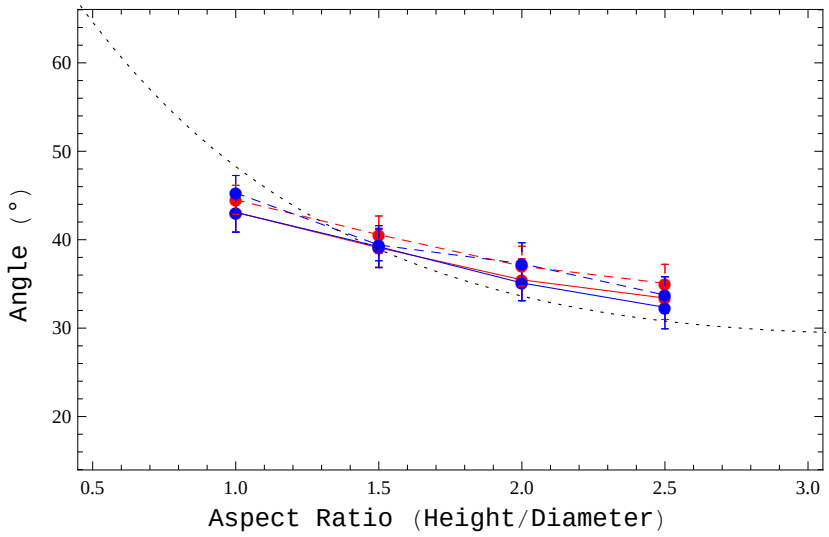

Figure 2.7: Average performance across all observers as an effect of aspect ratio (x-axis), volume (red lines are 1, blue lines are 2), and initial tilt angle (0° are solid, 90° are dashed). The physical critical angle is the black dotted line, plotted as a function of the aspect ratio. Note that for the lowest aspect ratio, observers underestimated the stability, while for the highest aspect ratios, they overestimated the stability.

was also seen in the group data, $F(1, 12) = 7.36, p < .05$. (Only 1 of the 13 observers, S10, exhibited an average difference of more than 5 degrees). Finally, observers' settings showed no reliable dependence on the overall volume of the conical frustum, $F(1, 12) = 1.48, p > .2$. This lack of dependence on volume was evident both in the group data, as well as in individual observers' data (see Fig. 2.8). This suggests that the perception of object stability is unaffected by the overall size of the object and—consistent with the physical definition of critical angle—is a function of its intrinsic shape only. There was no systematic effect of the shape manipulation on participant sensitivity to the critical angle as a function of aspect ratio (see Table 2.1 for within-subject variability).

We next wished to model observers' settings of object stability as a function of object shape (here, aspect ratio). Fig. 2.9 plots the individual data for the 13 observers—averaged over the two levels of volume and initial angle—as well as the group mean. An examination of the individual observer data suggests that the group pattern of underestimating stability for small aspect ratios and overestimating it for large aspect ratios may be the result of two factors: (a) the tendency of different observers to either somewhat overestimate or underestimate object stability – but with no consistent bias

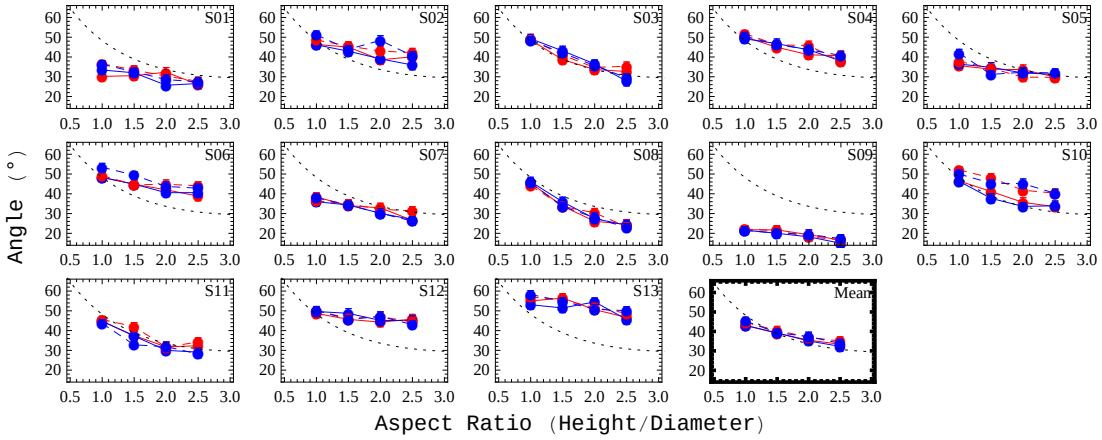

Figure 2.8: Individual observer performance for the critical angle task in Exp. 1A showing the effect of aspect ratio (x-axis), volume (red lines are 1, blue lines are 2), and initial tilt angle (0° are solid, 90° are dashed) on the perceived critical angle. The physical critical angle is the black dotted line, plotted as a function of the aspect ratio.

across observers; and (b) the fact that most observers' data curves exhibit a shallower slope than the physical prediction curve (i.e., a smaller dependency on aspect ratio than physically predicted).

In order to quantify these differences across observers, we fit a model to each individual observer's data, of the form:

$$y = \beta_0 + \beta_1 F(x), \tag{2.1}$$

where x = aspect ratio, y = perceived critical angle, β_0 and β_1 are free parameters, and $F(x)$ is the function that specifies the physical critical angle for each possible aspect ratio—i.e., the function plotted in the dotted black curves in Figs. 2.7, 2.8, & 2.9.[5] The fits of this model thus capture two ways in which individual observers' settings can deviate from the physical predictions. The curves in Fig. 2.9 show the fits to each observer's data. Based on these fits, we summarize each observer's stability settings in

[5]The functional form of the physical critical angle curve (in radians) for conical frustums with taper angles of 82° is as follows:

$$F(x) = \tan^{-1}\left[\frac{3-6x\cot\left(82\frac{\pi}{180}\right)+4x^2\cot\left(82\frac{\pi}{180}\right)^2}{x\left(3-8x\cot\left(82\frac{\pi}{180}\right)+6x^2\cot\left(82\frac{\pi}{180}\right)^2\right)}\right].$$

Table 2.1: Within-subject variability (standard deviation in degrees) for each observer as a function of aspect ratio, collapsed across volume and initial angle. Note that there is no systematic increase or decrease in the standard deviations as a function of the aspect ratio.

Observer	$AR = 2:2$	$AR = 3:2$	$AR = 4:2$	$AR = 5:2$
1	4.211	3.153	5.143	3.234
2	3.723	4.969	7.622	5.270
3	3.333	3.720	3.425	5.162
4	2.553	2.250	3.098	3.151
5	4.877	5.015	5.035	4.829
6	4.443	4.505	4.537	4.913
7	4.422	3.380	3.298	3.745
8	2.615	2.934	3.513	2.183
9	2.350	3.456	2.669	2.518
10	4.155	6.031	7.446	7.029
11	5.430	6.120	5.647	5.535
12	3.772	3.146	2.541	3.276
13	5.717	5.178	4.786	7.195
All	3.963	4.145	4.502	4.454

terms of two variables of interest:

(a) *Overall bias*, B, or the overall degree of underestimation or overestimation in physical stability (i.e., a conservative or liberal bias). We measure bias in terms of the signed difference between the fitted model to an observer's data and the corresponding physical prediction, summed over the four levels of aspect ratio.

$$B = \sum_{i=1}^{4} [\hat{y}(x_i) - F(x_i)] \tag{2.2}$$

(b) *Compression,* C, or the influence of aspect ratio on perceived critical angle relative to the corresponding influence of aspect ratio on the *physical* critical angle. This is simply the fitted parameter β_1 (hence $C = \beta_1$). When $\beta_1 > 1$, an observer's stability settings are more influenced by aspect ratio than is physical stability. When $\beta_1 < 1$, an observer's stability settings are less influenced by aspect ratio than is physical stability.

Fig. 2.10 summarizes each individual observer's data as a point within the 2D space defined by these two variables. Two trends are evident in this plot: First, although

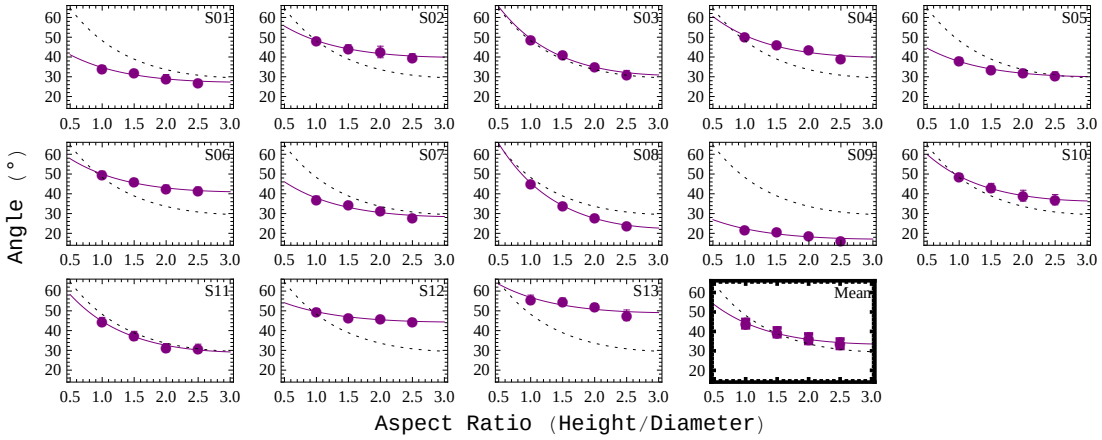

Figure 2.9: Individual observer performance for the critical angle task in Exp. 1A showing the effect of aspect ratio (x-axis), collapsed across volume and initial angle. The solid lines represent the models fit using Equation 2.1. The physical critical angle is the black dotted line, plotted as a function of the aspect ratio.

individual observers exhibit different biases, observers who overestimate stability (positive bias) and those who underestimate stability (negative bias) are roughly balanced. In other words, we see no systematic tendency to underestimate stability in this experiment (i.e., no systematic conservative or anticipatory bias), as was observed in the Samuel and Kerzel (2011) study. Second, the compression parameter C is consistently smaller than 1 – for all but one of the 13 observers – indicating that most observers' critical angle settings are less influenced by aspect ratio than are the corresponding physical predictions. This "compression" can also be seen in the individual data plots in Fig. 2.9, in that most observers' data curves are shallower in slope than the physical prediction curve.

2.2.3 Discussion

In Exp. 1A, we found that object stability – measured by critical angle – was, on average, underestimated for short-and-wide shapes with lower aspect ratios and overestimated for tall-and-narrow shapes with higher aspect ratios. There was an effect of aspect ratio, meaning that as the aspect ratio increased, observers changed their settings to reflect the change in the physical stability. There was no effect of the volume manipulation on the perceived critical angle, suggesting size/volume invariance. This invariance is

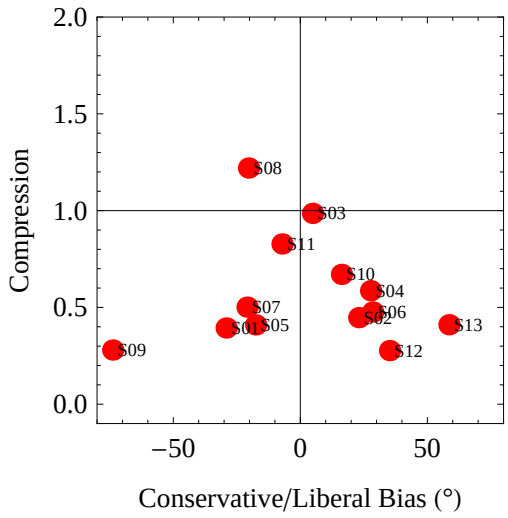

Figure 2.10: Graph illustrating observers' judgments relative to the physical predictions. Overall bias (B) is a measure of a observer's over/underestimation bias, while compression (C) is a measure of the influence of the aspect ratio on judgments. Each red dot represents a single observer (labeled with their ID number). Note that there is no consistent overestimation or underestimation bias across observers and that the observers' responses – as an effect of aspect ratio – were compressed relative to the physical prediction (the majority are < 1.

consistent with the prediction that critical angle judgments should be dependent upon geometric relations between the COM and the supporting base of the object, that stay constant as the volume is increased.

As the individual observers' results illustrated (Fig. 2.9 & Fig. 2.10), some observers had over and underestimation biases, but there was no consistent bias across all observers. In addition, the compression in the observers' responses illustrated that although there was an effect of aspect ratio on their critical angle judgments, the effect was not as large as the physical prediction for the majority of the observers.

2.3 Experiment 1B: Perception of Center of Mass

The pattern of settings in the visual estimation of object stability in Exp. 1A can be summarized as follows: (a) we see no systematic tendency across observers to overestimate or underestimate physical stability; and (b) observers' settings of object stability are consistently influenced to a lesser extent by aspect ratio than the corresponding

physical predictions. As noted above, previous empirical work on the visual estimation of COM has pointed to various biases in the visual estimation of COM (Baud-Bovy & Soechting, 2001; Baud-Bovy & Gentaz, 2004; Bingham & Muchisky, 1993). A natural question, therefore, is whether the observed pattern of biases in the estimation object stability reflects a corresponding misperception of the objects' COM. Specifically: (1) are perceptual COM estimates *also* less influenced by aspect ratio than are physical COMs? and (2) do individual observers who tend to underestimate object stability when judging the critical angle correspondingly perceive the COM of the frustum objects to be *higher* than it actually is (and vice versa)? Experiment 1B addresses these questions by obtaining visual estimates of COM on the same set of 3D objects from the same group of observers.

2.3.1 Methods

Observers

The same group of observers participated as in Experiment 1A.

Apparatus

The apparatus was the same as Experiment 1A.

Stimuli and Design

Observers participated in Exp. 1B after completing Exp. 1A and taking a short break. The method of adjustment was used to estimate their perceived COM for the same set of conical frustum shapes used in Experiment 1A. However, unlike the opaque surfaces in Exp. 1A, the conical frustums in Exp. 1B were rendered with a transparent surface through which the axis of symmetry of the frustum was visible – shown as a solid gray line (see Fig. 2.11). Along this line, the vertical height of a small red dot (technically, a sphere in the 3D rendered scene) could be adjusted by the observer.

The experiment was conducted using a 4×2 factorial design, with aspect ratio and volume as the independent variables and the same levels as in Experiment 1A. Each

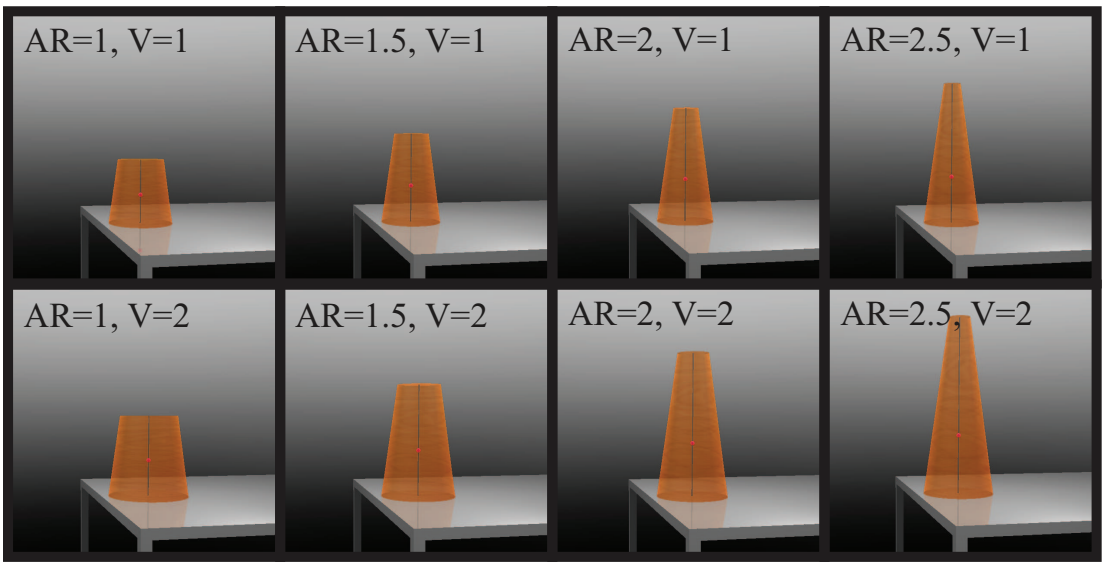

Figure 2.11: Cropped examples for Exp. 1B showing the four aspect ratios of the conical frustums (1, 1.5, 2, and 2.5) and the two volumes (1 and 2). Note that the 3D volumes were equated. In addition, the observer's COM judgment (red sphere inside object) was constrained to the vertical axis of symmetry (solid gray line).

observer made 10 adjustments of COM height for each combination of aspect ratio and volume, for a total of 80 trials. The initial location of the probe dot, at the start of each trial, was at the top of the object on half the trials, and at the bottom on the other half.

In the instructions to the observers, the concept of the COM of the object was explained by describing a serving tray, and noting the existence of a central point where the tray could be balanced on a single finger. Observers generally found this concept quite intuitive. They were then instructed that their task was to similarly localize the center or balance point of three-dimensional objects.

To make their COM setting, observers used the up and down arrow keys to adjust its vertical position along the axis of symmetry. They were instructed to adjust the height of the probe dot to localize the perceived COM of the object. As in Experiment 1A, pressing the Shift key allowed them to make faster adjustments, so observers were instructed to take advantage of the faster adjustment to get a coarse estimate of the COM, and then to release the Shift key to make a finer, final adjustment.

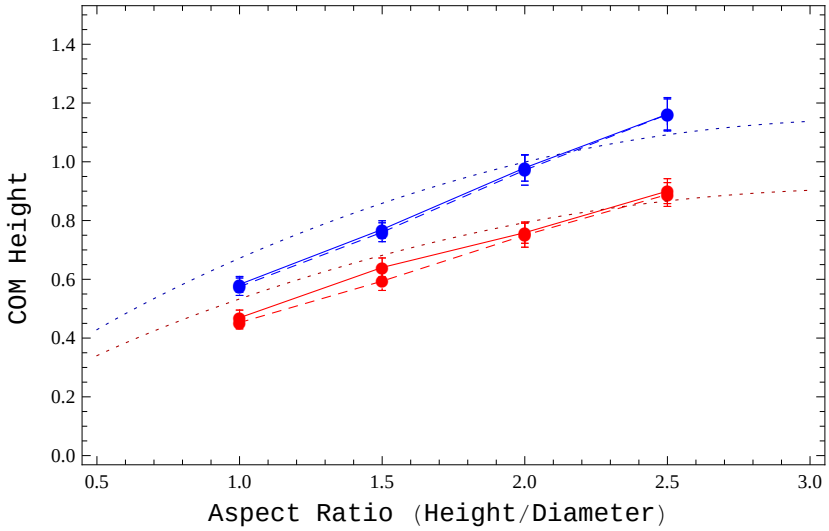

Figure 2.12: Average COM judgments across all observers as an effect of aspect ratio (x-axis), volume (red lines are 1, blue lines are 2), and initial COM start location (solid lines are estimates that began at the bottom of the object, dashed are estimates that began at the top). The physical COM locations for the two volumes are the dotted lines (red lines are volume = 1, blue lines are volume = 2), plotted as a function of the aspect ratio. Note that for the lowest aspect ratios, observers underestimated the COM height, while for the highest aspect ratio, they overestimated the COM height.

2.3.2 Results

Since our goal is to examine the degree of mutual consistency between settings of object stability and settings of COM, we only include data from the 13 observers whose stability data were reported in Experiment 1A.[6] Fig. 2.12 shows the group data across the 13 observers: the average COM height settings are plotted as a function of frustum aspect ratio, for the two volumes and two initial probe locations. The two dashed curves show the physical predictions of the COM height for the two different volumes. (The COM heights are of course *not* invariant to the size of the object.) Although the deviations from the physical COM predicts are not large, for most aspect ratios, observers tend to exhibit an overall tendency to underestimate the height of the COM (i.e., to perceive the COMs as being located slightly lower within the frustums than they actually are).

[6]We note, moreover, that the same two observers who were excluded from the Exp. 1A analysis also produced very noisy data in the COM task as well.

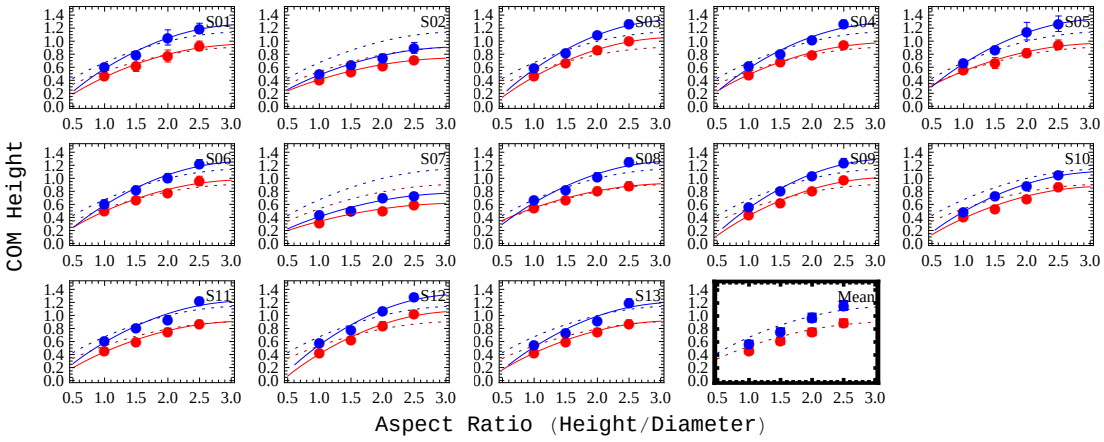

Figure 2.13: Individual observer performance for the COM task in Exp. 1B. Data have been collapsed across initial COM height, so these show the effect of aspect ratio (x-axis) and volume (red lines are 1, blue lines are 2) on the perceived critical angle. The physical COM locations for the two volumes are the dotted lines (red lines are volume = 1, blue lines are volume = 2), plotted as a function of the aspect ratio.

A repeated-measures ANOVA on the group data revealed a highly significant effect of aspect ratio, $F(3, 36) = 275.7, p < 10^{-20}$. All 13 observers exhibited a highly significant influence of aspect ratio in their individual data (see Fig. 2.13). Similarly, there was a highly significant influence of volume on observers' COM settings, $F(1, 12) = 235.5, p < 10^{-8}$, with all observers exhibiting a significant influence in their individual data. The effect of the initial location of the probe dot was not significant, $F(1, 12) = 2.54, p > .1$. None of the interactions were significant and there was no systematic effect of the shape manipulation on participant sensitivity to the critical angle as a function of aspect ratio (see Table 2.2 for within-subject variability).

In order to compare observers' COM settings to their estimates of object stability from Experiment 1A, we convert their observed COM settings into the critical angles they *would* generate, were the observers using these COM estimates in the physically correct manner to estimate the critical angles. This transformation allows for the direct comparison of the results from the two experiments to determine if observers are using the COM in a physically-consistent manner when judging the object's critical angle. These "implied critical angles" can simply be calculated using the radius of the object's

Table 2.2: Within-subject variability (standard deviation of COM height) for each observer as a function of aspect ratio and volume, collapsed across initial height.

Observer	$AR = 2:2$ $V = 1$	$AR = 3:2$ $V = 1$	$AR = 4:2$ $V = 1$	$AR = 5:2$ $V = 1$	$AR = 2:2$ $V = 2$	$AR = 3:2$ $V = 2$	$AR = 4:2$ $V = 2$	$AR = 5:2$ $V = 2$
1	0.0520	0.1475	0.1479	0.1199	0.0865	0.0619	0.1870	0.1258
2	0.0402	0.0448	0.0524	0.0572	0.0408	0.0577	0.0841	0.1346
3	0.0451	0.0484	0.0484	0.0724	0.0505	0.0355	0.0360	0.0837
4	0.0266	0.0346	0.0591	0.0678	0.0251	0.0474	0.0413	0.0945
5	0.0679	0.1375	0.0939	0.1105	0.0447	0.0627	0.2179	0.1923
6	0.0600	0.0657	0.0671	0.1137	0.0981	0.0811	0.1008	0.0985
7	0.0905	0.0907	0.0420	0.0463	0.0978	0.0415	0.0869	0.0800
8	0.0218	0.0589	0.0777	0.1066	0.0287	0.0603	0.0947	0.0968
9	0.0390	0.0462	0.0383	0.0590	0.0419	0.0717	0.0589	0.0987
10	0.0401	0.0498	0.0853	0.0735	0.0441	0.0671	0.0856	0.0641
11	0.0459	0.0443	0.0873	0.0740	0.0330	0.0712	0.0924	0.0779
12	0.0506	0.0456	0.1024	0.0199	0.0407	0.0376	0.0493	0.0877
13	0.0257	0.0443	0.0563	0.0819	0.0470	0.0711	0.0463	0.1000
All	0.0462	0.0665	0.0736	0.0772	0.0524	0.0588	0.0908	0.1028

base (R_{base}) and the height of the observer's COM response (h_{COM})[7]:

$$\Theta_{CA} = ArcTan\left(\frac{R_{base}}{h_{COM}}\right) * \frac{180}{\pi} \tag{2.3}$$

The group data for these implied critical angles are plotted in Fig. 2.14. Individual performance is plotted in Fig. 2.15. (In these plots, there is only one prediction curve because the physical critical angles are invariant to object size. Consistent with this prediction, a repeated-measures ANOVA on these transformed data revealed that there was no longer a main effect of volume, $F(1, 12) = 2.02, p > .1$.)

As expected, the group COM data replotted in terms of implied critical angle now exhibit, for all aspect ratios but the highest, a systematic tendency to overestimate the critical angle. (By definition, an underestimation an object's COM height automatically implies an overestimation of its critical angle; recall Fig. 2.3). In other words, were observers to use their perceptually estimated COMs in the physically correct way to

[7]Note that since the objects in these experiments have been constrained to have constant volume, the base radius (R_{base}) for a conical frustum with a taper angle of 82° is as follows:

$$R_{base}(AR, V) = \frac{\left(\frac{3}{2}\right)^{1/3} V^{1/3}}{\left(3AR\pi - 6AR^2\pi\tan\left(82\frac{\pi}{180}\right) + 4AR^3\pi\tan\left(82\frac{\pi}{180}\right)^2\right)^{1/3}}$$

Plugging this into Eq. 2.3, the implied critical angle (in degrees) for an observer's response (h_{COM}) is:

$$CA_i(AR, V, h_{COM}) = \tan^{-1}\left(\frac{\left(\frac{3}{2}\right)^{1/3} V^{1/3}}{h_{COM}\left(3AR\pi - 6AR^2\pi\tan\left(82\frac{\pi}{180}\right) + 4AR^3\pi\tan\left(82\frac{\pi}{180}\right)^2\right)^{1/3}}\right) * \frac{\pi}{180}$$

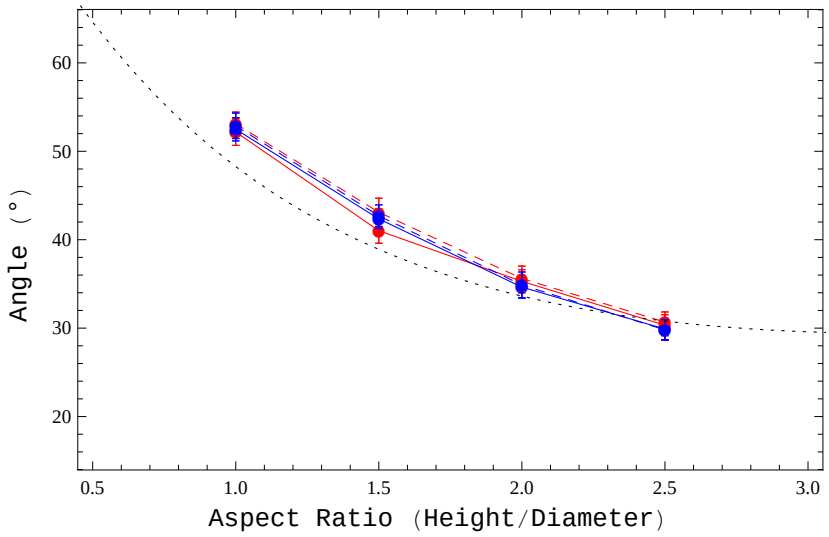

Figure 2.14: Average COM judgments as implied critical angles plotted as a function of aspect ratio (x-axis), volume (red lines are 1, blue lines are 2), and initial COM start location (solid lines are estimates that began at the bottom of the object, dashed are estimates that began at the top). The physical critical angle is the black dotted line, plotted as a function of the aspect ratio.

estimate the critical angle, their stability data from Exp. 1A should look like Fig. 2.14. How does this compare to the settings of critical angle they actually made in Experiment 1A? A comparison of the implied critical angles in Fig. 2.14 with observers' settings of perceived critical angle in Fig. 2.7 suggests that the two are not mutually consistent. For instance, the underestimation of the perceived COMs seen in Fig. 2.13 implies that the critical angles for frustums with the smallest aspect ratio (short-and-wide shapes) should be systematically overestimated. But we see in Fig. 2.7 that observers' critical angle settings for these frustums were actually underestimated. So the group data in the critical angle task seem not to be consistent with a strategy of deriving critical angles from perceived COMs.

We next examine the degree of consistency between the two sets of results at the level of individual observers. As in Experiment 1A, we summarize individual observers' performance using the two parameters of compression (from Eq. 2.1) and bias (from Eq. 2.2) using the implied critical angles (see Eq. 2.3). Fig. 2.16 shows the fits of this model to individual observers' implied critical angle data in Exp. 1B.

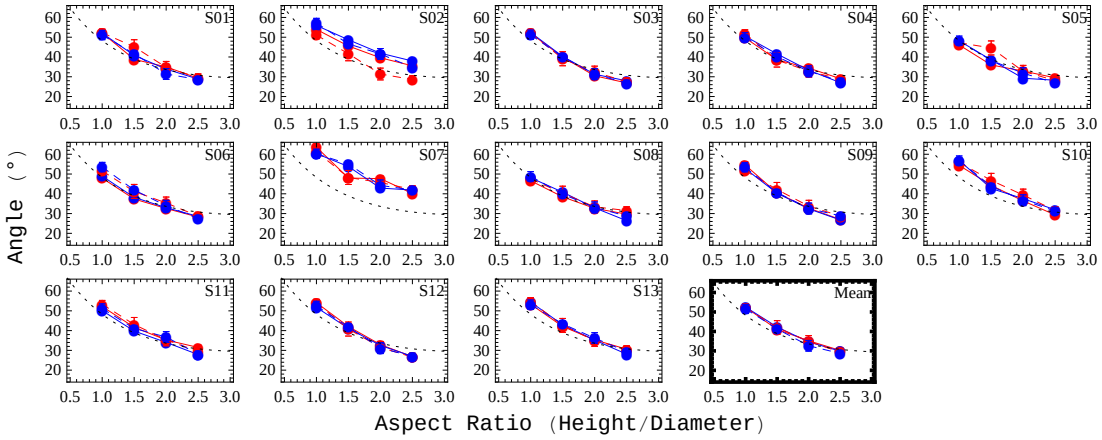

Figure 2.15: Individual observers' implied critical angle performance as a function of aspect ratio (x-axis), volume (red lines are 1, blue lines are 2), and initial COM start location (solid lines are estimates that began at the bottom of the object, dashed are estimates that began at the top). The physical critical angle is the black dotted line, plotted as a function of the aspect ratio.

As before, we summarize each observer's data in terms of two variables: compression and overall bias. The blue dots in Fig. 2.17 summarize each individual observer's data as points within the 2D space defined by these two variables. A visual comparison with the corresponding data from Exp. 1A (red dots) indicates large differences between the two. First, in contrast to Exp. 1A where the compression parameter was consistently smaller than 1, in the COM experiment, this fitted parameter is larger than 1 for all 13 observers. Thus, in visually estimating the COM of conical frustums, observers' settings were influenced to a *greater* extent than would be physically predicted by the aspect ratio of the frustums. Second, there is small overall bias in the positive direction (the overall bias is positive for 10 of the 13 observers). In other words, observers tended to underestimate the height of the COM, which in turn is consistent with an overestimation of the critical angle entailed by these COMs.

In Fig. 2.17, we compare the results of Exp. 1A and Exp. 1B. There was a large reduction in the bias parameter for the majority of observers (observers were more accurate) when they were asked to judge the objects' COMs. Observers who tended to underestimate object stability when judging the critical angle also did not appear to perceive the COM of the frustum objects to be higher than it actually was (and

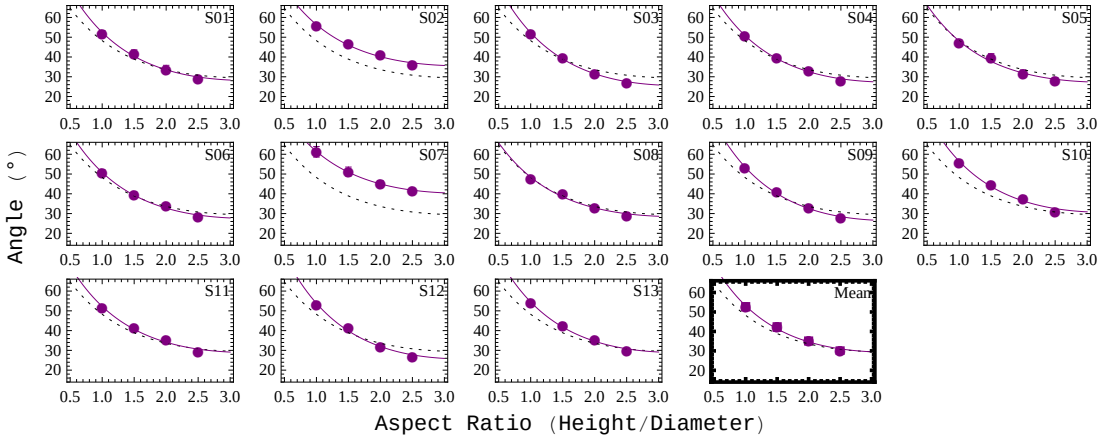

Figure 2.16: Individual observers' implied critical angle performance, collapsed across initial COM height and volume. The solid lines represent the fitted models for each individual observer that were used to determine their bias and compression. The physical critical angle is the black dotted line, plotted as a function of the aspect ratio.

vice versa), which is inconsistent with the critical angle results. Thus, the majority of observers were much closer to the physical prediction in the COM task than in the critical angle task.

Observers had no compression – in fact, all observers had an expansion of the influence of shape on their judgments, because the compression parameter was greater than 1. So, aspect ratio had a greater effect on their perceptual COM estimates than would be predicted by the physical COMs. This suggests that individuals were using different perceptual stability estimation strategies in the two tasks.

2.3.3 Discussion

In Exp. 1B, we found that the same observers from Exp. 1A, whose responses were compressed relative to the physical prediction and who exhibited no systematic bias, now had responses that were much closer to the physical prediction. For all 13 observers, the compression in their responses was greater than 1, indicating that they put a larger emphasis on the aspect ratio when making their COM judgments, than would be predicted physically. This is in contrast to their responses on the critical angle task, where the compression was less than 1.

In addition, the magnitude of bias was consistently smaller in Exp. 1B (i.e., accuracy

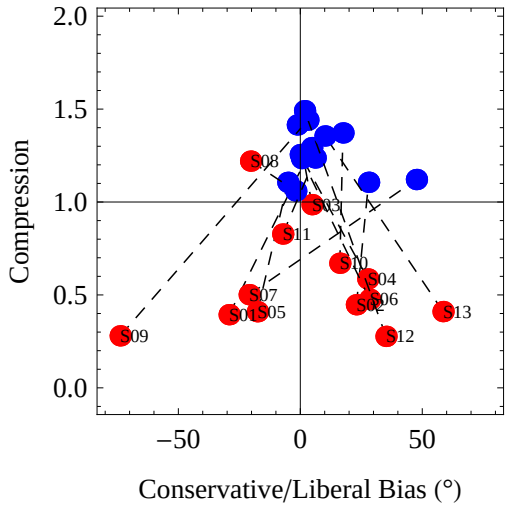

Figure 2.17: Compression and overall bias for model fits in Exp. 1A (red points) and Exp. 1B (blue points). The dashed lines connect the model fits for individual observers.

is better in the COM task than stability task) and the sign of bias is not balanced across all observers in Exp. 1B; unlike Exp. 1A, the bias tended to be more in the positive direction. However, is the sign of the bias generally preserved across the two tasks (i.e., do observers with positive bias in the implied critical angles from the COM task also tend to have positive bias in the critical angle settings)?

2.4 Experiment 2: The Role of Parts

One of the findings in Exp. 1 was that when the shape of an object is changed (such as the manipulation of aspect ratio), observers' stability estimates also change, but not quite as much as would be physically predicted. (For stability judgments, the compression parameter was consistently smaller than 1.) In Experiment 2, we consider a different shape change, namely, the addition of a protruding part to a conical frustum.

Exp. 2 was designed to further investigate the importance of shape in this adjustment task and to study the influence of part structure on the perceived stability of shape. Adding parts to a shape will shift the object's COM in the direction of the added part(s), thereby altering the object's stability, but how well do observers use this additional information when judging stability?

2.4.1 Methods

Observers

Twelve observers at Rutgers University participated in the experiment. All were naïve as to the purpose of the experiment, and received course credit for their participation.

Apparatus

The apparatus was the same as Exp. 1A & 1B.

Stimuli and Design

Stimuli were presented in the same rendered scene as Exp. 1A & 1B. The primary manipulation was the addition of a part onto the object – defined using a bivariate Gaussian distribution. The object was positioned on the table so that the part could face towards the edge of the table or away – towards the center of the table (see Fig. 2.18). Therefore, we had three part conditions, a baseline "no part" condition and two conditions with the attached part: "part towards" and "part away". The base shapes could have one of three aspect ratios (Height/Base Diameter): 1.5, 2, and 2.5. The conical frustum with an aspect ratio of 1 was not used because it was too short to accommodate the attached part. The taper angle of the conical frustums was fixed at 82°.

The method of adjustment was used to estimate observers' perceived critical angle for each object. Observers used the left and right arrow keys to adjust its angle of tilt until the object was at its perceived critical angle. As in the other experiments, the rotation of the object occurred about the point on its supporting base that was closest to the edge of the table.

We used a 3 × 3 factorial design, with aspect ratio and part condition ("no part", "part towards", and "part away") as the independent variables. Each observer made 20 adjustments of critical angle for each combination of aspect ratio and part condition, for a total of 180 adjustments. The initial tilt of the object, at the start of each trial, was 0° (vertically upright) on half the trials, and 90° (horizontal, rotated in the direction

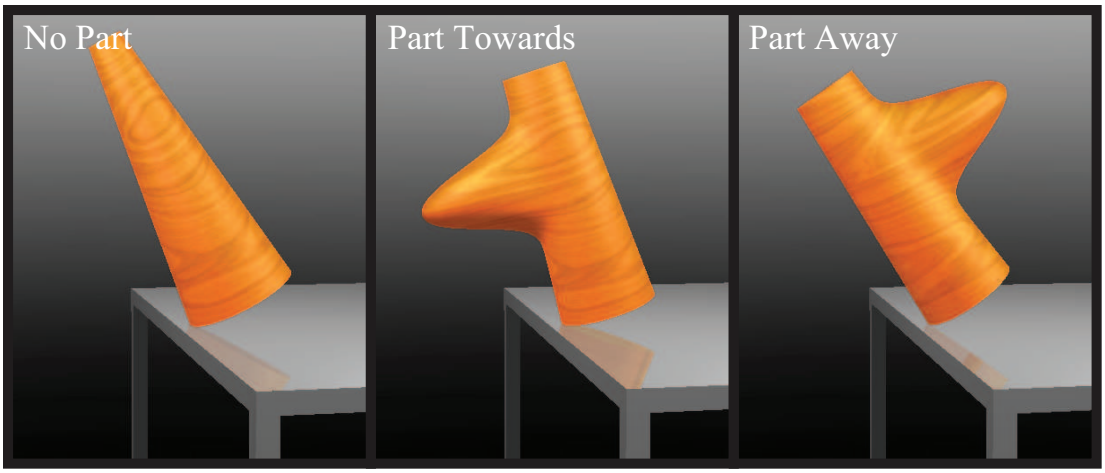

Figure 2.18: Cropped examples for Exp. 2 showing representative stimuli with no part (left), with the part facing towards the edge of the table (center), and with the part facing away from the edge of the table (right).

of the precipitous edge) on the other half.

2.4.2 Results

Observer performance for the part conditions was compared to the physical predictions for the different objects. Note that the physical predictions for the part conditions ("part towards" and "part away" from the edge) will be different from the "no part" condition because the presence of the part will shift the COM of the object towards the additional mass of the part. As shown in Fig. 2.19, the "no part" condition exhibits a similar performance trend as in Exp. 1A (underestimation of stability for lower aspect ratios and overestimation for higher aspect ratios). In addition, we see a shift in the perceived critical angles for conditions where a part is present, consistent with the physical predictions – that is, higher perceived stability when the part faces away from the edge and lower perceived stability when the part faces towards the edge[8]. In addition, the higher aspect ratios exhibit a systematic overestimation, while the lower aspect ratios exhibit underestimation (consistent with the aspect ratio-based over and underestimation Exp. 1A).

[8]It should be noted that asymmetric objects, such as the frustum with part, have different critical angles in different directions. Here we are referring here to the objects' stability in the direction in which they are being tilted, namely, directly towards the precipitous edge of the table.

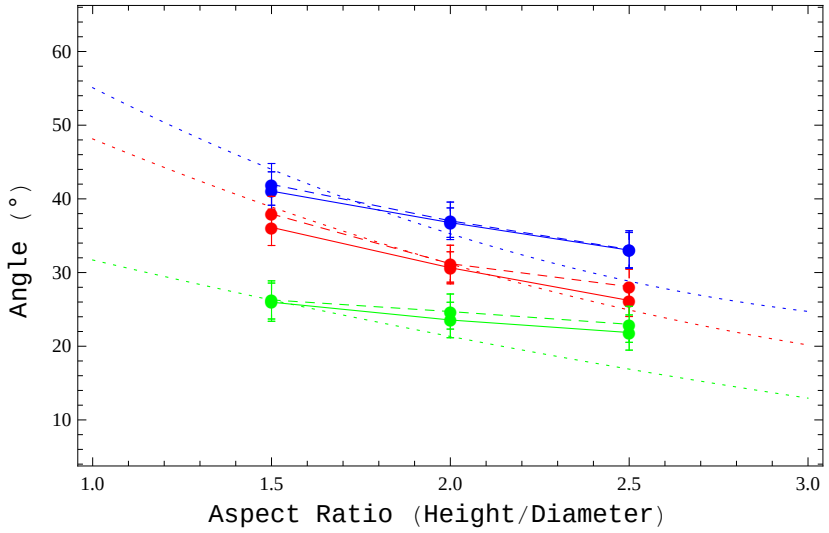

Figure 2.19: Group results for Exp. 2, illustrating the effects of aspect ratio, part condition (red = "no part", green = "part towards", and blue = "part away"), and initial tilt angle (solid = 0°, dashed = 90°). The dotted lines illustrate the physical critical angle curves for the respective part conditions.

As was the case in the previous experiments, there was individual variability, with some observers having an overestimation bias and others an underestimation bias (see Fig. 2.20). We fitted model curves to the observers' critical angle settings – using the model fitting technique described in Exp. 1A – for the three part conditions and overlaid these curves on the observers' data (see Fig. 2.21). The majority of the observers responded in the predicted manner, taking into account the presence of the part. Next we wished to compare the perceptual effect of the part to its physical effect on the objects' stability.

To evaluate the extent to which observers take into account the presence of the part the presence of the part (regardless of any stability biases), we measured the relative influence of the part. First, we define the influence of a part to be the difference in critical angle between the "part away" and "part towards" conditions. We define the relative influence to be the ratio of perceptual influence to the physical influence of a part. If observers perfectly take into account the contribution of the part when judging perceived stability, then the relative influence for any given aspect ratio should be 1 (i.e., the magnitude of the perceptual influence is equal to the physical influence). If

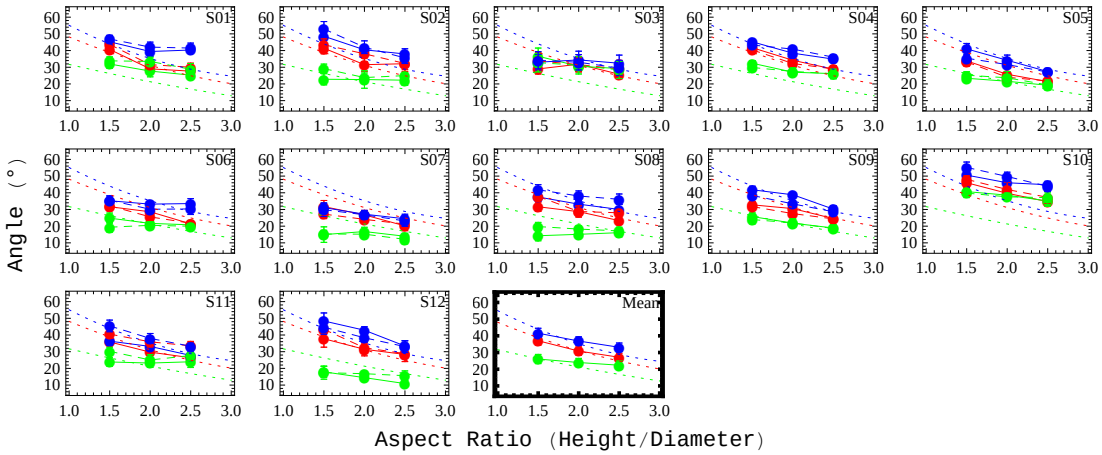

Figure 2.20: Individual results for Exp. 2 illustrating the effects of aspect ratio, part condition (red = "no part", green = "part towards", and blue = "part away"), and initial tilt angle (solid = 0°, dashed = 90°). The dotted lines illustrate the physical critical angle curves for the respective part conditions.

there is perceptual down-weighting of the part, the relative influence should be less than 1 (an influence of 0 would mean that the presence of the part does not affect an observer's stability settings at all). Alternatively, if the observer gives too much emphasis on the part when judging the overall stability of the object, then we would expect a relative influence greater than 1.

Fig. 2.22 shows the relative influence for each individual observer for the three aspect ratios. Seven of the thirteen observers consistently down-weighted the influence of the parts, three consistently over-emphasized the influence, and two wavered around the unity line. On average, there was a slight down-weighting of the influence of the presence of the part on perceived stability, consistent with a robust-statistics approach used to determine the influence of a potentially separate part on global estimation (Cohen & Singh, 2006; Denisova et al., 2006).

2.5 Conclusion

The experiments presented here suggested that people can use purely visual information to infer the forces acting upon 3D objects in a scene. Using these inferences, observers were able to make stability judgments using either a critical angle (Exp. 1A and 2) or

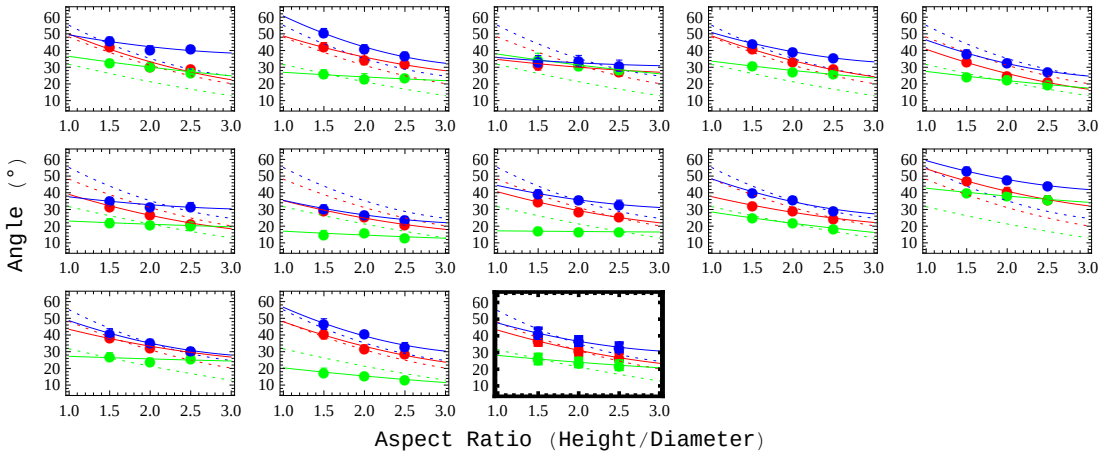

Figure 2.21: Individual results for Exp. 2 with data collapsed across the initial tilt angle. The red lines are the "no part" conditions, the green lines are the "part towards" conditions, and the blue line are the "part away" conditions. The dashed lines represent the model fits to the different conditions. The dotted lines illustrate the physical critical angle curves for the respective part conditions.

COM (Exp. 1B) task.

In Exp. 1A, we showed that, on average, observers are quite accurate when making their judgments of object stability using a critical angle task. Their visual judgments of stability were invariant to size/volume, and appeared to be a function of only shape. There was a bias to underestimate the stability of low aspect ratio shapes and overestimate the stability of high aspect ratio shapes in the average data; however, this was due to: (i) some individual variability in bias (with some observer underestimating stability, others overestimating it) and (ii) a compression in the data curves relative to the physical predictions (i.e., a smaller perceptual influence of aspect ratio than physically predicted). Contrary to recent results with 2D shapes, stability judgments were not always "on the safe side" (Samuel & Kerzel, 2011).

The critical angle results were contrasted with the COM estimates in Exp. 1B, showing that observers were much closer to the physical prediction when they were asked to judge the center of mass of the same objects. There was much less bias (observers were more accurate) and the compression observed in Exp. 1A – in observers' stability estimates as a function of aspect ratio – was no longer present. Observers settings of center of mass were inconsistent with their settings of critical angle and they did

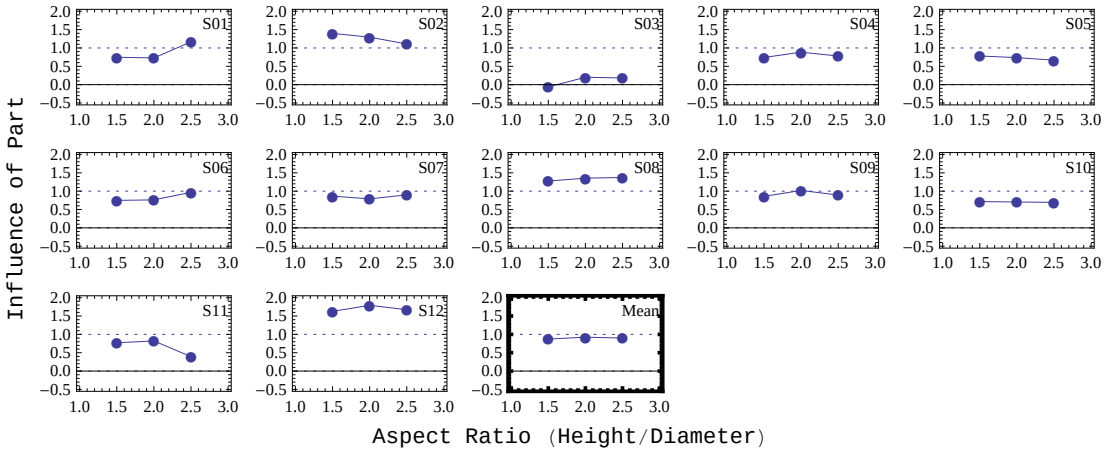

Figure 2.22: Plots showing the relative influence of the part for individual observers. The dotted black horizontal line identifies the unity line, where observer performance would lie if they perfectly utilized the contributions of the parts. The solid black horizontal line illustrates the situation where there is no influence of the presence of the parts on perceived stability.

not appear to rely on the COM in making judgments of physical stability. Therefore, comparing the results, observers do not seem to be using COM – at least not in the physically correct manner – when making judgments of object stability.

Finally, in Exp. 2, we found that observers were able to combine information from different parts of a shape in order to judge the physical stability of objects with multiple parts. However, even though on average observers did a very good job taking into account the contribution of the part to the stability of the shape, there was some down-weighting of the relative influence of the parts.

Chapter 3

Perception of the physical stability of asymmetrical three-dimensional objects

3.1 Introduction

In addition to estimating the *current properties* of objects and surfaces based on visual inputs, human observers are very good at predicting how objects are likely to behave in the near future. For example, observers can visually extrapolate the trajectory of a moving object (Becker & Fuchs, 1985; Pavel et al., 1992; Verghese & McKee, 2002), and predict where an object that disappears behind an occluder is likely to re-emerge from (Scholl & Pylyshyn, 1999; Graf et al., 1995; Shah et al., 2012). Even more impressive are cases where observers can make visual predictions about object behavior based on the inference of unseen forces, such as momentum (S.-H. Kim, Feldman, & Singh, 2012; Newman et al., 2008), gravity, and support relations (Barnett-Cowan et al., 2011; Hamrick, Battaglia, & Tenenbaum, 2011; Samuel & Kerzel, 2011). Indeed, infants as young as 8 months of age have been shown to be visually sensitive to support relations and gravity; and are surprised when shown a scene in which an inadequately supported object appears to maintain its position in space (Baillargeon & Hanko-Summers, 1990; Baillargeon et al., 1992). Predictions such as these rely on a "causal understanding" of the scene based on visual information (Cooper et al., 1995).

Traditional work on naïve physics has documented various ways in which people's intuitions are often inconsistent with Newtonian mechanics (e.g., McCloskey et al., 1980, 1983). However, when shown dynamic "real-time" displays simulating physical behavior, observers can be quite accurate at detecting deviations from Newtonian mechanics (Kaiser et al., 1985, 1992; Proffitt & Gilden, 1989). More recent work has also demonstrated that observers correctly take into account acceleration due to gravity –

consistent with Newton's laws of motion – when timing their hand movements in order to catch a falling ball (McIntyre et al., 2001; Zago & Lacquaniti, 2005). These results are also consistent with our day-to-day experiences of manipulating and interacting with objects, where we are generally quite good at predicting the physical behavior objects and guiding our motor actions.

In a recent study on the perception of object stability, Samuel and Kerzel (2011) used planar polygonal objects, shown sitting on a supporting edge/base, with varying degrees of "imbalance" – measured in terms of where the COM of the object lies relative to the center of the supporting edge (including the possibility of being outside this supporting base – in which case the object would *not* physically stay upright). Subjects indicated whether a given object (shown resting on its supporting edge) would stay upright or fall over. Their responses exhibited a conservative (or anticipatory) bias – i.e., in the direction of perceiving an object to be unstable, even though physically it would maintain its upright posture. These results were interpreted in terms of a conservative tendency to keep judgments of object stability stay "on the safe side."

In the current paper, our interest is in the visual estimation of the degree of physical stability of 3D objects which are in stable equilibrium (in the sense that, if left unperturbed, they would maintain their current position). For example, the two objects in Fig. 3.1 are both in stable equilibrium (in each case, the COM of each object is directly above the center of a circular base). However, it is visual apparent that the object in Fig. 3.1a is physically more stable than the one in Fig. 3.1b. In other words, based on vision alone, one would naturally expect that the object in Fig. 3.1a is more resistant to the action of perturbing forces than is the object in Fig. 3.1b. One natural way of capturing object stability, therefore, is in terms of the extent to which an object can be tilted away from its "upright" position of stable equilibrium, and maintain an unstable equilibrium at that position where it was released. We refer to this angle of tilt as the *critical angle* (see Fig. 3.2). At this angle of tilt, the center of mass (COM) of the object is directly vertically above the point of contact on the base, around which the object is being rotated (see Fig. 3.2b). By definition, any tilt greater in magnitude than this critical angle will result in the object toppling over, rather than returning to its

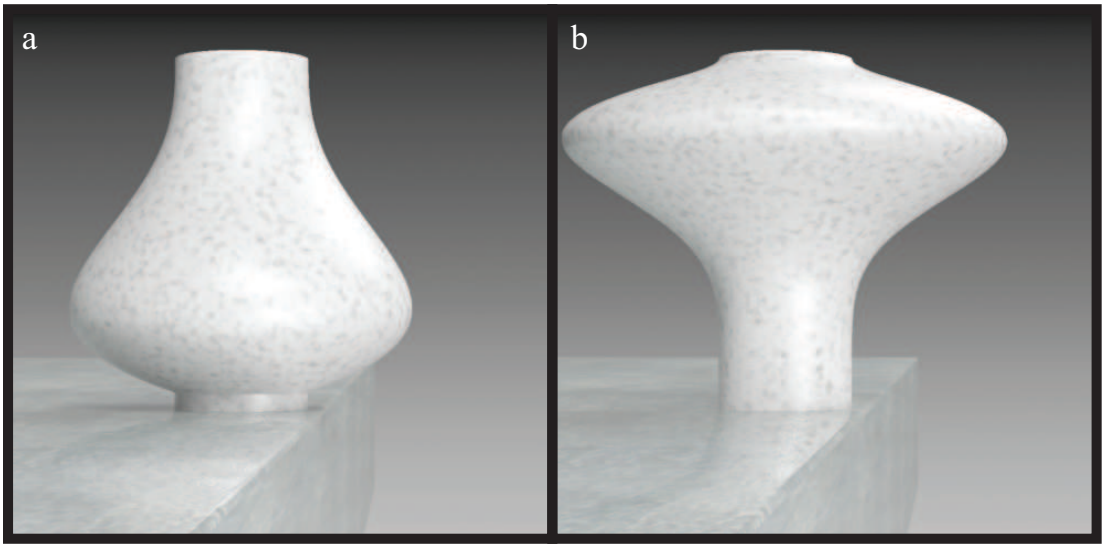

Figure 3.1: Two objects sitting near the edge of a table, one that is very perceptually stable (a) and one that is very perceptually unstable (b).

upright position. With this definition in mind, it is easy to appreciate that the object in Fig. 3.1a is physically more stable because it has a larger critical angle than the one in Fig. 3.1b.

In previous work, we have used the visual estimation of critical angle to measure the perception of stability for three-dimensional objects that were rotationally symmetric (Barnett-Cowan et al., 2011; Cholewiak, Singh, Fleming, & Pastakia, 2010). While critical angle provides a natural measure of overall physical stability for such objects, the situation is more complicated for asymmetric 3D objects. Specifically, for an asymmetric object, the critical angle is not a single value, but depends on the direction in which the object is tilted. Since the object can be tilted in any radial direction varying from 0° to 360°, the critical angle is really a function defined on $[0^\circ, 360^\circ)$. However, as we will see, observers can reliably judge the *overall* stability of such an asymmetric 3D object. This raises the question of how people combine the information about different critical angles in different possible tilt directions into a single overall estimate of the physical stability of an object? To address this question, we use two experimental methods: visual estimation of critical angle in different directions (Experiment 1) and perceptual matching of overall stability across objects with different shapes (Experiment 2 & Experiment 3).

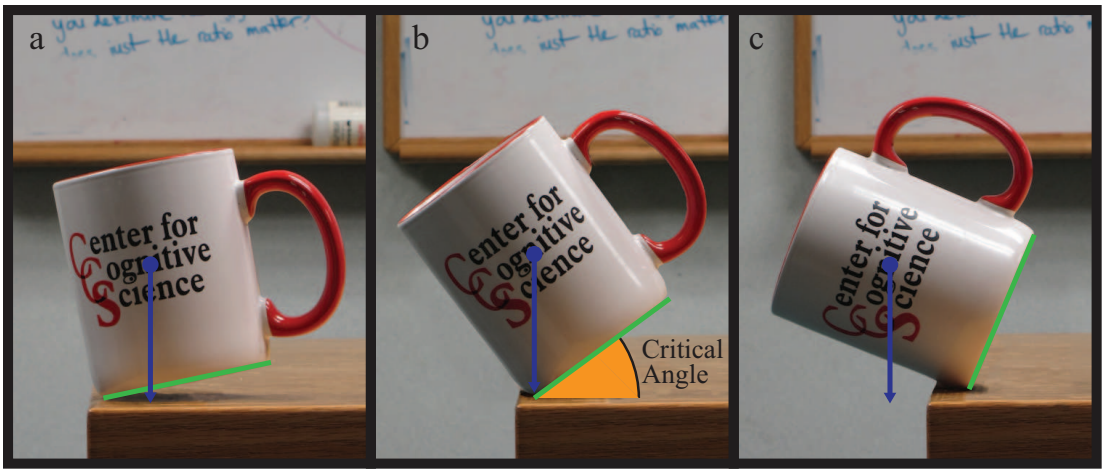

Figure 3.2: Coffee cup with COMs – represented by the blue circle and blue line representing gravity vector – vertically above the base (green) (a), directly over the contact point when the object is at its critical angle (b), and outside the base (c).

In Experiment 1, we explicitly test how well people can estimate the critical angle of an object as a function of the direction in which the object is tilted. In Experiments 2 and 3, we ask how these different critical angles in different tilt directions are combined into a single estimate of stability. Specifically, we compare two natural combination rules: (i) that the overall perceived stability is determined by the average critical angle across all possible tilt directions; (ii) overall perceived stability is determined by the minimum critical angle (i.e., the critical angle in the least stable direction).

3.2 Experiment 1: Measuring Critical Angle in Different Directions

In the first experiment, we investigated whether observers could accurately track the critical angle of asymmetric 3D objects as a function of the direction in which they are tilted. The objects used in these experiments were skewed conical frustums (see Fig. 3.3). In what follows, it will be important to distinguish between: (i) the direction in which the object is tilted (the magnitude of tilt is adjusted interactively by the observer); and (ii) the intrinsic direction of skew of the conical frustum objects. The angle of relevance to us is the direction in which the object was tilted relative to the intrinsic direction of skew of the object. We refer to this angle as α. In the experiments, the object was always tilted directly over the precipitous edge of a table,

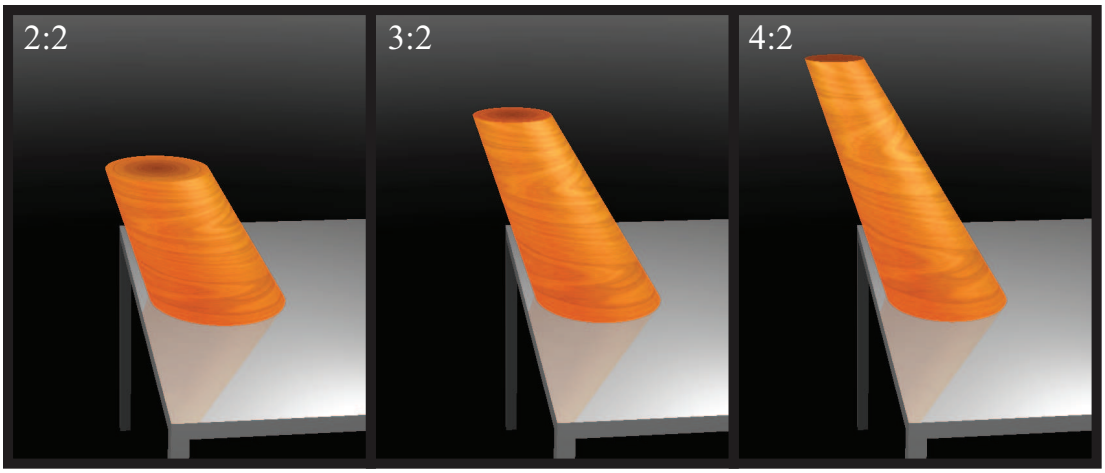

Figure 3.3: Cropped examples for Exp. 1 showing the three aspect ratios of the asymmetric conical frustums (2:2, 3:2, 4:2) with a constant skew. Note that 3D volumes were equated and all of the objects were skewed by 25° from the vertical.

but the direction of intrinsic skew of the object was varied from trial to trial, thereby manipulating α (see Fig. 3.4).

3.2.1 Methods

Observers

Fourteen Rutgers University undergraduate students participated for course credit. All reported normal or corrected-to-normal vision.

Apparatus

The stimuli were generated in MATLAB 2012a using Psychotoolbox-3 (Brainard, 1997; Pelli, 1997; Kleiner et al., 2007) and presented on a Sony Trinitron 20 inch CRT with a 1024 x 768 pixel resolution at a refresh rate of 140Hz. Within Psychtoolbox-3, experimental scenes were rendered using the Matlab OpenGL (MOGL) toolbox and were presented stereoscopically using an NVIDIA Quadro 4000 graphics card and 3D Vision 2 LCD shutter glasses. Observers were comfortably seated with a chin-rest supporting their head 80 cm from the screen.

The individual object meshes and all relevant quantities (volumes, COM locations, critical angles, etc.) were calculated using Mathematica 8.

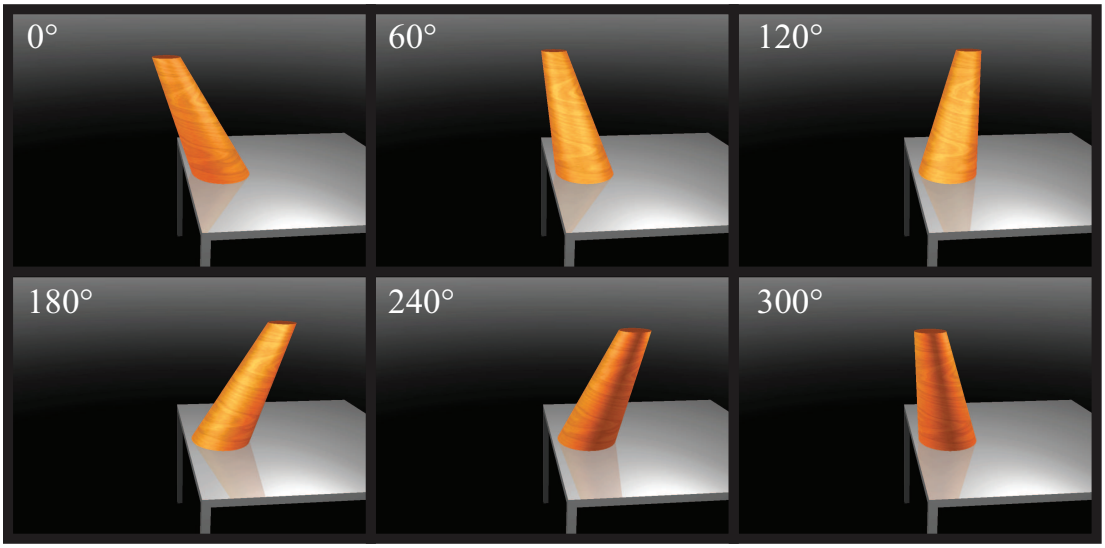

Figure 3.4: Examples for Exp. 1 of the 6 possible skew stimuli ($\alpha = 0°, 60°, 120°, 180°, 240°, 300°$) for a frustum with a constant aspect ratio (4:2). Note that the aspect ratio or skew angle may appear to change in these illustrative figures; however the stimuli were presented stereoscopically, so a skew direction of $\alpha = 120°$ was facing into the screen/scene and $\alpha = 300°$ was facing out toward the observer

Stimuli and Design

The experiment used the method of adjustment to measure the perceived critical angle for objects in a 3 aspect ratios $\times$ 6 skew directions factorial design. The objects were conical frustums that were placed close to the edge of a virtual table. The objects had 3 possible aspect ratios (Height:Base diameter; 2:2, 3:2, 4:2) and subtended approximately 6.4-10.7 DVA (see Fig. 3.3). The frustums were skewed by 25° from the vertical in one of 6 directions relative to the edge of the table ($\alpha = 0°, 60°, 120°, 180°, 240°, 300°$) (see Fig. 3.4). At 0° the object's skew was directed towards the precipice, in the range $0° - 180°$ the object was facing away from the observer, at 180° the object was skewed in the opposite direction of the precipice, and in the range $180° - 360°$ the object was skewed toward the observer.

Objects were always tilted directly toward the edge of the table, so the skew direction determines the tilt direction relative to the object's intrinsic skew. The observers' viewpoint in the scened was fixed. The objects had a woodgrain texture to reinforce the percept of solid, uniform density objects. They were described to observers as solid

blocks of wood (as if cut out from the trunk of a tree). Visual cues – including shading, a metallic reflection of the objects on the table, and dynamic lighting – were added to aid in the realism of the scene and, in addition, scenes were presented stereoscopically. The volumes of objects were equated across shape manipulations.

Procedure

The observers' task was to adjust the tilt of the object until it was perceived to be equally likely to fall off the table versus return to its upright position on the table (the perceived critical angle). As noted previously, the object's motion was constrained to move orthogonal to the edge of the table, with the axis of rotation at the point on the base of the object closest to the table's edge.

On each trial, the conical frustum was shown with an initial tilt angle of either 0° (upright with base fully on the table) or 90° (tilted so that the entire object was over the precipice). The starting angle was counterbalanced to later analyze for possible hysteresis.

Each observer performed a total of 144 adjustments: 8 adjustments for each of the 3×6 combinations of aspect ratio and skew directions. Half of these had an initial tilt angle of 0°, and the other half had an initial tilt angle of 90°.

3.2.2 Results

Observer performance was evaluated by examining their critical angle settings as a function of the skew direction (α) and aspect ratio. A repeated measures ANOVA was conducted on the pooled observer data, showing a highly significant effects for aspect ratio ($F(2, 26) = 86.57, p < 0.01$), α ($F(5, 65) = 280.31, p < 0.01$), and initial tilt angle ($F(1, 13) = 11.95, p < 0.01$). There was a small but significant effect of initial tilt angle on the observers' responses.

Fig. 3.5 shows the average data plotted as a function of α along with the predicted critical angles for all three aspect ratios. The only notable exception was for $\alpha = 0°$ (especially at aspect ratios of 3:2 and 4:2), where observers overestimated the critical angle (and hence the stability) of the object – which would have caused the object to

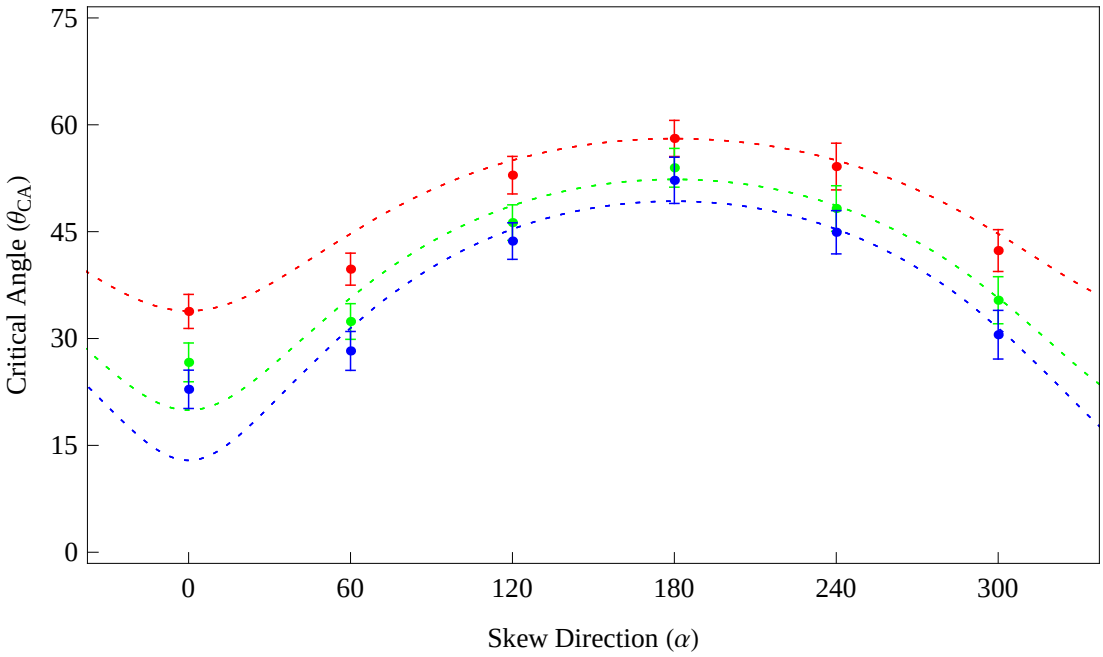

Figure 3.5: Average group critical angle performance for the 3 object aspect ratios (red = 2:2, green = 3:2, blue = 4:2) and 6 skew directions ($\alpha = 0°, 60°, 120°, 180°, 240°, 300°$). Dotted lines show the veridical critical angle curves for the 3 aspect ratios. Error bars are standard error. On average, observers tracked the physical critical angle quite well.

fall off the table in the real world. Observers' settings showed that they tracked the critical angle as a function of the skew remarkably well. Fig. 3.6 shows the individual observers' data plotted as a function of α.

3.2.3 Discussion

In the first experiment, we found that not only were observers able to perform the task, they were also very good at tracking the critical angle as a function of the skew direction. For all three aspect ratios, observers adjustments followed the physical prediction as a function of α.

Interestingly, on average, observers' perceptual judgments were very close to the physical predictions, indicating that there was no systematic conservative bias for judgments "on the safe side" (Samuel & Kerzel, 2011). And for $\alpha = 0°$, observers actually made liberal critical angle estimates, suggesting that there may be a more complex interaction between shape and the observers' biases to over or underestimate the critical

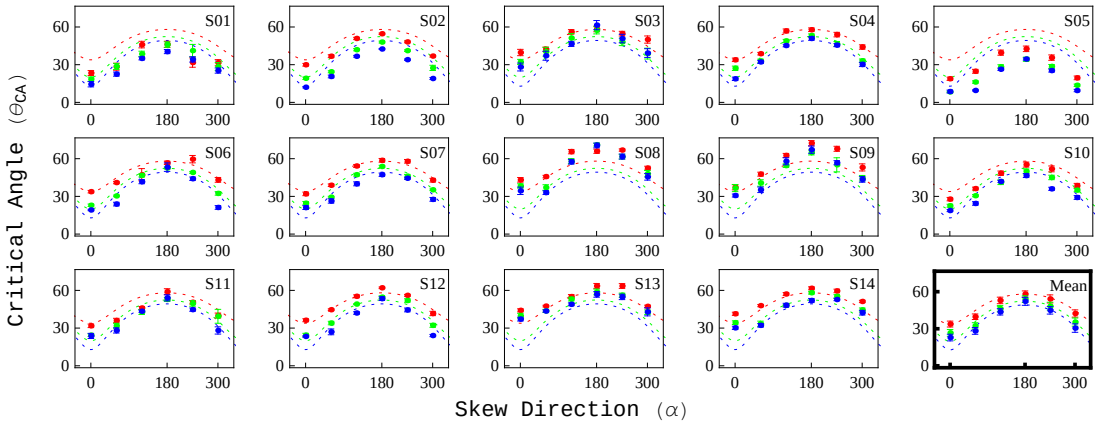

Figure 3.6: Individuals' critical angle response data for the 3 object aspect ratios (red = 2:2, green = 3:2, blue = 4:2) and 6 skew directions ($\alpha = 0°, 60°, 120°, 180°, 240°, 300°$). Dotted lines show the veridical critical angle curves for the 3 aspect ratios.

angle.

3.3 Experiment 2: Matching Overall Stability

3.3.1 Motivation

The results of the first experiment showed that observers tracked the critical angle as a function of the tilt direction relative to the intrinsic skew of the object (α). However, in addition to judging the critical angle in any given direction, observers can also estimate overall object stability. For example, in Fig. 3.7a it is visually apparent that the cylindrical object on the right is more stable than the skewed frustum; whereas in Fig. 3.7b the cylindrical object is less stable.

This raises the question of how observers combine information about the various critical angles into a unitary percept of object stability. Because the critical angle task inherently measures the perceived stability in a single direction of tilt, we can only answer this question by using a different task that assesses the overall stability of an object, not just stability in a given direction. To do this, we use an overall stability matching task.

Observers were asked to compare the overall stabilities of two objects – a standard

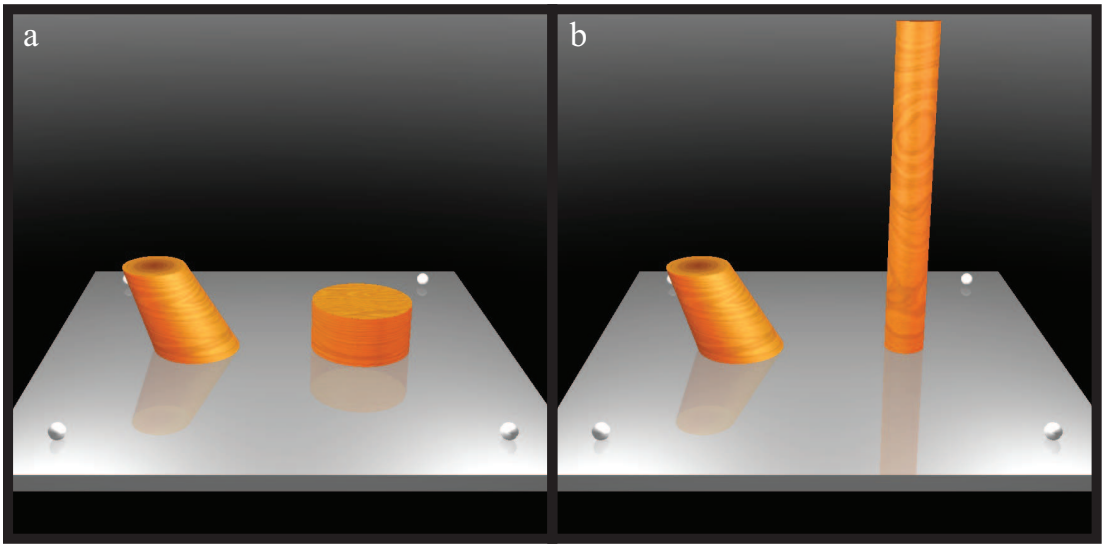

Figure 3.7: Example scenes illustrating situations where a cylinder is perceptually more stable than a skewed conical frustum (a) and where a cylinder is perceptually less stable than the skewed frustum (b).

object (corresponding to one of the skewed conical frustums from the previous experiment) and a simple cylindrical comparison object – and to adjust the aspect ratio of the comparison object until it was perceived to be equally stable as the standard. When the stabilities of the two objects were perceptually matched, the two shapes could be considered stability metamers.

It was not obvious *a priori* whether observers would be able to perform such matches. A pilot study revealed, however, that observers find this a natural task, and their settings are quite precise. This is consistent with the idea that physical stability is natural perceptual dimension.

How do observers combine the various critical angles into a single stability judgment? Two natural combination rules that could be used are: (1) to take the average of all the critical angles; and (2) to simply use the minimal critical angle. If observers assume that an object could have a force impulse applied from any direction (uniformly sampled from every direction around the perimeter of the object), then it would make sense to integrate across all possible tilt directions, which would result in the average critical angle strategy (Hamrick et al., 2011). This average critical angle model incorporates information from every potential force vector direction, so it can be used to take into

account the minimum and maximum critical angle, as well as every critical angle in-between, when judging the overall stability.

Alternatively, observers could use the object's minimum critical angle as a proxy for the perceived overall stability, which may be a more salient feature if individuals are looking for the critical angle that is most informative about a potential change in the object's state of equilibrium. A natural way to think of physical stability is in terms of the minimum force required to change the equilibrium state of the object, so if we consider the minimum of the forces in all directions, then the absolute minimum would be in the least stable direction. That is, when a force is applied in the direction of the minimum critical angle, it has the highest likelihood of changing the equilibrium state.

The average and minimum critical angle models were compared to see which model better described the observers' settings.

3.3.2 Methods

Observers

Thirteen Rutgers University undergraduate students, with normal or corrected-to-normal visual acuity, participated in the experiment.

Stimuli and Design

The scene was composed of two objects, a standard and a comparison object, sitting next to each other on a virtual table. The standard objects – skewed conical frustums as in the first experiment – had 3 possible aspect ratios (2:2, 3:2, 4:2) and subtended approximately 4.3-6.8 DVA (see Fig. 3.8). The frustums were skewed by 25° from the vertical and were skewed towards the left or right (see left panes in Fig. 3.9). In addition, the standard objects were placed on either the left or the right of the comparison object (see center panes in Fig. 3.9). The comparison objects – cylinders – had one of 2 initial aspect ratios (1:2 or 16:2), the two opposite ends of the aspect ratio spectrum: short-and-wide and narrow-and-tall, that subtended approximately 3.0 and 12.3 DVA, respectively (see right panes in Fig. 3.9). They had the same wood grain

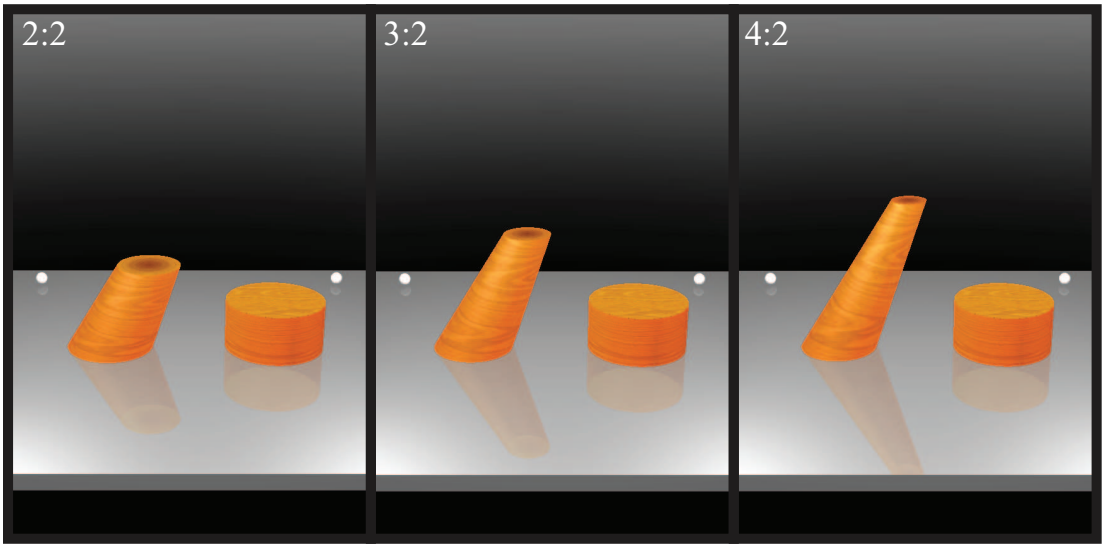

Figure 3.8: Cropped examples for Exp. 2 of the 3 possible aspect ratios (2:2, 3:2, 4:2) for a constant skew direction ($\alpha = 180°$), with the comparison cylinder at it's lowest aspect ratio (1:2) on the right.

texture and material properties as the conical frustums and had a variable aspect ratio, to be adjusted by the observers.

The experiment used the method of adjustment for stability matching using a 3 standard aspect ratios $\times$ 2 skew directions $\times$ 2 presentation locations $\times$ 2 initial comparison object aspect ratios factorial design.

Procedure

On each trial, a standard conical frustum was shown alongside a comparison cylinder. The observers' task was to adjust the aspect ratio of the comparison object until it was judged to have the same overall stability as the standard object. The comparison object's volume was held constant across changes in aspect ratio, hence the observer's adjustments affected both height and radius. Since the two objects had the same surface properties and there were no other stability cues than the visual ones, observers had to rely on shape alone in making their judgments.

When the observer finished their aspect ratio adjustment (i.e., when the perceived stabilities of the comparison and standard were subjectively the same), the two objects could be considered stability metamers (similar to color metamers, where two colors are

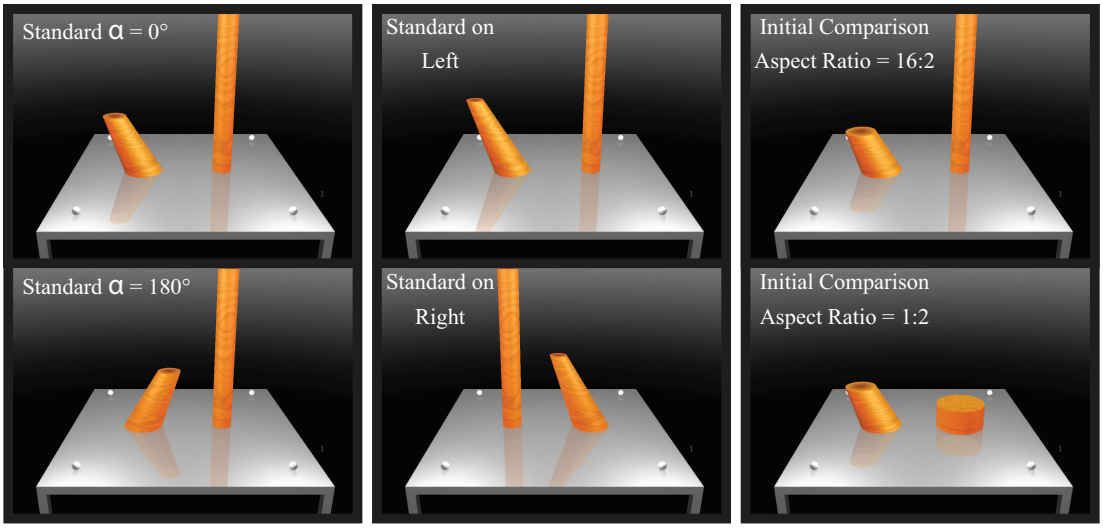

Figure 3.9: Examples of the two standard skew directions ($\alpha = 0°and180°$), the two standard object locations (left and right), and the 2 initial comparison aspect ratios (1:2 and 16:2).

perceived to be the same even though they have differing wavelength compositions).

Each observer performed a total of 192 adjustments: 8 adjustments for each of the $3 \times 2 \times 2 \times 2$ combinations of aspect ratio, skew direction, presentation location, and initial comparison aspect ratio.

3.3.3 Results

A repeated measures ANOVA was conducted on the pooled observer data, showing significant effects for the standard aspect ratio ($F(2, 24) = 50.80, p < 0.01$) and initial comparison aspect ratio ($F(1, 12) = 21.12, p < 0.01$) (see Fig. 3.10). There was no effect of skew direction ($F(1, 12) = 3.67, p > 0.05$) or presentation location ($F(1, 12) = 1.23, p > 0.05$). There was a small but significant effect of initial aspect ratio on the observers' responses (see Fig. 3.11 for individual observers' data). Further analyses were collapsed across initial comparison aspect ratio.

Observers' settings were compared against predictions derived from (i) the average critical angle model and (ii) the minimum critical angle model. If observers used the lowest critical angle to make their judgments, then we would expect their data to be close to the minimum critical angle prediction (blue dashed curves in Fig. 3.10 &

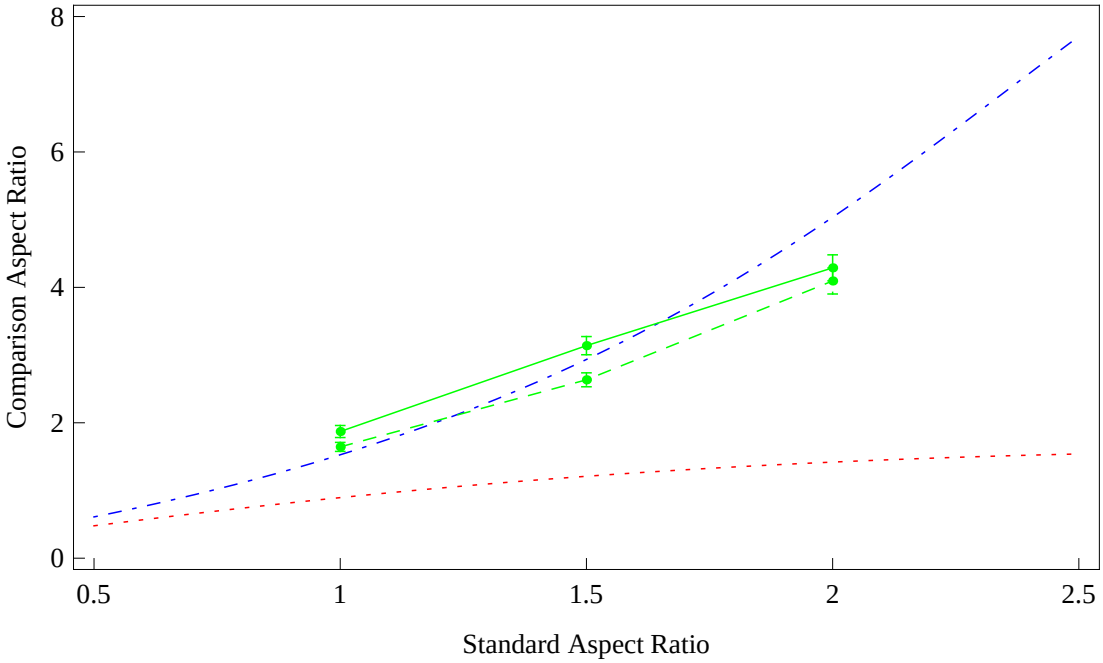

Figure 3.10: Average group performance for the 3 object aspect ratios (2:2, 3:2, 4:2) collapsed across skew direction and presentation location. The green lines represent the observers' responses, separated by initial comparison aspect ratio (solid = 16:2, dashed = 1:2). The blue line represents the predicted comparison aspect ratio if observers used the minimum critical angle and the red line represents the average prediction. Error bars represent 95% confidence intervals.

Fig. 3.11). Conversely, if observers used an estimate that uniformly took into account the object's critical angle in all possible directions, then their judgments should be closer to the average critical angle prediction (red dashed curves in Fig. 3.10 & Fig. 3.11). On average, the observers' settings were closer to the minimum critical angle model's predictions than the average critical angle model.

In order to evaluate which model (average critical angle or minimum critical angle) better described observers' performance, we calculated the likelihood ratios for each observer's data. The likelihood ratio test allows us to compare the two stability estimation models and judge which model better explains the observed data.

Normally, we would compare performance using the Bayes factor (K), which is the ratio of the probability of the data given the first model ($Pr(D|M_{avg})$) over the probability of the data given the second model ($Pr(D|M_{min})$)(see Eq. 3.1).

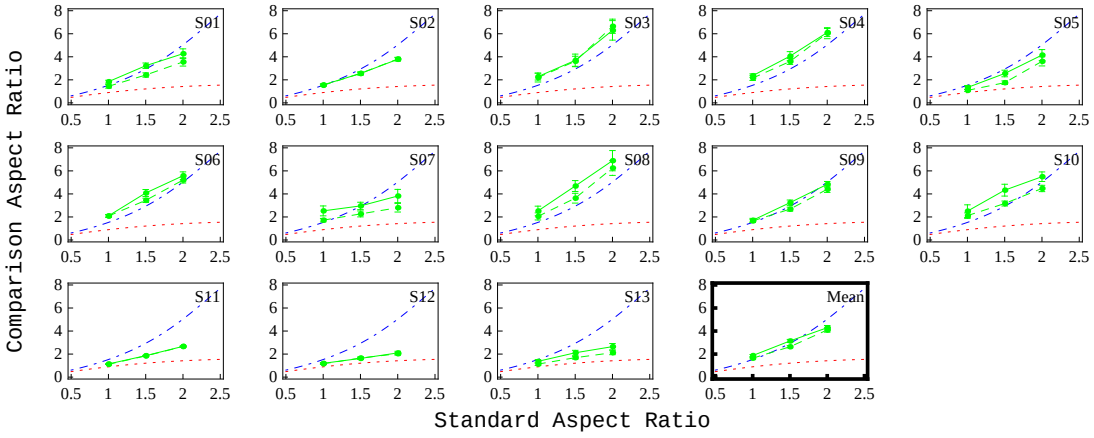

Figure 3.11: Individual observer performance for the 3 object aspect ratios (2:2, 3:2, 4:2) collapsed across skew direction and presentation location. The green lines represent the observers' responses, separated by initial comparison aspect ratio (solid = 16:2, dashed = 1:2). The blue line represents the predicted comparison aspect ratio if observers used the minimum critical angle and the red line represents the average prediction. Error bars represent 95% confidence intervals.

$$K = \frac{Pr(D|M_{avg})}{Pr(D|M_{min})} \tag{3.1}$$

However, in this case the two models we are comparing have no free parameters, which means the Bayes Factors simply reduces to the ratio of the two model likelihoods. This likelihood ratio can now be used to judge which model better explains the data, with likelihood ratio values greater than 1 supporting M_{avg} and values less than 1 supporting M_{min}. The ratios of the average and minimum likelihoods were calculated for each observer (see Eq. 3.2). Because the raw likelihoods can be extremely small or large, we calculated the log likelihoods for the individual models and for the likelihood ratios – meaning positive log likelihoods support M_{avg} and negative log likelihoods support M_{min}.

$$\Lambda_{observer} = \frac{\prod_{i=1}^{n} Pr(D_i|M_{avg})}{\prod_{i=1}^{n} Pr(D_i|M_{min})} \tag{3.2}$$

For 10 of the 13 observers, the calculated log likelihood ratios supported the minimum model over the average model (see Table 3.1), indicating that the minimum critical angle provides a better model of the observers' stability matches than the average

Table 3.1: Log likelihoods for each model and the log likelihood ratios ($Log(Likelihood_{avg}/Likelihood_{min})$) for each observer. Note that for 10 of the 13 observers, the log likelihood ratio favored the minimum model – that is, the likelihood ratio was negative.

Observer	$Log(Likelihood_{avg})$	$Log(Likelihood_{min})$	$Log(\Lambda)$	Model Favored
1	−507.33	−154.81	−352.51	Minimum
2	−1920.61	−374.93	−1545.69	Minimum
3	−561.97	−218.72	−343.25	Minimum
4	−1094.45	−258.80	−835.66	Minimum
5	−328.60	−213.95	−114.65	Minimum
6	−1659.79	−254.89	−1404.89	Minimum
7	−367.33	−243.18	−124.15	Minimum
8	−585.69	−246.68	−339.01	Minimum
9	−1054.09	−116.44	−937.65	Minimum
10	−683.06	−218.44	−464.62	Minimum
11	−8317.27	−29086.70	20769.40	Average
12	−270.65	−3203.57	2932.92	Average
13	−231.59	−702.86	471.27	Average

critical angle.

3.3.4 Discussion

Observers' judgments were better explained by the minimum critical angle, rather than the mean critical angle. Thus the least-stable direction has a disproportionately large influence in visually estimating the overall stability of an object. The direction of least stability could be considered the "worst case scenario" and it tends to dominate observers' judgments.

3.4 Experiment 3: Matching Overall Stability in Different Directions

3.4.1 Motivation

The results of the stability matching task in Experiment 2 indicated that observers' overall stability judgments were informed by the minimum critical angle of the asymmetric objects. The idea behind the stability matching task presented in Exp. 2 was that, unlike the critical angle task, the stability matches for a given object should be stable as the direction of tilt varies relative to the intrinsic skew of the object. Here we

test if this is indeed the case.

Dependencies on the viewing direction are common in 3D shape perception – and are particularly acute when the axis of elongation of an object is foreshortened (Marr & Nishihara, 1978; Biederman, 1987; Humphrey & Jolicoeur, 1993; Lawson & Humphreys, 1998). Because of this, one may expect some effect of viewing direction on visual judgments of object stability (if the shape appears different, its perceived stability will of course also be affected). However, we would expect that any such effects are much smaller than the large influence of skew direction on perceived critical angles, observed in Experiment 1.

In this experiment, observers compared the overall stabilities of two objects – a standard and a comparison – and adjusted the comparison object until it was perceived to be the same stability as the standard, just as in Exp. 2. However, this experiment differed from Exp. 2 in that the direction of skew was also manipulated (analogous to the manipulation of α in the first experiment).

3.4.2 Methods

Observers

Thirteen Rutgers University undergraduate students, with normal or corrected-to-normal visual acuity, participated in the experiment.

Stimuli and Design

The experiment used the same stability matching task as Exp. 2. It used a 3 standard aspect ratios $\times$ 6 skew directions $\times$ 2 presentation locations $\times$ 2 initial comparison object aspect ratios factorial design.

As in the second experiment, the rendered scene contained two objects, a standard and a comparison object, sitting next to each other on top of a table. The standard objects had 3 possible aspect ratios (2:2, 3:2, 4:2), were skewed by 25° from the vertical, and were skewed in 1 of 6 skew directions ($0°, 60°, 120°, 180°, 240°, 300°$). In addition, the standard objects were placed on either the left or the right of the comparison object

and the comparison objects had one of two initial aspect ratios (1:2 or 16:2). See Fig. 3.9 for examples of the scene layout.

Procedure

The testing procedure was identical to Experiment 2.

Each observer performed a total of 216 adjustments: 6 adjustments for each of the $3 \times 6 \times 2$ combinations of aspect ratio, skew direction, and presentation location. Half of these used an initial aspect ratio of 1:2 for the comparison object; the other half used an initial aspect ratio of 16:2.

3.4.3 Results

Observer performance was evaluated by examining their stability matches (aspect-ratio settings for the comparison object) as a function of the skew direction. A repeated measures ANOVA was conducted on the pooled data, showing a highly significant effect of aspect ratio ($F(2, 24) = 153.21, p < 0.01$) and a significant effect of initial comparison aspect ratio ($F(1, 12) = 7.53, p < 0.05$). There was also a significant effect of skew direction ($F(5, 60) = 39.94, p < 0.01$), but a Post-Hoc Tukey Test confirmed that the slant direction effect was due to the dip in performance at 60° and 120° and that there were no other significant differences for any other slant directions.

As shown in Fig. 3.12, on average, judgments were affected by the change in the standard aspect ratio and the direction of the skew, which had a much smaller effect. There was a slight dip in the comparison aspect ratios at 60° and 120°. It is likely this may have been due to perceived foreshortening when the slant was directed into the screen.

3.4.4 Discussion

The results from the third experiment support the hypothesis that observers are able to match the overall stabilities of objects in a consistent manner, even when the asymmetric objects are rotated relative to the observer's viewpoint.

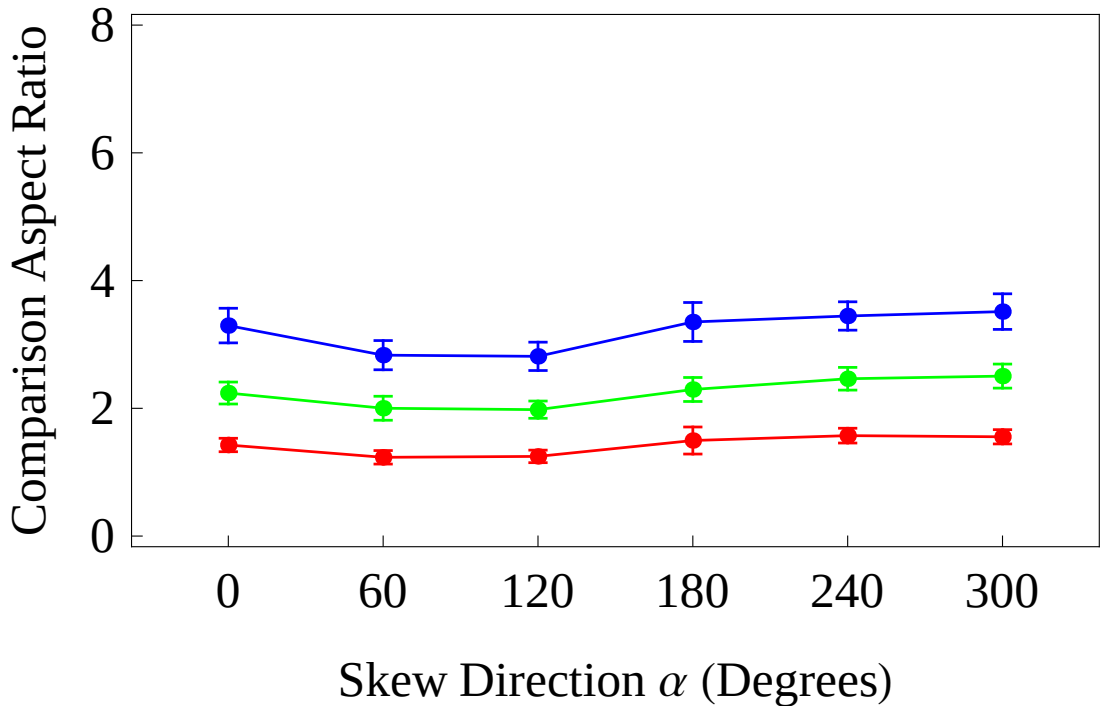

Figure 3.12: Average group performance in Exp. 3 for the 3 object aspect ratios (red = 2:2, green = 3:2, blue = 4:2) collapsed across the other independent variables (standard location and initial comparison aspect ratio) as a function of the skew direction. The dashed lines represent the minimum critical angle predictions for each aspect ratio. Error bars represent standard error.

Although the effect of skew direction was statistically reliable, it was quite small when compared to the influence of skew direction on the perceived critical angle observed in Exp. 1. Given the well-known effects of foreshortening of the axis on shape perception, it seems likely that the observed influence of skew direction on perceived stability is most likely due to the misperception of 3D shape from those viewpoints (Marr & Nishihara, 1978; Biederman, 1987; Humphrey & Jolicoeur, 1993; Lawson & Humphreys, 1998). Nevertheless, the stability matches are surprisingly flat, especially when compared with the large influence of skew direction on the perceived critical angles observed in Exp. 1.

3.5 Conclusion

The critical angle is a good measure of stability for three-dimensional objects, incorporating information about mass distribution and shape to define an ecologically important property of real-world objects. We have previously found that people are good at visually estimating the critical angles of symmetric objects (Barnett-Cowan et al., 2011; Cholewiak et al., 2010); however, it was not clear how these results would extend to more general, asymmetric objects. Since the critical angle is not a single value for asymmetric objects, but depends on the direction in which the object is tilted, we investigated how well observers could visually estimate the critical angles in different tilt directions for asymmetric objects.

Observers were clearly able to track the critical angle as asymmetric conical frustums were tilted in different directions relative to their intrinsic skews in Exp. 1, indicating that their judgments were appropriately informed by the shape's asymmetry. These results extend our previous results for rotationally symmetric objects to asymmetric objects. This is reassuring because anecdotally we have few issues making guided actions that are informed by our percepts of real-world object stability. In contrast to the findings of Samuel and Kerzel (2011) with 2D polygonal objects, however, our results show no systematic conservative bias – i.e., for stability settings to be judged "on the safe side".

Although our Exp. 1 results showed that individuals could reliably judge stability, as reflected in the work by Samuel and Kerzel (2011), there was an important contrast: observers did not always make their critical angle judgments "on the safe side". In fact, although Samuel and Kerzel (2011) found that their observers systematically made conservative judgments – judging the objects to be less than physically stable, observers in our experiments were quite accurate at visually estimating physical stability. Although there was of course some individual variability across observers (with some tending to overestimate and others tending to underestimate stability), we did not see any systematic conservative bias in the pooled data.

Surprisingly, observers were able to reliably match the perceived stability of two

objects with different shapes in Exp. 2. These results suggest that stability may be represented along a unitary dimension. The observers were able to infer the force of gravity acting upon the shapes and compare their overall stabilities even though the shapes were quite different. Observers' stability matches were better explained by the minimum model than the average model, suggesting that observers' estimates were disproportionately influenced by the direction of least stability. Since physical stability is defined as the minimum force required to change the equilibrium state of the object, the direction with the smallest critical angle defines where the object has the highest likelihood of changing its equilibrium state. Although the average critical angle is a measure of the central tendency of the stability for the object – taking into account the maximum and minimum stability, and all of the critical angles in-between – on average, people appeared to use the minimum critical angle as a proxy for the perceived overall stability.

Finally, Exp. 3 demonstrated that the matches were a function of the aspect ratio of the 3D shapes – with observed data exhibiting only a slight dependence on viewpoint (likely due to foreshortening).

As a whole, these results are evidence that visual estimates of overall object stability are strongly influenced by the minimum critical angle and that perceived shape plays an important role to inform the people of the objects' physical properties.

Chapter 4

Visual adaptation to the physical stability of objects

4.1 Introduction

How does the brain represent Newtonian forces? It has been suggested by research in naïve – intuitive – physics that people incorrectly infer forces and object motion due to faulty internal models (McCloskey et al., 1980; McCloskey, 1983b, 1983a). However, there is an alternative body of research that has shown that while people make mistakes when relying upon higher-level, slower reasoning, their lower level perceptual judgments are much more consistent with physically accurate models – especially when they are shown real-time simulations of physical behavior (Kaiser et al., 1985, 1992; Proffitt & Gilden, 1989). We have previously demonstrated that judgments of object stability are fairly consistent with physical predictions (Cholewiak et al., 2010; Cholewiak, Fleming, & Singh, 2011, 2012); here we show clear evidence in support of lower level representation of perceived stability, demonstrating that stability – and the inference of forces – is likely an perceptual attribute that is subject to adaptation effects.

People can usually judge, based on vision alone, whether an object is physically stable or unstable; that is, whether it will stay in its current physical state or fall due to gravity. Anecdotally, these stability judgments appear to occur automatically and unconsciously, and we seem quickly identify these salient situations where objects appear unstable (for example, see Fig. 4.1).

The perception of physical stability requires the inference of forces in order to judge whether or not an object will fall. Previous work has documented observers' ability to estimate object stability (Barnett-Cowan et al., 2011; Cholewiak et al., 2010, 2011, 2012; Samuel & Kerzel, 2011) and has shown that people use aspects of shape – such as aspect ratio and part structure –when making stability judgments. Cholewiak et

(a) Stones balanced at Aghnacliff dolmen in Ireland (Dempsey, 2008)

(b) Bricks carefully balanced (Dan, 2007)

(c) Former Transport Ministry of Georgia (Zollinger, 2008)

Figure 4.1: Photographs illustrating how scenes can convey the physical interactions and support relations between objects in a scene. Sometimes the support structures and interactions are clear, (a) and (b). Other times, foundations conceal the forces that support the objects, (c).

al. (2012)'s results suggest that perceived stability may be represented as a unitary dimension, where objects are perceptually judged on a continuum from very unstable to stable. The ability to make judgments of a object's critical angle or its COM, however, does not necessarily imply that object stability is a natural perceptual dimension. So, in the experiments described herein, we asked whether it is possible to obtain adaptation aftereffects with perceived object stability.

Color, motion, and prismatic aftereffects have long been used as evidence for the claim that visual perception operates at an earlier stage of processing (Harris, 1963; Singer & Day, 1966a, 1966b) and that there are specific neuronal pools dedicated to the representation of perceptual variables. The reliability of perceptual adaptation – continued exposure to previously explored stimuli affecting the neural representation – has led to aftereffects to being dubbed the *psychophysicists microelectrode*. Recent neuroscience studies have supported these claims and have shown that perceptual aftereffects lead to neuronal response rate tuning in both non-humans (Dragoi, Sharma, & Sur, 2000; Dragoi, Sharma, Miller, & Sur, 2002; Kohn & Movshon, 2003, 2004) and humans (Tootell et al., 1995). Recently, there has also been research demonstrating that some processes that were traditionally held to be dependent upon higher-level processing, specifically visual judgments of numerosity, may be represented at a lower perceptual level than traditionally believed (Burr & Ross, 2008; Burr, Anobile, & Turi, 2011).

We want to answer the question of whether judgments of stability are purely based on high-level knowledge/reasoning, or may they be represented perceptually? In the following experiments, we test whether perceived stability is indeed a bona fide unitary perceptual dimension that is susceptible to adaptation aftereffects.

4.2 Experiment 1: 2D Curvature Probe

In the first experiment, we tested whether visually adapting to stable and unstable shapes would lead to a stability aftereffect that causes under and overestimation, respectively, of the perceived stability of test shapes. When observers adapt to stable shapes (see Fig. 4.2), a stability aftereffect would cause them perceive test shapes as *less* stable and vice versa, if they adapt to unstable shapes, they will perceive the test shapes as *more* stable. The test shapes in Exp. 1 had axes with variable curvature and constant rib-lengths (see Fig. 4.3). The curvature of the object's axis was increased while its base remained fully in contact with the ground plane/supporting surface. With sufficiently high curvature, the COM would no longer lie above the object's base; and the object would become unstable (i.e., would no longer physically stay upright). Thus the curvature manipulation allowed us to manipulate the stability of the shape in a controlled manner.

4.2.1 Methods

Observers

Ten Rutgers University students. All reported normal or corrected-to-normal vision.

Apparatus

The stimuli were generated in MATLAB 2012a using Psychtoolbox-3 (Brainard, 1997; Pelli, 1997; Kleiner et al., 2007) and presented on a Sony Trinitron 20 inch CRT with a 1024 x 768 pixel resolution at a refresh rate of 140Hz. Observers were comfortably seated with a chin-rest supporting their head 80 cm from the screen.

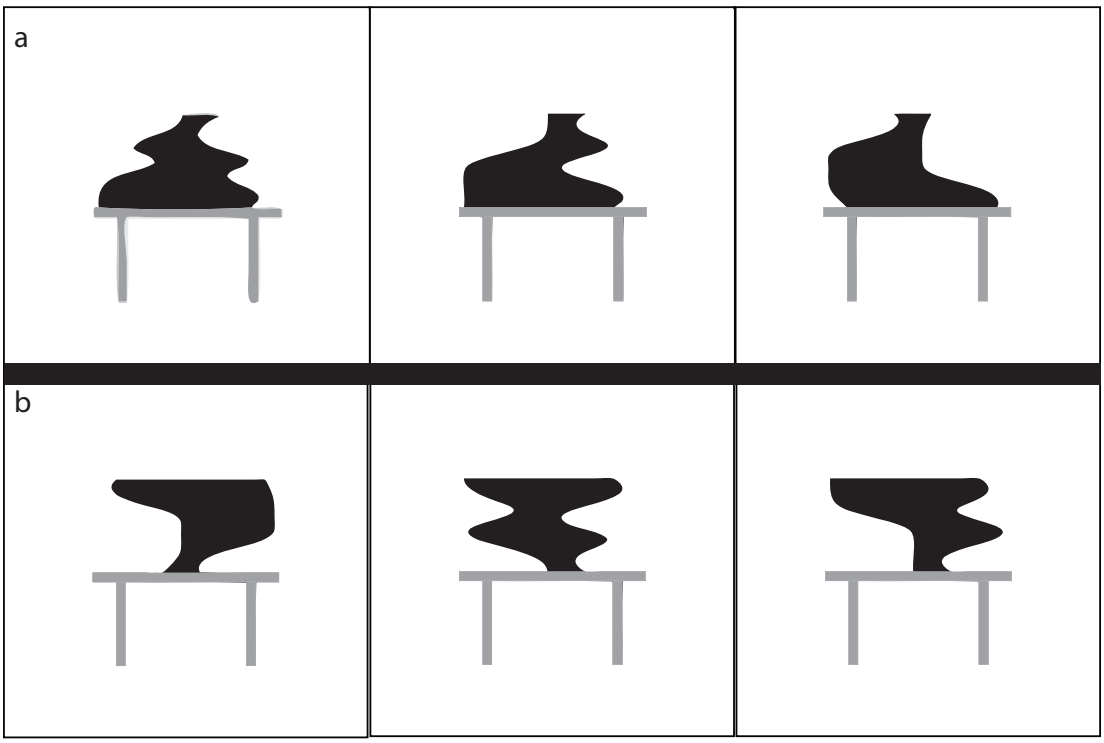

Figure 4.2: Examples of the 2D adaptation stimuli. The stimuli in the top row (a) are examples of very stable shapes, while the stimuli in the bottom row (b) are examples of very unstable shapes. Note that the shapes in row (a) were vertically flipped in the experiment to produce very unstable adaptation shapes (not illustrated in this figure).

The individual object contours and all relevant quantities (areas, COM locations, critical angles, etc.) were calculated using Mathematica 8.

Adaptation Stimuli

The adaptation shapes were 2D silhouettes that were either very stable – bottom heavy with very high critical angles – or very unstable – top heavy with very low or negative critical angles (negative meaning that the shapes would not physically stand up as presented) (see Fig. 4.2). The silhouettes were placed on horizontal supporting surface – a "table" composed of 3 rectangles. In order to ensure that any adaptation was due to the perceived stability and not an artifact of the specific shapes used, the same set of shapes was used for both the high and low stability adaptation conditions; they were simply rotated through 180°.

The adaptation shapes were constrained to have a fixed area. The contours of the

left and right sides of the shape were analytically defined using B-spline functions with 7 control points each, while the top and bottom were straight horizontal lines connecting the endpoints of the B-splines, ensuring that the shapes could be flipped vertically. Unique adapting shapes were generated by randomly varying the control points of the B-spline functions. The final set of 45 adapting stimuli were picked by selecting the sets of B-spline functions that created shapes with constant area and critical angles greater than 50° ($Range = [50.33°, 73.03°], M = 63.52°, SD = 5.37°$).

The low stability shapes were the same 45 shapes, vertically flipped. By vertically flipping the high stability stimuli, we were able to create a series of unstable shapes that either had small or negative (completely unstable) critical angles. The critical angles for the unstable stimuli ranged from $-21.69°$ to $17.90°$ ($M = 3.60°, SD = 10.57°$).

Test Stimuli

We wanted a novel set of shapes that would allow us to probe the observers' judgments of stability. The base shape that we used for probing the observer's judgments was an analytically-defined, vertically symmetric elongated shape with a rounded bulge at the top, making it top heavy (see Fig. 4.3).

We manipulated the test shape's stability by adding different levels of curvature to its primary axis while constraining its thickness function along the axis of symmetry (Biederman, 1987; Blum, 1967; Feldman & Singh, 2006; Marr & Nishihara, 1978). With no curvature, the object was vertically upright and stable (critical angle = 10.52° in either direction) (see shape *a* in Fig. 4.3). Increasing the curvature of the primary axis bent the shape, shifting the object's COM. The physical stability – defined using the critical angle – decreased as the curvature increased, as the horizontal position of the COM approached the edge of the object's base. Once the COM was no longer vertically above the base, the object was unstable and would not stay upright, as presented (see shape *c* in Fig. 4.3). The curvature where the object was equally likely to stay upright or fall – when the COM was directly over the edge of the base – was defined as the tipping point (see shape *b* in Fig. 4.3).

A set of 201 versions of the test shape were generated, with curvatures ranging from

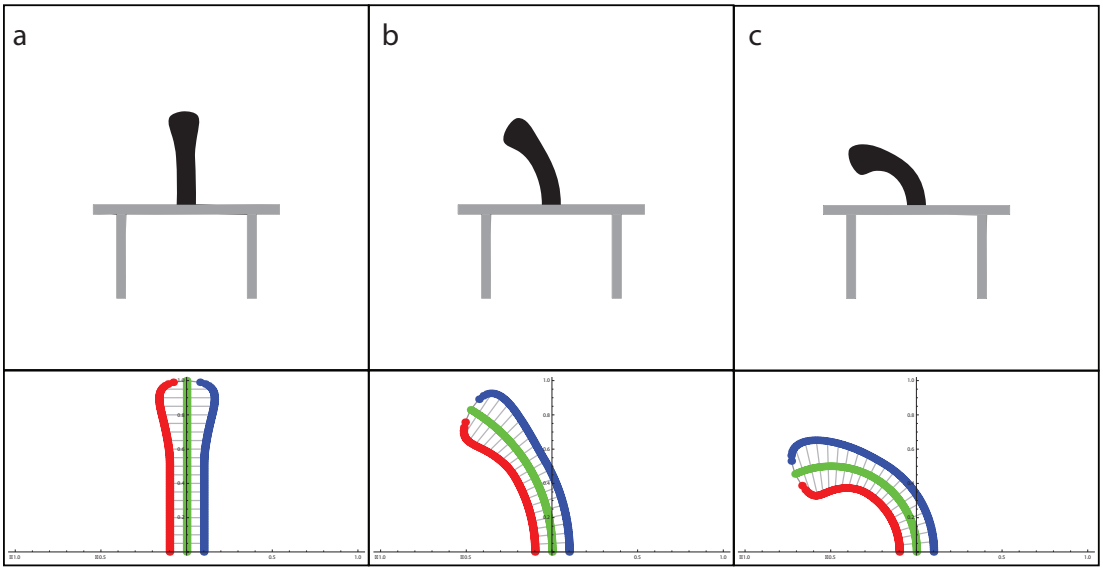

Figure 4.3: Examples of the 2D curvature test shapes. The top shapes show examples of the stimuli shown to observers and the bottom plots illustrate how the shapes' axes were curved while ribs were kept perpendicular to their axis tangents. The left-most shape (a) has the minimum curvature and is completely stable, the right-most shape (c) has the maximum curvature and is completely unstable, and the center shape (b) is at its tipping point.

0 DVA^{-1} to 0.54 DVA^{-1}. The critical curvature ("tipping point") for the test shape was 0.28 DVA^{-1}. The curvatures were converted to a 0 to 2 scale, where 0 was no curvature (0 DVA^{-1}) and 2 was the maximum curvature presented (0.54 DVA^{-1}), making the critical curvature 1.04. During the experiment, the test shape was shown curved either to the left or the right.

Design

The experiment used a yes/no paradigm, where observers were asked to judge whether a test stimulus would stay upright or fall over. There were a total of four conditions, a pre-test with no adaptation, the two adaptation conditions counterbalanced across subjects, and a post-test without adaptation. Observers completed the baseline condition, a single adaptation condition, took a 5 minute break, completed the second adaptation condition, and finished with the post-test.

Observers were instructed to judge whether the test shapes would fall or stay upright (by pressing "f" if the shape would fall and "j" if the shape would stay upright).

They were shown an example of an extremely stable test shape ($curvature = 0$) and an extremely unstable test shape ($curvature = 2$) to illustrate the range of possible curvatures. In addition, they were instructed to judge each shape as if it were a frame from a movie, where the object could fall or stay upright in the next frame. Observers were given 10 practice trials and all observers confirmed that they understood the task and felt that they could readily judge whether a shape would fall or stay upright.

For each condition, stimuli were chosen using the Psi adaptive staircase method, described by Kontsevich and Tyler (1999), implemented in MATLAB with the Palamedes toolbox (Kingdom & Prins, 2010). The Psi method allows for estimation of the point of subjective equality (PSE) – the tipping point in these experiments – and slope – the difference threshold – of the psychometric function for observers' judgments.

For the pre-test condition, observers were shown a fixation cross for 1000 ms, a test stimulus – drawn from the pool of 201 test curvatures (selected using the Psi adaptive staircase method) and randomly curved to the left or right – for 250 ms, and then a screen with only the "table" and were asked to respond if the test stimulus would fall or stay upright. A total of 50 trials were shown for the pre-test, with a forced break between the 25th and 26th trials. After confirming that the observer had a clear understanding of the task, he/she then began either the stable or unstable adaptation condition (counterbalanced across subjects).

In the adaptation conditions, we used a top-up procedure to adapt observers to either stable or unstable shapes (Hong & Papathomas, 2006; Burr et al., 2011). For the first trial, observers were shown a fixation cross for 1000 ms, a series of 40 adaptation stimuli – drawn randomly without replacement from the 45 generated – that were shown for 500 ms each (20 seconds total), another fixation cross for 500 ms, a test stimulus for 250 ms, and then a screen with only the table and were asked to respond if the test stimulus would fall or stay upright. Subsequent to the first trial, the adaptation was topped up by showing a sequence of 10 adapting shapes prior to each test shape. This was repeated until the break, after which observers were shown another random series of 45 shapes, with the 10 shape top-up procedure for the subsequent trials.

4.2.2 Results

The Psi method was used to estimate the observers' PSEs for each condition with 95% confidence intervals (Kingdom & Prins, 2010). The pre-test condition data were found to be noisy for most observers – with large 95% confidence intervals and non-converging data, presumably because most observers were naïve to the testing procedure and used the pre-test as an extended "practice" –, so only the adaptation conditions were used for further analysis. Because the post-test condition immediately followed the second adaptation condition, it was excluded due to potential residual adaptation aftereffects.

A shift in the adaptation condition PSEs could indicate the presence of priming – i.e., judgments biased in the direction of the adapting shapes – or of an aftereffect – where adaptation leads to judgments in the *opposite* direction of the adapting shapes. Seven out of 10 observers had significantly different PSEs for the Stable and Unstable Adaptation conditions (PSEs for each condition fell outside of the 95% confidence intervals for the other condition). Fig. 4.4 illustrates the individual observers' PSEs, standardized by removing the bias. And, as predicted, all of the observers with significant differences were biased to underestimate stability after adapting to high-stability shapes and overestimate stability after adapting to low-stability shapes – consistent with a stability aftereffect.

In addition, bias was measured for each observer by averaging the two adaptation conditions to see if there was a systematic under or overestimation bias. As shown in Fig. 4.5, 7 out of 10 of the observers underestimated the stability on average while the other 3 overestimated stability, with an average PSE of 0.97 (0.26 DVA^{-1}), which is below the physical tipping point of 1.04 (0.28 DVA^{-1}). Although there was a bias to underestimate stability, it was not large.

4.2.3 Discussion

The observers in Exp. 1 exhibited a stability aftereffect when asked if the curved test shape would fall or stay upright. After viewing highly stable shapes, they judged test shapes with lower curvature to be unstable and after viewing highly unstable shapes,

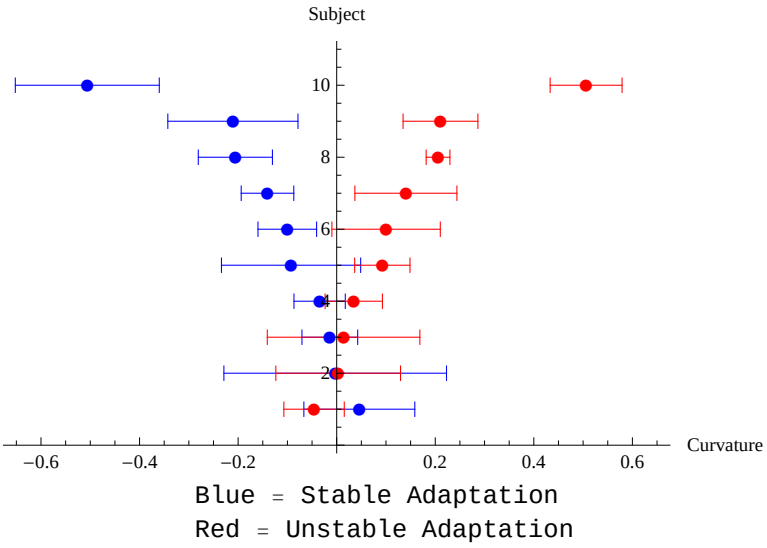

Figure 4.4: PSE results using 2D curvature test shapes standardized by removing bias (average PSE for the adaptation conditions). Subjects (y-axis) were sorted by magnitude of the aftereffect (PSE for Unstable Adaptation - PSE for Stable Adaptation), with individuals showing the smallest aftereffect at the bottom and those with the largest at the top. Note: Curvatures are presented using a 0 (0 DVA^{-1}) to 2 (0.54 DVA^{-1}) scale.

they would judge test shapes with higher curvature to be stable. This means that their percept of the tipping point is affected by the stability of the adapting shapes and that the shift in their percept is consistent with a stability aftereffect prediction (rather than priming).

4.3 Experiment 2: 2D Shift Probe

Exp. 1 showed that observers shifted their perceived tipping point when they were shown highly stable or unstable adapting stimuli. We wanted to test the robustness of our finding by making sure that it wasn't somehow specific to the curvature manipulation. Therefore, in Exp. 2, we used test shapes that provided a very different manipulation of shape (top/bottom shift) that could also be used to demonstrate a stability aftereffect when judging the tipping point of shapes.

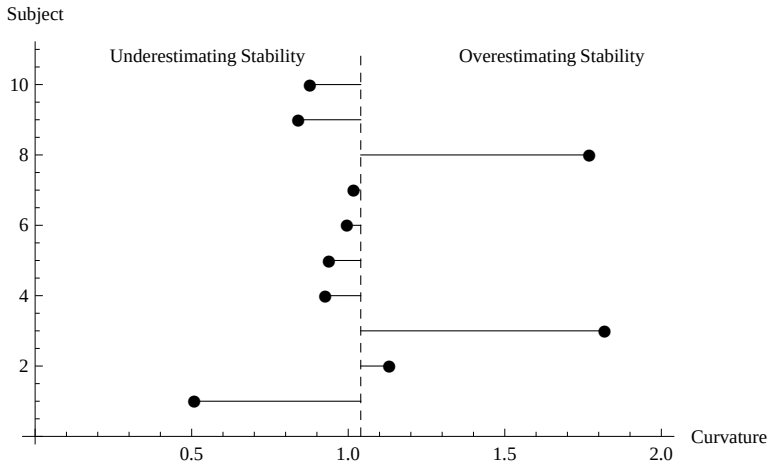

Figure 4.5: Bias results for the 2D curvature experiment. Subjects (y-axis) have the same ordering as in Fig. 4.4, where individuals showing the smallest aftereffect are at the bottom and those with the largest at the top. Note that the vertical dashed line is the physical tipping point for this test measure. Note: Curvatures are presented using a 0 (0 DVA^{-1}) to 2 (0.54 DVA^{-1}) scale, with the critical curvature at 1.04 (0.28 DVA^{-1}).

4.3.1 Methods

Observers

Ten Rutgers University undergraduate students. All reported normal or corrected-to-normal vision.

Apparatus

As in Exp. 1, the stimuli were generated in MATLAB 2012a using Psychtoolbox-3 and observers were comfortably seated with a chin-rest 80 cm from the screen.

Adaptation Stimuli

The adaptation shapes were identical to the 2D adaptation shapes used in Exp. 1, either very stable – bottom heavy with very high critical angles – or very unstable – top heavy with very small or negative critical angles (see Fig. 4.2 for examples). And as in Exp. 1, a total of 45 unique high stability adapting shapes were generated, with unstable shapes being the same objects turned upside-down.

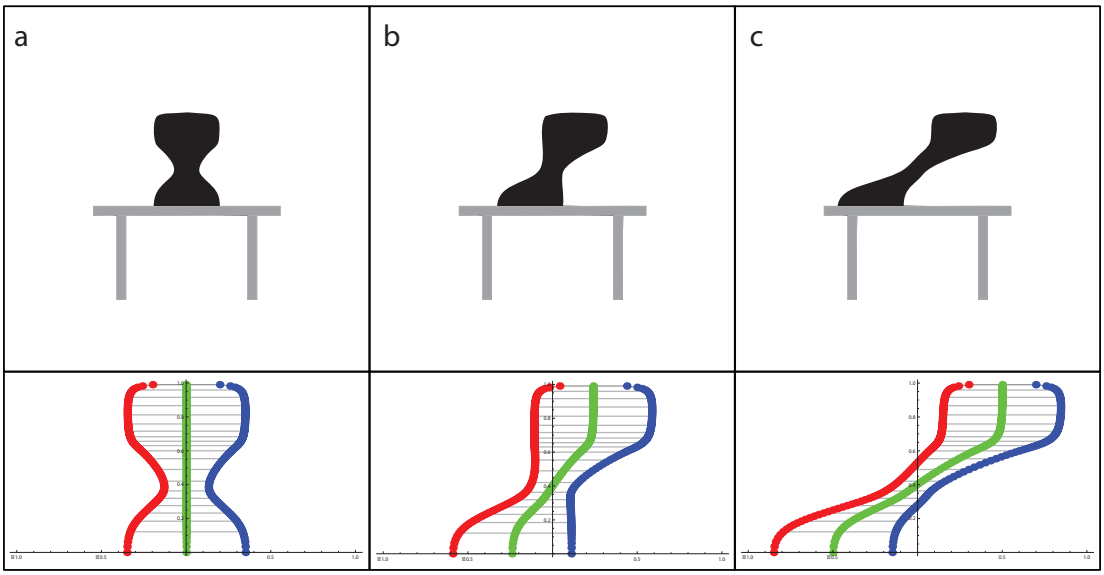

Figure 4.6: Examples of the 2D shift test shapes. The top shapes show examples of the stimuli shown to observers and the bottom plots illustrate how the axes bent as the B-spline control points were shifted. The left-most shape (a) has the no shift and is completely stable, the right-most shape (c) has the maximum shift presented and is completely unstable, and the center shape (b) is at its tipping point.

Test Stimuli

The primary differences from Exp. 1 were the base shape and the transformation used for probing the observer's judgments. For this experiment, the object was an analytically-defined bar-bell-like shape with a rounded bulge at both the top and the bottom (see Fig. 4.6). The top was slightly rounded while the bottom had a flat bottom.

The test shapes were manipulated by shifting the top and bottom parts in opposite directions, so that as the lateral separation between the top and bottom increased, the shape would become less stable. In order to give the perceptual appearance of the top and bottom moving in opposite directions, the test shape was manipulated by shifting the B-spline functions' control points, rather than simply applying a skew to the object. Each side of the shape was composed of 7 control points, with the first 6 of each side defining the barbell shape and the 7^{th} shared as the top-most point. To apply the shift, the bottom 2 points for the left and right functions were moved in one direction and the top 3 points were moved in the opposite direction, while the 3^{rd} and 4^{th} points were kept stationary. This lead to the object shifting its top and bottom features without

introducing a strong perceived skew (see Fig. 4.6).

With no shift, the object was vertically upright and stable. Increasing the lateral shift between the top and bottom shifted the location of the COM relative to the supporting base. So, as the shift increased, the physical stability – defined using the critical angle – decreased. And as with the curvature measure, once the COM was no longer vertically above the base, the object was unstable and would not stay upright as presented. The magnitude of lateral shift for which the object was equally likely to stay upright or fall – when the COM was directly over the edge of the base – was defined as the tipping point.

51 test stimuli were generated with shifts ranging from 0 DVA to 3.72 DVA. The tipping point for these test shapes was 1.79 DVA (see shape b in Fig. 4.6). The shifts were converted to a 0 to 0.5 scale, where 0 was no shift (0 DVA) and 0.5 was the maximum shift presented (3.72 DVA), making the critical lateral shift 0.24. During the experiment, the top of the test shape was shifted either to the left or the right.

Design

As in Exp. 1, this design used a yes/no paradigm to judge if the test stimulus would stay upright or fall. There were four conditions, a pre-test with no adaptation, the two adaptation conditions counterbalanced across subjects, and a post-test without adaptation. As in Exp. 1, observers completed the baseline condition, a single adaptation condition, took a 5 minute break, completed the second adaptation condition, and finished with the post-test.

The experimental procedure was the same as in Exp. 1.

Stimuli were chosen using the Psi adaptive staircase method so that we could estimate the PSE – the tipping point in these experiments – of the psychometric function for observers' judgments. In the adaptation conditions, we used the same top-up procedure to adapt observers to either high-stability or low-stability shapes as was used in Exp. 1.

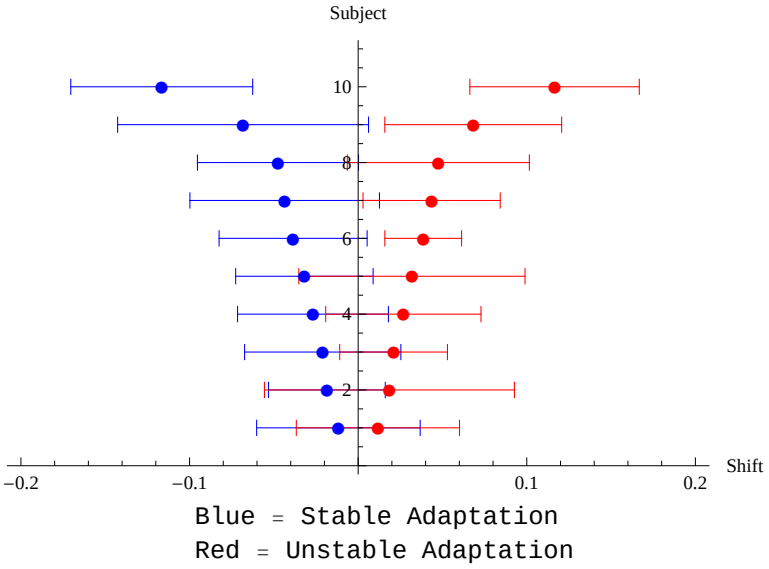

Figure 4.7: PSE results using a 2D shift test shape standardized by removing bias (average PSE for the adaptation conditions). Subjects (y-axis) were sorted by magnitude of the aftereffect (PSE for Unstable Adaptation - PSE for Stable Adaptation), with individuals showing the smallest aftereffect at the bottom and those with the largest at the top. Note: Lateral shifts are presented using a 0 (0 DVA) to 0.5 (3.72 DVA) scale.

4.3.2 Results

The Psi method was used to estimate the observers' PSEs with 95% confidence intervals (Kingdom & Prins, 2010). All 10 subjects showed an effect of adaptation in the expected direction, i.e. all were biased in the direction of underestimating stability after adapting to stable objects and overestimating stability after adapting to unstable objects – consistent with a stability aftereffect. As shown in Fig. 4.7, this difference was statistically significant for 6 out of the 10 observers (PSEs for each condition fell outside of the 95% confidence intervals for the other condition).

Bias was measured for each observer by averaging their PSEs in the two adaptation conditions to see if there was a systematic under or overestimation bias. As shown in Fig. 4.8, 7 out of 10 of the observers overestimated the stability on average while the other 3 underestimated stability, with an average PSE of 0.29 (2.16 DVA), which is above the physical tipping point of 0.24 (1.79 DVA).

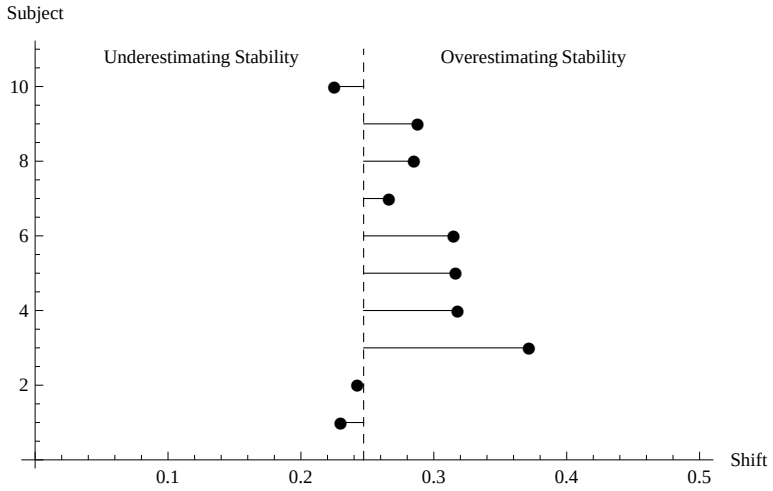

Figure 4.8: Bias results for the 2D shift experiment. Subjects (y-axis) have the same ordering as in Fig. 4.7, where individuals showing the smallest aftereffect are at the bottom and those with the largest at the top. Note that the vertical dashed line is the physical tipping point for this test measure. Note: Lateral shifts are presented using a 0 (0 DVA) to 0.5 (3.72 DVA) scale, with the physical tipping point at 0.24 (1.79 DVA).

4.3.3 Discussion

Exp. 2 used an alternative manipulation of the test shape to measure the adaptation effects of perceived stability. We found that high-stability adapting shapes led to underestimation of the test shape's stability and that low-stability adapting shapes led to overestimation of the test shape's stability, both of which are consistent with Exp. 1's findings.

The effect clearly is not simply a "curvature aftereffect" nor is it a "shift aftereffect", but appears to be a bonafide stability aftereffect. Since the results of Exp. 1 and Exp. 2 support the presence of a stability aftereffect, they, *ipso facto*, provide support for the "stability as a unitary dimension" hypothesis.

4.4 Experiment 3: 3D Curvature Probe

After conducting Exps. 1 and 2, we wanted to see if the aftereffect would generalize to a more naturalistic setting. So, for Exp. 3, we took the stimuli from Exp. 1, inflated the 2D silhouettes into 3D shapes, and tested for a stability aftereffect in stereoscopic

3D renderings. Since it may be difficult to interpret physical stability for 2D shapes – we rarely interact with planar objects similar to those presented in Exps. 1 and 2 – in Exp. 3, we generated 3D shapes that could have created the 2D shapes in Exps. 1 and 2, presented them stereoscopically to subjects, and tested to see if adapting to stable and unstable objects would cause a change in perceived stability.

4.4.1 Methods

Observers

Ten Rutgers University undergraduate students. All reported normal or corrected-to-normal vision.

Apparatus

The 3D stimuli were generated in MATLAB 2012a using Psychtoolbox-3 and presented on a Sony Trinitron 20 inch CRT with a 1024 x 768 pixel resolution at a refresh rate of 140Hz using NVIDIA 3D Vision 2 stereoscopic glasses (for a stereoscopic refresh rate of 70Hz). Observers were seated 80 cm from the screen.

Adaptation Stimuli

The adaptation objects were 3D shapes derived from the 2D silhouettes generated in Exps. 1 and 2. To generate the 3D objects, slices locally perpendicular to the shape's axis were taken along the length of the shape's axis. Each slice was turned into a circular disk, where the disk's diameter was the width of the slice and the disk was centered in the middle of the slice. These disks were stacked and the vertices for the slices were connected to create a smooth surface. This created a shape with a central axis that followed the curvature of the two sides of the shape in the x-y plane but had no curvature in the y-z plane. An analogy would be that the shapes were generated as if extruded from a nozzle, similar to an icing pipette, with width and location varying as a function of height. Normals and texture coordinates were calculated for the surface to create a smooth surface in OpenGL and the shapes were pre-processed for rapid

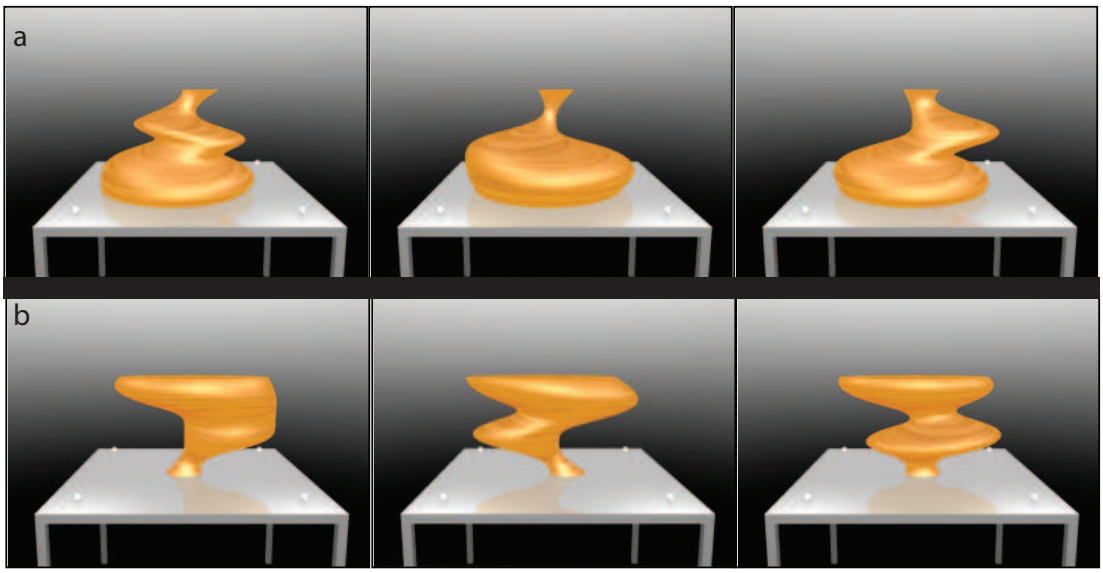

Figure 4.9: Examples of the 3D adaptation stimuli. The stimuli in the top row (a) are examples of high-stability shapes, while the stimuli in the bottom row (b) are examples of low-stability shapes. Note that the shapes in row (a) were vertically flipped in the experiment to produce low-stability adaptation shapes (whose analogs are not illustrated in this figure).

presentation. See Fig. 4.9 for examples of the 3D adaptation stimuli.

As with the 2D adaptation stimuli, the 3D adaptation stimuli were either very stable – bottom heavy with very high critical angles – or very unstable – top heavy with very low or negative critical angles (again, negative meaning that the shapes would not stand up as presented) (see Fig. 4.9). The objects were placed on a virtual table with a reflection to simulate dull metal. Identical shapes were used for both the high and low stability adaptation conditions, with the low-stability shapes being the high-stability shapes turned upside down.

Test Stimuli

Analogous to Exp. 1, the base shape used for probing the observer's judgments was an analytically-defined cylinder with a rounded bulge at the top, making it top heavy. The base shape was inflated using the method described above, to create a 3D tubular object with a bulge at the top (see Fig. 4.10).

The test shape's stability was manipulated by adding curvature to its axis while

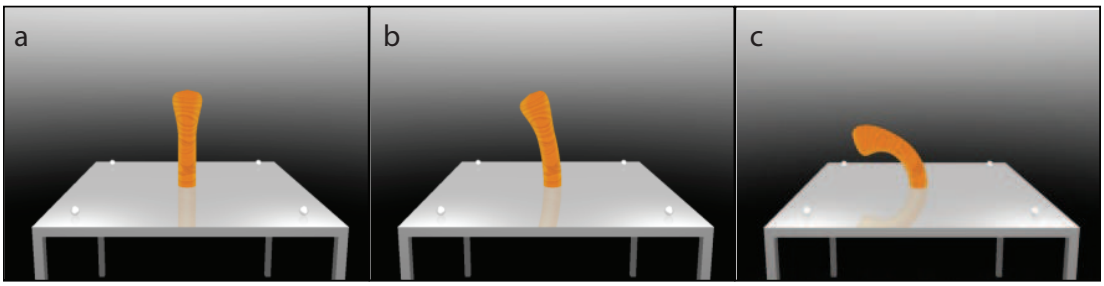

Figure 4.10: Examples of the 3D curvature test shape stimuli. The left-most shape (a) has the minimum curvature and is completely stable, the right-most shape (c) has the maximum curvature and is completely unstable, and the center shape (b) is at its tipping point.

maintaining the thickness function along the axis (Biederman, 1987; Blum, 1967; Feldman & Singh, 2006; Marr & Nishihara, 1978). With no curvature, the object was vertically upright and stable. And, as in Exp. 1, as curvature was added, the object's COM would shift until it was no longer over the base, which would cause the object to fall. The curvature where the object was equally likely to stay upright or fall was defined as the tipping point.

A set of 201 test stimuli were generated by with curvatures ranging from 0 DVA^{-1} to 0.27 DVA^{-1}. The critical curvature ("tipping point") for these curved 3D test shapes was 0.07 DVA^{-1}. The curvatures were converted to a 0 to 2 scale, where 0 was no curvature (0 DVA^{-1}) and 2 was the maximum curvature presented (0.27 DVA^{-1}), making the critical curvature 0.52 (0.07 DVA^{-1}). During the experiment, the test shape was shown curved either to the left or the right.

Design

As in Exps. 1 and 2, this design used a yes/no paradigm with four conditions, a pre-test with no adaptation, the two adaptation conditions counterbalanced across subjects, and a post-test without adaptation.

The experimental procedure was the same as in Exp. 1.

Stimuli were chosen using the Psi adaptive staircase method so that we could estimate the PSE of the psychometric function for observers' judgments. In the adaptation conditions, we used the same top-up procedure to adapt observers to either

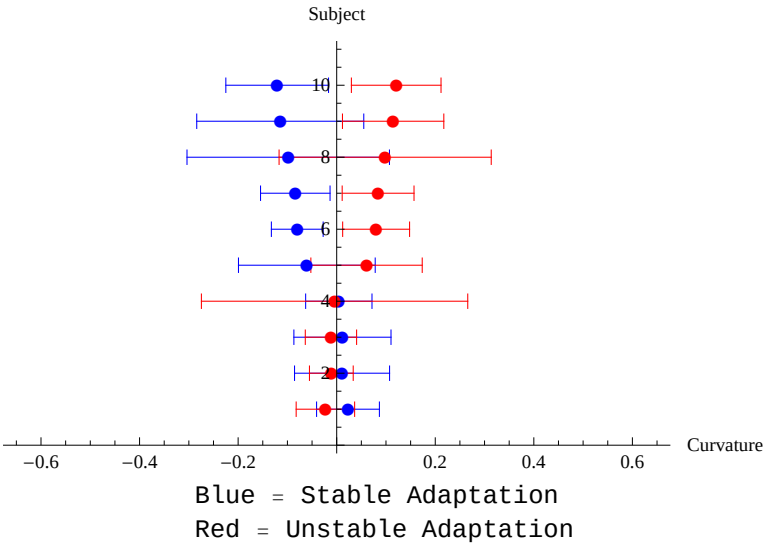

Figure 4.11: PSE results using a 3D curvature probe standardized by removing bias (average PSE for the adaptation conditions). Subjects (y-axis) were sorted by magnitude of the aftereffect (PSE for Unstable Adaptation - PSE for Stable Adaptation), with individuals showing the smallest aftereffect at the bottom and those with the largest at the top.

high-stability or low-stability shapes, as was used in Exps. 1 and 2.

4.4.2 Results

The Psi method was used to estimate the observers' psychometric curves for each condition and provided an estimate of the PSEs with 95% confidence intervals. As shown in Fig. 4.11, 6 of the 10 observers were biased in direction predicted by the stability aftereffect, 4 having significantly different PSEs for the Stable and Unstable Adaptation conditions.

As shown in Fig. 4.12, 8 out of 10 of the observers overestimated the stability on average while the other 2 underestimated stability, with an average PSE of 0.95 (0.13 DVA^{-1}), which is above the physical tipping point of 0.52 (0.07 DVA^{-1}). On average, the observers in this experiment had a larger bias to overestimate stability than those in Exp. 1, perhaps due to perceived foreshortening of the 3D objects causing them to neglect the additional mass in depth, which contributes more mass to the bulge at the top of the test shapes than the thinner "body".

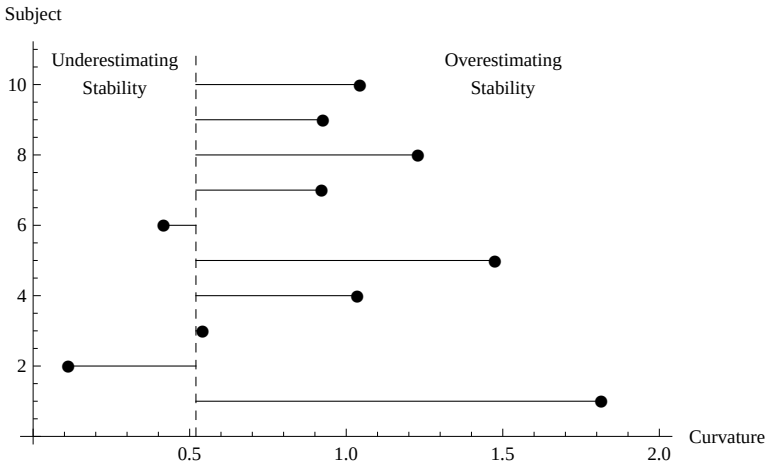

Figure 4.12: Bias results for the 3D curvature experiment. Subjects (y-axis) have the same ordering as in Fig. 4.11, where individuals showing the smallest aftereffect are at the bottom and those with the largest at the top. Note that the vertical dashed line is the physical tipping point for this test measure. Note: Curvatures are presented using a 0 (0 DVA^{-1}) to 2 (0.27 DVA^{-1}) scale, with the critical curvature at 0.52 (0.07 DVA^{-1}).

4.4.3 Discussion

The results of this experiment demonstrate that while the majority of observers had a significant aftereffect for 3D stimuli, on average, the effect was weaker than for 2D stimuli (see Fig. 4.4 for 2D results). However, it is difficult to say definitively that this was due to the manipulation of 2D (Exp. 1) versus 3D (Exp. 3) because different observers participated in the two experiments.

4.5 Experiment 4: 3D Shift Probe

In the final experiment, we used the 3D adapting shapes from Exp. 3 with 3D test shapes that were generated from the shift silhouettes in Exp. 2 and tested to see if if adaptation to object stability would also be observed using this different geometric manipulation of the test shape.

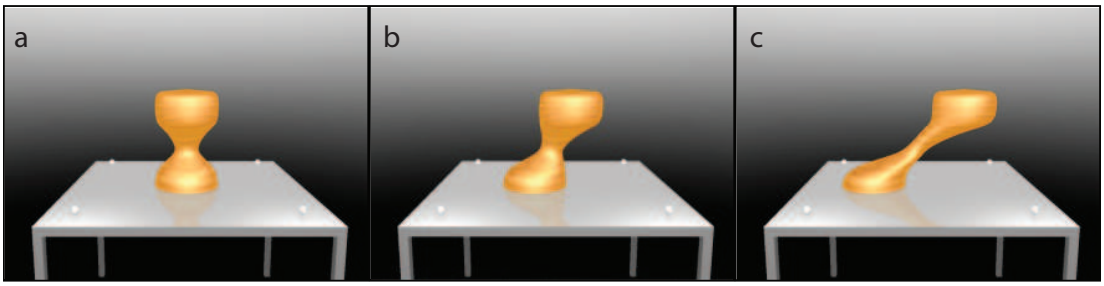

Figure 4.13: Examples of the 3D shift test shape stimuli. The left-most shape (a) has the no shift and is completely stable, the right-most shape (c) has the maximum shift presented and is completely unstable, and the center shape (b) is at its tipping point.

4.5.1 Methods

Observers

Ten Rutgers University undergraduate students. All reported normal or corrected-to-normal vision.

Apparatus

This experiment used the same apparatus as Exp. 3.

Adaptation Stimuli

This experiment used the same adapting stimuli as Exp. 3. See Fig. 4.9 for examples of the 3D adaptation stimuli.

Test Stimuli

As in Exp. 2, the base shape used for probing the observer's judgments was an analytically-defined bar-bell-like shape with a rounded bulge at both the top and the bottom. The 2D shape was inflated using the method described in Exp. 3, to create a 3D cylindrical object (see Fig. 4.13 for example test shapes).

The test shape's stability was manipulated by shifting the top and bottom in opposite directions, in the same manner described in Exp. 2. With no shift, the object was vertically upright and stable. And, as in Exp. 2, as the top and bottom were shifted in opposite directions, the object's base would shift relative to its COM until it was no

longer stable. As in the previous experiments, the shift where the object was equally likely to stay upright or fall was defined as the tipping point.

Fifty-one test stimuli were generated by with top/bottom shifts ranging from 0 DVA to 7.42 DVA. The tipping point for these test shapes was 2.98 DVA. The shifts were converted to a 0 to 0.5 scale, where 0 was no shift (0 DVA) and 0.5 was the maximum shift presented (7.42 DVA), making the critical lateral shift 0.20 (2.98 DVA). During the experiment, the top of the test shape was randomly shifted either to the left or the right.

Design

As in the previous experiments, this design used a yes/no paradigm with four conditions: a pre-test with no adaptation, the two adaptation conditions counterbalanced across subjects, and a post-test without adaptation.

The experimental procedure was the same as in Exp. 2.

Stimuli were chosen using the Psi adaptive staircase method so that we could estimate the PSE of the psychometric function for observers' judgments. In the adaptation conditions, we used the same top-up procedure to adapt observers to either stable or unstable shapes as was used in the previous experiments.

4.5.2 Results

The Psi method was used to estimate the observers' PSEs with 95% confidence intervals. All 10 observers were biased in the direction predicted by a stability aftereffect, with 5 of the 10 observers having significantly different PSEs for the Stable and Unstable Adaptation conditions (see Fig. 4.14).

As shown in Fig. 4.15, 8 out of 10 of the observers overestimated the stability on average while the other 2 underestimated stability, with an average PSE of 0.30, which is above the physical tipping point of 0.20. As with the results from Exp. 3, on average, the observers in this experiment had a larger biased to overestimate stability than those in Exp. 2.

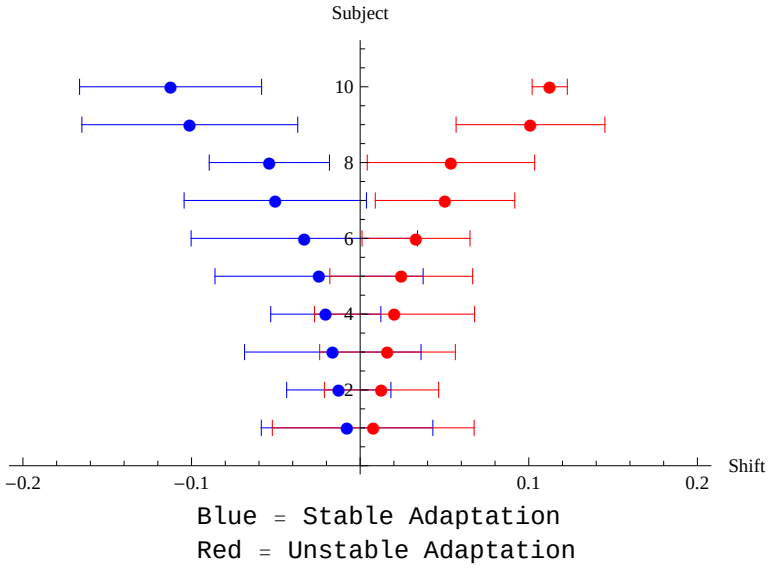

Figure 4.14: PSE results using a 3D shift test shape standardized by removing bias (average PSE for the adaptation conditions). Subjects (y-axis) were sorted by magnitude of the aftereffect (PSE for Unstable Adaptation - PSE for Stable Adaptation), with individuals showing the smallest aftereffect at the bottom and those with the largest at the top. Note: Lateral shifts are presented using a 0 (0 DVA) to 0.5 (7.42 DVA) scale.

4.6 Conclusion

We found converging evidence that people adapt to object stability, and exhibit a "stability aftereffect" when making stability judgments after observing using different shape manipulations of the test object, such curving the axis and introducing lateral shift between the top and bottom halves. This visual adaptation is quite robust, causing aftereffects for both 2D and 3D stereoscopically presented scenes. Stability adaptation is quite surprising because estimating the stability of an object requires integration of a number of different aspects – using the object's shape to estimate COM and inference of gravitational forces on the object – so judging stability may have been dependent upon higher level reasoning. However, the presence of the aftereffect argues for a lower level perceptual representation of object stability.

From a purely physical perspective, it would be surprising for the perceived stability to be affected by previously observed objects. But it may be possible that our visual system is tuned to emphasize instability, given the fact that the majority of objects

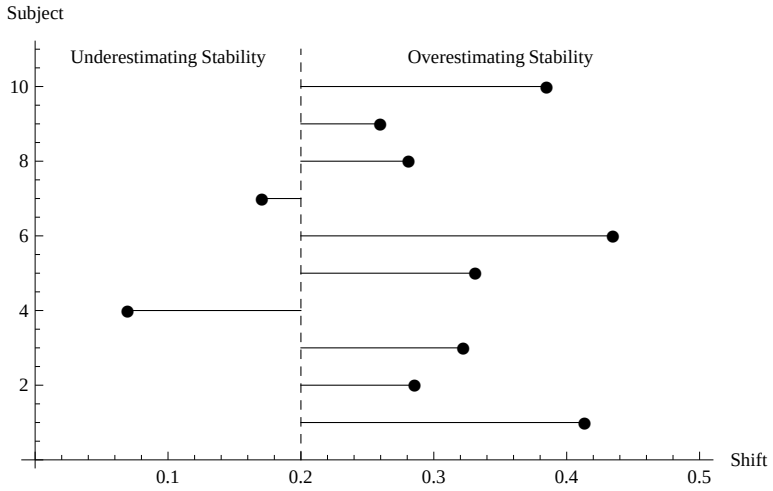

Figure 4.15: Bias results for the 3D shift experiment. Subjects (y-axis) have the same ordering as in Fig. 4.14, where individuals showing the smallest aftereffect are at the bottom and those with the largest at the top. Note that the vertical dashed line is the physical tipping point for this test measure. Note: Lateral shifts are presented using a 0 (0 DVA) to 0.5 (7.42 DVA) scale, with the physical tipping point at 0.20 (2.98 DVA).

we observe and interact with are normally in a stable equilibrium. If this were the case, we would see systematic underestimation of stability if observers are told to judge whether an object is stable or not and, in fact, this is what Samuel and Kerzel (2011) found. In our experiments presented here, observers were biased to judge the stability of test objects "on the safe side" after viewing very stable objects, consistent with the results of Samuel and Kerzel (2011), however, we also found that the direction of the bias could be reversed, causing them to judge the stability of probe objects "recklessly" after adapting to unstable objects.

These results, coupled with the previous results in Cholewiak et al. (2012), suggest that stability is a physical aspect of shape that is judged along a unitary dimension. People are able to infer the force of gravity acting upon the shapes and predict whether the objects will stay upright or fall, regardless of whether they are presented as 2D silhouettes (Exp. 1 and 2) or as volumetric 3D objects (Exp. 3 and 4). In addition, observers' stability judgments are affected regardless of the test shape's manipulation, whether the probe's curvature (Exp. 1 and 3) or the top-bottom shift (Exp. 2 and 4) were manipulated, meaning that we were not simply observing a curvature or shift

aftereffect. Although the visual estimation of object stability is sometimes considered to be a higher-level judgment, our results suggest that it is a bona fide perceptual variable that is susceptible to adaptation effects.

This conclusion is consistent with our previous finding, using a stability matching task, that subjects find it easy and natural to adjust the aspect ratio of one object so that it is perceived as being equally stable as another, despite the fact that the two objects have different shapes. Similar to color metamerism, where colors that are composed of different wavelengths appear the same, shapes with the same perceived stability would be stability metamers. In Cholewiak et al. (2012), we demonstrated that observers had no difficulty comparing the stability of 3D shapes (slanted conical frustums and cylinders) and readily estimated stability metamers that could be predicted using aspects of stability – specifically the minimum critical angles of the two objects. In the experiments herein, we show that observers were able to estimate the tipping point, regardless of the underlying shape manipulation, meaning that the manipulated shapes at their tipping points were stability metamers.

Our results indicated that some judgments of physical attributes, such as object stability tested here, actually involve unidimensional perceptual variables.

Chapter 5

Conclusion

The inference of forces is an ecologically important aspect of visual perception. We use it to make judgments of physical interactions – including collisions (Scholl & Nakayama, 2002), support relations (Baillargeon & Hanko-Summers, 1990; Baillargeon et al., 1992) and stability (Barnett-Cowan et al., 2011; Samuel & Kerzel, 2011) – in the service of future actions. The reported research provides evidence for the visual estimation of stability, which requires the inference of gravitational forces acting upon objects.

As shown in Chapter 2, observers judgments of an object's stability are invariant to the volume of the object and appeared to only be a function of the object's shape. This is significant for the representation of the object's physical parameters, such as the COM and bounding contour, because it suggests we use an objects shape – rather than relying on purely retinotopic representations – when making stability judgments.

The critical angle tasks described in Chapter 2 identified a shape-dependent stability effect, specifically that stability was underestimated for short-and-wide shapes, and overestimated for tall-and-narrow shapes. This contradicts the assertion by Samuel and Kerzel (2011) – in the context of 2D shapes – that stability judgments would always be "on the safe side". And although there were biases to under and overestimate the stability of the object, observers were on average close to the physical prediction, suggesting that they used an physically correct internal model to make their judgments. When asked to estimate the COM, observers were even closer to the physical predictions. On the individual level though, observers do not appear to rely on the COM in making judgments of physical stability. Their COM stability estimates are much less biased and have a larger effect of aspect ratio.

When adding a part to the conical frustums, observers tended on average to down-weight the influence of the attached part on the object's physical stability. Although their perceived influence was often close to the physical influence of the part on overall stability, there was a tendency to underestimate the part's contribution and decrease the perceived influence of the part's additional mass. This down-weighting is consistent with a robust-statistics approach to determining the influence of a potentially separate part on global shape estimation (Cohen & Singh, 2006; Denisova et al., 2006). It provides some evidence for part-based representation of shape (versus an unstructured, template-like account of shape representation, where all points within a shape are treated equally).

Chapter 3 addressed the question of whether stability is a unitary dimension. Do people use an "internal scale" of very stable and unstable objects when judging the stability of other objects (perhaps calibrated to their own perceptual biases)? Moreover, a potential concern with using the critical angle task (as introduced in Chapter 2) as a measure of *overall* stability is that with asymmetric objects, the critical angle is not a single number, but instead a function of the direction of tilt.

Therefore, the first experiment in Chapter 3 investigated how well observers could track the critical angle as a function of the direction of skew for asymmetric 3D objects. We found that observers were quite accurate for most skew directions (as would have been expected from the critical angle results in Chapter 2). Given that observers' performance for asymmetric objects was established, the subsequent experiments addressed the idea that if perceived stability were a one dimensional attribute, then observers should have been able to assign a single value to describe an object's stability. We investigated how are the critical angles in different directions combined into a single estimate of object stability.

This required a separate task that assessed overall stability, so we asked observers to match different objects' stabilities and tested to see if there was a predictable relationship between the critical angles of asymmetric shapes and their perceived stabilities. The results showed that, for most observers, the minimum critical angle was a better model for their stability estimate than the mean, namely, that the critical angle in the

least stable direction of tilt was a better predictor for the overall perceived stability than the mean critical angle. Given that observers readily matched the perceived overall stabilities of different objects and that their judgments were consistent across the aspect ratio manipulation, the results of Chapter 3 suggested that stability is judged as along a unitary dimension. However, is it a truly perceptual dimension?

In Chapter 4, we found converging evidence that people visually adapt to object stability and exhibit a "stability aftereffect." Observers adapted to 2D and 3D objects that were flashed on the screen and were then asked to judge the stability of test objects. Across two adaptation conditions, the sets of adaptation objects were either all highly stable, or all highly unstable. The test objects were manipulated in two different ways (curvature and top/bottom shift) and all of the results across the four experiments supported the assertion that observers adapt to the perceived stability of objects and exhibit an aftereffect, perceiving the test object as more stable after adapting to very unstable objects and less stable after adapting to very stable objects.

Although the estimation of object stability is sometimes considered to be a high-level judgment, this research project's results suggest that it is a bona fide perceptual variable that is susceptible to adaptation effects. The results suggest that some judgments of physical attributes, such as object stability tested here, actually involve unidimensional perceptual variables.

However, although these experiments provide supportive evidence for a perceptual representation of stability, this research project did not directly investigate the hierarchy of perceptual processing and how a representation of stability is generated from lower-level features. It is still an open question of how the brain takes low-level surface features, for example orientation, and processes them into more complex representations, like contour and shape; and similarly takes representations of shape and computes higher-level visual estimates of object stability. Therefore, future research could focus on how "simple features" of objects and scenes are combined into a more complex perceptual representation of shape, upon which the brain applies physical models of forces to judge a composite of the lower-level features, the object's stability.

Given the surprising result of perceptual adaptation to 2D and 3D object stability,

it would be important in future studies to examine this phenomenon in greater detail, especially with respect to the time course of the adaptation. For example: How long does the adaptation persist? How resistant is it to repeated presentations of the test stimuli? Given that perceptual adaptation has been shown to exhibit build-up and decay over time – for example, as demonstrated with motion (Hoffmann, Dorn, & Bach, 1999), visual gratings (Greenlee, Georgeson, Magnussen, & Harris, 1991), audition (Anstis & Saida, 1985), and chromatic adaptation (Fairchild & Reniff, 1995) – future experiments investigating the time course of stability adaptation would provide further evidence for a purely perceptual representation of shape.

References

Anderson, B. L., Singh, M., & Fleming, R. (2002). The interpolation of object and surface structure. *Cognitive Psychology*, *44*, 148–190. doi: 10.1006/cogp.2001.0765

Anstis, S., & Saida, S. (1985). Adaptation to auditory streaming of frequency-modulated tones. *Journal of Experimental Psychology: Human Perception and Performance*, *11*, 257–271. doi: 10.1037/0096-1523.11.3.257

Baillargeon, R., & Hanko-Summers, S. (1990). Is the top object adequately supported by the bottom object? young infants' understanding of support relations. *Cognitive development*, *5*, 29–53. doi: 10.1016/0885-2014(90)90011-H

Baillargeon, R., Needham, A., & DeVos, J. (1992). The development of young infants' intuitions about support. *Early Development and Parenting*, *1*, 69–78. doi: 10.1002/edp.2430010203

Barnett-Cowan, M., Fleming, R. W., Singh, M., & Bülthoff, H. H. (2011). Perceived object stability depends on multisensory estimates of gravity. *PLoS ONE*, *6*, 1–5. doi: 10.1371/journal.pone.0019289

Baud-Bovy, G., & Gentaz, E. (2004). The visual localization of the centre of triangles in young children and adults. *Current Psychology Letters*, *13*, 2–11.

Baud-Bovy, G., & Soechting, J. (2001). Visual localization of the center of mass of compact, asymmetric, two-dimensional shapes. *Journal of Experimental Psychology: Human Perception and Performance*, *27*, 692–706. doi: 10.1037/0096-1523.27.3.692

Becker, W., & Fuchs, A. F. (1985). Prediction in the oculomotor system: Smooth pursuit during transient disappearance of a visual target. *Experimental Brain Research*, *57*, 562–575. doi: 10.1007/BF00237843

Biederman, I. (1987). Recognition-by-components: A theory of human image understanding. *Psychological Review*, *94*, 115–147. doi: 10.1037/0033-295X.94.2.115

Bingham, G. P., & Muchisky, M. M. (1993). Center of mass perception and inertial frames of reference. *Perception & Psychophysics*, *54*, 617–632. doi: 10.3758/BF03211785

Blum, H. (1967). A transformation for extracting new descriptors of shape. *Models for the perception of speech and visual form*, 362–380.

Brainard, D. (1997). The Psychophysics Toolbox. *Spatial Vision*, *10*, 433–436. doi: 10.1163/156856897X00357

Burr, D. C., Anobile, G., & Turi, M. (2011). Adaptation affects both high and low (subitized) numbers under conditions of high attentional load. *Seeing and Perceiving*, *24*, 141–150. doi: 10.1163/187847511X570097

Burr, D. C., & Ross, H. (2002). Direct evidence that "speedlines" influence motion mechanisms. *The Journal of Neuroscience*, *22*, 8661–8664.

Burr, D. C., & Ross, H. (2008). A visual sense of number. *Current Biology*, *18*, 1–4. doi: 10.1016/j.cub.2008.02.052

Carello, C., Fitzpatrick, P., Domaniewicz, I., Chan, T.-C., & Turvey, M. T. (1992). Effortful touch with minimal movement. *Journal of Experimental Psychology: Human Perception and Performance*, *18*, 290-302. doi: 10.1037/0096-1523.18.1.290

Cholewiak, S. A., Fleming, R., & Singh, M. (2011). Perception of physical stability of asymmetrical three-dimensional objects [abstract]. *Journal of Vision*. doi: 10.1167/11.11.44

Cholewiak, S. A., Fleming, R. W., & Singh, M. (2012). Perception of the physical stability of asymmetrical three-dimensional objects. *Journal of Vision*, Under Review.

Cholewiak, S. A., Singh, M., Fleming, R., & Pastakia, B. (2010). The perception of physical stability of 3d objects: The role of parts [abstract]. *Journal of Vision*, *10*, 77. doi: 10.1167/10.7.77

Cohen, E. H., & Singh, M. (2006). Perceived orientation of complex shape reflects graded part decomposition. *Journal of Vision*, *6*, 805–821. doi: 10.1167/6.8.4

Cooper, P. R., Birnbaum, L. A., & Brand, M. E. (1995). Causal scene understanding. *Computer vision and image understanding*, *62*(2), 215–231. doi:

10.1006/cviu.1995.1051

Dan, B. (2007). *Balancing bricks . . . again . . .* Retrieved from http://www.flickr.com/photos/rocker/2068407802/

Dempsey, J. (2008). *Stone age jenga.* Retrieved from http://www.flickr.com/photos/stonemason/2545658903/

Denisova, K., Singh, M., & Kowler, E. (2006). The role of part structure in the perceptual localization of a shape. *Perception*, *35*, 1073–1087. doi: 10.1068/p5518

Dragoi, V., Sharma, J., Miller, E. K., & Sur, M. (2002). Dynamics of neuronal sensitivity in visual cortex and local feature discrimination. *Nature Neuroscience*, *5*, 883–891. doi: 10.1038/nn900

Dragoi, V., Sharma, J., & Sur, M. (2000). Adaptation-induced plasticity of orientation tuning in adult visual cortex. *Neuron*, *28*, 287–298. doi: 10.1016/S0896-6273(00)00103-3

Fairchild, M. D., & Reniff, L. (1995). Time course of chromatic adaptation for color-appearance judgments. *Journal of the Optical Society of America*, *12*, 824–833. doi: 10.1364/JOSAA.12.000824

Feldman, J., & Singh, M. (2006). Bayesian estimation of the shape skeleton. *Proceedings of the National Academy of Sciences*, *107*, 18014–18019. doi: 10.1073/pnas.0608811103

Freyd, J. J. (1983). The mental representation of movement when static stimuli are viewed. *Perception & Psychophysics*, *33*, 575–581. doi: 10.3758/BF03202940

Freyd, J. J., & Finke, R. A. (1984). Representational momentum. *Journal of Experimental Psychology: Learning, Memory, and Cognition*, *10*, 126–132. doi: 10.1037/0278-7393.10.1.126

Freyd, J. J., & Jones, K. T. (1994). Representational momentum for a spiral path. *Journal of Experimental Psychology: Learning, Memory, and Cognition*, *20*, 968–976. doi: 10.1037/0278-7393.20.4.968

Freyd, J. J., Pantzer, T. M., & Cheng, J. L. (1988). Representing statics as forces in equilibrium. *Journal of Experimental Psychology: General*, *117*, 395–407. doi: 10.1037/0096-3445.117.4.395

Friedman, W. J. (2002). Arrows of time in infancy: The representation of temporal-causal invariances. *Cognitive Psychology*, *44*, 252–296. doi: 10.1006/cogp.2001.0768

Geilser, W. S. (1999). Motion streaks provide a spatial code for motion direction. *Nature*, *400*, 65–69. doi: 10.1038/21886

Gibson, J. J. (1954). The visual perception of objective motion and subjective movement. *Psychological Review*, *61*, 304–314. doi: 10.1037/h0061885

Graf, E. W., Warren, P. A., & Maloney, L. T. (1995). Explicit estimation of visual uncertainty in human motion perception. *Vision Research*, *45*, 3050–3059. doi: 10.1016/j.visres.2005.08.007

Greenlee, M. W., Georgeson, M. A., Magnussen, S., & Harris, J. P. (1991). The time course of adaptation to spatialcontrast. *Vision Research*, *31*, 223–236. doi: 10.1016/0042-6989(91)90113-J

Hamrick, J., Battaglia, P. W., & Tenenbaum, J. B. (2011). Internal physics models guide probabilistic judgments about object dynamics. In *Proceedings of the 33rd cognitive science society annual conference.*

Harris, C. S. (1963). Adaptation to displaced vision: Visual, motor, or proprioceptive change? *Science*, *140*, 812–813. doi: 10.1126/science.140.3568.812

Hoffmann, M., Dorn, T. J., & Bach, M. (1999). Time course of motion adaptation: Motion-onset visual evoked potentials and subjective estimates. *Vision Research*, *39*, 437–444. doi: 10.1016/S0042-6989(98)00186-2

Hong, J., & Papathomas, T. V. (2006). Influences of attention on auditory aftereffects following purely visual adaptation. *Spatial Vision*, *19*, 569–580. doi: 10.1163/156856806779194044

Humphrey, G. K., & Jolicoeur, P. (1993). An examination of the effects of axis foreshortening, monocular depth cues, and visual field on object identification. *The Quarterly Journal of Experimental Psychology, Section A: Human Experimental Psychology*, *46*, 137–159. doi: 10.1080/14640749308401070

Kaiser, M. K., Proffitt, D. R., & Anderson, K. (1985). Judgments of natural and anomalous trajectories in the presence and absence of motion. *Learning, Memory,*

and Cognition, *11*, 795–803. doi: 10.1037/0278-7393.11.1-4.795

Kaiser, M. K., Proffitt, D. R., Whelan, S. M., & Hecht, H. (1992). Influence of animation on dynamical judgments. *Journal of Experimental Psychology*, *18*, 669–690. doi: 10.1037/0096-1523.18.3.669

Kim, I. K., & Spelke, E. S. (1992). Infants' sensitivity to effects of gravity on visible object motion. *Journal of Experimental Psychology: Human Perception and Performance*, *18*, 385–393. doi: 10.1037/0096-1523.18.2.385

Kim, S.-H., Feldman, J., & Singh, M. (2012). Curved apparent motion initiated by a causal launch. *Psychological Science*, In Press.

Kingdom, F. A. A., & Prins, N. (2010). *Psychophysics: A practical introduction.* London: Academic Press.

Kleiner, M., Brainard, D., & Pelli, D. (2007). What's new in psychtoolbox-3? *Perception*, *36*, ECVP Abstract Supplement.

Koenderink, J. J. (1998). Pictorial relief. *Philosophical Transactions of the Royal Society of London Series A*, *356*, 1071–1086. doi: 10.1098/rsta.1998.0211

Koenderink, J. J., van Doorn, A. J., & Kappers, A. M. L. (1992). Surface perception in pictures. *Perception & Psychophysics*, *52*, 487–496. doi: 10.3758/BF03206710

Kohn, A., & Movshon, J. A. (2003). Neuronal adaptation to visual motion in area mt of the macaque. *Neuron*, *39*, 681–691. doi: 10.1016/S0896-6273(03)00438-0

Kohn, A., & Movshon, J. A. (2004). Adaptation changes the direction tuning of macaque mt neurons. *Nature Neuroscience*, *7*, 764–772. doi: 10.1038/nn1267

Kontsevich, L. L., & Tyler, C. W. (1999). Bayesian adaptive estimation of psychometric slope and threshold. *Vision Research*, *39*, 2729–2737. doi: 10.1016/S0042-6989(98)00285-5

Korte, A. (1915). Kinematoskopische untersuchungen [Kinematoscope investigations]. *Zeitschrift für Psychologie*, *72*, 193–296.

Lasseter, J. (1987). Principles of traditional animation applied to 3d computer animation. In *Siggraph '87 proceedings of the 14th annual conference on computer graphics and interactive techniques* (Vol. 21, pp. 35–44). New York, NY: ACM. doi: 10.1145/37401.37407

Lawson, R., & Humphreys, G. W. (1998). View-specific effects of depth rotation and foreshortening on the initial recognition and priming of familiar objects. *Perception & Psychophysics*, *60*, 1052–1066. doi: 10.3758/BF03211939

Lederman, S. J., Ganeshan, S. R., & Ellis, R. E. (1996). Effortful touch with minimum movement: Revisited. *Journal of Experimental Psychology: Human Perception and Performance*, *22*, 851-868. doi: 10.1037/0096-1523.22.4.851

Marr, D. (1982). *Vision.* San Francisco, CA: W H Freeman.

Marr, D., & Nishihara, H. K. (1978). Representation and recognition of the spatial organization of three-dimensional shapes. *Proceedings of the Royal Society of London, Series B, Biological Sciences*, *200*, 269–294. doi: 10.1098/rspb.1978.0020

McCloskey, M. (1983a). Intuitive physics. *Scientific American*, *248*, 122–130. doi: 10.1038/scientificamerican0483-122

McCloskey, M. (1983b). Naive theories of motion. In D. Gentner & A. L. Stevens (Eds.), *Mental models* (pp. 299–324). Hillsdale, NJ: Lawrence Erlbaum Associates, Inc.

McCloskey, M., Caramazza, A., & Green, B. (1980). Curvilinear motion in the absence of external forces: Naive beliefs about the motion of objects. *Science*, *210*, 1139–1141. doi: 10.1126/science.210.4474.1139

McCloskey, M., & Kohl, D. (1983). Naive physics: The curvilinear impetus principle and its role in interactions with moving objects. *Journal of Experimental Psychology: Learning, Memory, and Cognition*, *9*, 146–156. doi: 10.1037/0278-7393.9.1.146

McCloskey, M., Washburn, A., & Felch, L. (1983). Intuitive physics: The straight-down belief and its origin. *Journal of Experimental Psychology: Learning, Memory, and Cognition*, *9*, 636–649. doi: 10.1037/0278-7393.9.4.636

McIntyre, J., Zago, M., Berthoz, A., & Lacquaniti, F. (2001). Does the brain model Newton's laws? *Nature Neuroscience*, *4*, 693–694. doi: 10.1038/89477

Melcher, D., & Kowler, E. (1999). Shapes, surfaces and saccades. *Vision Research*, *39*, 2929–2946. doi: 10.1016/S0042-6989(99)00029-2

Morales, T. (2009). *Amputee aims to scale new peaks.* Retrieved from `http://www.cbsnews.com/stories/2003/05/06/earlyshow/living/main552498.shtml`

Morgan, M. J., Hole, G. J., & Glennerster, A. (1990). Biases and sensitivities in geometrical illusions. *Vision Research*, *30*, 1793–1810. doi: 10.1016/0042-6989(90)90160-M

Moscatelli, A., Polito, L., & Lacquaniti, F. (2011). Time perception of action photographs is more precise than that of still photographs. *Experimental Brain Research*, *210*, 25–32. doi: 10.1007/s00221-011-2598-y

Needham, A., & Baillargeon, R. (1993). Intuitions about support in 4.5-month-old infants. *Cognition*, *47*, 121–148. doi: 10.1016/0010-0277(93)90002-D

Newman, G. E., Choi, H., Wynn, K., & Scholl, B. J. (2008). The origins of causal perception: Evidence from postdictive processing in infancy. *Cognitive Psychology*, *57*, 262–291. doi: 10.1016/j.cogpsych.2008.02.003

Pavel, M., Cunningham, H., & Stone, V. (1992). Extrapolation of linear motion. *Vision Research*, *32*, 2177–2186. doi: 10.1016/0042-6989(92)90078-W

Pelli, D. G. (1997). The VideoToolbox software for visual psychophysics: Transforming numbers into movies. *Spatial Vision*, *10*, 437–442. doi: 10.1163/156856897X00366

Proffitt, D. R., & Gilden, D. L. (1989). Understanding natural dynamics. *Journal of Experimental Psychology*, *15*, 384–393. doi: 10.1037/0096-1523.15.2.384

Roncato, S., & Rumiati, R. (1986). Naive statics: Current misconceptions on equilibrium. *Journal of Experimental Psychology: Learning, Memory, and Cognition*, *12*, 361–377. doi: 10.1037/0278-7393.12.3.361

Samuel, F., & Kerzel, D. (2011). Is this object balanced or unbalanced? Judgments are on the safe side. *Journal of Experimental Psychology: Human Perception and Performance*, *37*, 529–538. doi: 10.1037/a0018732

Scholl, B. J., & Nakayama, K. (2002). Causal capture: Contextual effects on the perception of collision events. *Psychological Science*, *13*, 493–498. doi: 10.1111/1467-9280.00487

Scholl, B. J., & Pylyshyn, Z. W. (1999). Tracking multiple items through occlusion: Clues to visual objecthood. *Cognitive Psychology*, *38*, 259–290. doi: 10.1006/cogp.1998.0698

Shah, S., Fulvio, J., & Singh, M. (2012). Perceptual decisions in the visual extrapolation of curved motion trajectories. *Journal of Vision*, Under Review.

Singer, G., & Day, R. H. (1966a). The effects of spatial judgments on the perceptual aftereffect resulting from prismatically transformed vision. *Australian Journal of Psychology*, *18*, 63–70. doi: 10.1080/00049536608255717

Singer, G., & Day, R. H. (1966b). Spatial adaptation and aftereffect with optically transformed vision: Effects of active and passive responding and the relationship between test and exposure responses. *Journal of Experimental Psychology*, *71*, 725–731. doi: 10.1037/h0023089

Singh, M. (2004). Modal and amodal completion generate different shapes. *Psychological Science*, *15*, 454–459. doi: 10.1111/j.0956-7976.2004.00701.x

Tootell, R. B. ., Reppas, J. B., Dale, A. M., Look, R. B., Sereno, M. I., Malach, R., ... Rosen, B. R. (1995). Visual motion aftereffect in human cortical area MT revealed by functional magnetic resonance imaging. *Nature*, *375*, 139–141. doi: 10.1038/375139a0

Verghese, P., & McKee, S. P. (2002). Predicting future motion. *Journal of Vision*, *2*, 513–523. doi: 1167/2.5.5

Vishwanath, D., & Kowler, E. (2003). Localization of shapes: eye movements and perception compared. *Vision Research*, *43*, 1637–1653. doi: 10.1016/S0042-6989(03)00168-8

Vishwanath, D., & Kowler, E. (2004). Saccadic localization in the presence of cues to three-dimensional shape. *Journal of Vision*, *4*, 445–458. doi: 10.1167/4.6.4

Wertheimer, M. (1912). Experimentelle Studien über das Sehen von Bewegung. [Experiments on the perception of motion]. *Zeitschrift für Psychologie*, *61*, 161-265.

White, B. Y. (1983). Sources of difficulty in understanding newtonian dynamics. *Cognitive Science*, *7*, 41–65. doi: 10.1207/s15516709cog0701_2

Winawer, J., Huk, A. C., & Boroditsky, L. (2008). A motion aftereffect from still photographs depicting motion. *Psychological Science*, *19*, 276–283. doi: 10.1111/j.1467-9280.2008.02080.x

Zago, M., & Lacquaniti, F. (2005). Visual perception and interception of falling objects: A review of evidence for an internal model of gravity. *Journal of Neural Engineering*, *2*, 198–208. doi: 10.1088/1741-2560/2/3/S04

Zollinger, D. (2008). *Tbilisi (georgia) - former transport ministry.* Retrieved from `http://www.flickr.com/photos/danielzolli/2497272343/`